



Miss Anchale Tresatayawed

A Dissertation Submitted in Partial Fulfillment of the Requirements
for the Degree of Doctor of Engineering in Chemical Engineering
Department of Chemical Engineering
Faculty of Engineering
Chulalongkorn University
Academic Year 2019
Copyright of Chulalongkorn University

เอทานอลดีไฮเดรชันบนตัวเร่งปฏิกิริยา WO_3/TiO_2 โดยใช้ตัวรองรับไทเทเนียมที่สังเคราะห์จาก
วิธีโซลเจลและโซลโวกเทอร์มอลที่มีการปรับปรุงด้วยแพลเลเดียม



วิทยานิพนธ์นี้เป็นส่วนหนึ่งของการศึกษาตามหลักสูตรปริญญาวิศวกรรมศาสตรดุษฎีบัณฑิต
สาขาวิชาวิศวกรรมเคมี ภาควิชาวิศวกรรมเคมี
คณะวิศวกรรมศาสตร์ จุฬาลงกรณ์มหาวิทยาลัย
ปีการศึกษา 2562
ลิขสิทธิ์ของจุฬาลงกรณ์มหาวิทยาลัย

Thesis Title
By Miss Anchale Tresatayawed
Field of Study Chemical Engineering
Thesis Advisor Professor BUNJERD JONGSOMJIT

Accepted by the Faculty of Engineering, Chulalongkorn University in Partial Fulfillment of the Requirement for the Doctor of Engineering

..... Dean of the Faculty of Engineering
(Professor SUPOT TEACHAVORASINSKUN, Ph.D.)

DISSERTATION COMMITTEE

..... Chairman
(Assistant Professor Ekrachan Chaichana)
..... Thesis Advisor
(Professor BUNJERD JONGSOMJIT)
..... Examiner
(Associate Professor KASIDIT NOOTONG)
..... Examiner
(Associate Professor SEEROONG PRICHANONT)
..... Examiner
(Dr. RUNGTHIWA METHAAPANON)



จุฬาลงกรณ์มหาวิทยาลัย
CHULALONGKORN UNIVERSITY

อัญจารี ตรีสัตยาเวทย์ : เอทานอลดีไฮเดรชันบนตัวเร่งปฏิกิริยา WO_3/TiO_2 โดยใช้ตัวรองรับไทเทเนียมที่สังเคราะห์จากวิธีโซลเจลและโซลโวเทอร์มอลที่มีการปรับปรุงด้วยแพลเลเดียม . () อ.ที่ปรึกษาหลัก : ศ. ดร. บรรเจิด จงสมจิตร

งานวิจัยนี้ได้ศึกษาถึงคุณลักษณะและประสิทธิภาพของตัวเร่งปฏิกิริยาของทั้งสแตนบนตัวรองรับไทเทเนียมที่สังเคราะห์จากวิธีโซลเจลและโซลโวเทอร์มอลโดยมีการปรับปรุงด้วยแพลเลเดียม โดยงานวิจัยนี้แบ่งออกเป็น 2 ส่วน ในงานวิจัยส่วนแรกเป็นการศึกษาหาประสิทธิภาพของตัวเร่งปฏิกิริยา (WO_3/TiO_2-SV , WO_3/TiO_2-SG) และ ตัวรองรับ (TiO_2-SV , TiO_2-SG) ในกระบวนการเอทานอลดีไฮเดรชัน จากผลการทดสอบพบว่าวิธีการสังเคราะห์ตัวรองรับตัวเร่งปฏิกิริยาไทเทเนียมจากวิธีโซลเจล (TiO_2-SG) และโซลโวเทอร์มอล (TiO_2-SV) ส่งผลให้คุณลักษณะทั้งกายภาพและเคมีภาพของตัวเร่งปฏิกิริยาแตกต่างกัน ทั้งนี้ตัวเร่งปฏิกิริยาที่สังเคราะห์จากวิธีโซลโวเทอร์มอลให้พื้นที่ผิว ขนาดรูพรุน และปริมาณความเป็นกรด ที่มากกว่าตัวเร่งปฏิกิริยาที่สังเคราะห์จากวิธีโซลเจล ดังนั้นตัวรองรับที่มีคุณลักษณะที่แตกต่างกันจึงส่งผลต่อคุณสมบัติของตัวเร่งปฏิกิริยา WO_3/TiO_2 เมื่อนำตัวเร่งปฏิกิริยา (WO_3/TiO_2-SV , WO_3/TiO_2-SG) และ ตัวรองรับ (TiO_2-SV , TiO_2-SG) ทำการทดสอบในกระบวนการเอทานอลดีไฮเดรชันพบว่าตัวเร่งปฏิกิริยา WO_3/TiO_2-SV ให้ผลผลิตเอทิลีนสูงสุดที่ร้อยละ 77 ที่อุณหภูมิ 400 องศาเซลเซียส อีกทั้งให้ผลผลิตไดออกซิอีเทอร์สูงสุดที่ร้อยละ 26 ที่อุณหภูมิ 250 องศาเซลเซียส ทั้งนี้อันเนื่องมาจากขนาดรูพรุน ปริมาณความเป็นกรดที่ได้จากการเติมโลหะทั้งสแตน (W) วิธีการเตรียมตัวรองรับ และ การกระจายตัวของทั้งสแตนที่เหมาะสมบนตัวเร่งปฏิกิริยา สำหรับงานวิจัยส่วนที่สองเป็นการพัฒนาตัวเร่งปฏิกิริยา WO_3/TiO_2-SV โดยการเติมโลหะแพลเลเดียมด้วยวิธีการเคลือบผงที่มีลำดับขั้นตอนต่างกันเพื่อให้ได้ตัวเร่งปฏิกิริยา $Pd/W/TiO_2$, $W/Pd/TiO_2$ และ $Pd/W/TiO_2$ ผลการวิจัยพบว่าตัวเร่งปฏิกิริยา $Pd/W/TiO_2$ ที่ได้จากการเคลือบผงร่วมกันให้ประสิทธิภาพการเกิดผลผลิตไดออกซิอีเทอร์สูงสุดที่ร้อยละ 41.4 ที่อุณหภูมิ 300 องศาเซลเซียส นอกจากนี้พบว่า $W/Pd/TiO_2$ ที่ได้จากการเคลือบผงที่มีลำดับต่างกัน โดยเคลือบผงด้วยแพลเลเดียมก่อนแล้วตามด้วยทั้งสแตนให้ประสิทธิภาพการเกิดผลผลิตเอทิลีนสูงสุดที่ร้อยละ 68.1 ที่อุณหภูมิ 400 องศาเซลเซียส จากงานวิจัยพบว่านอกจากการปรับปรุงด้วยโลหะแพลเลเดียมบนตัวเร่งปฏิกิริยาจะมีผลต่อประสิทธิภาพของตัวเร่งปฏิกิริยาแล้วนั้น ขั้นตอนเติมโลหะด้วยการเคลือบผงที่แตกต่างกันมีบทบาทสำคัญต่อประสิทธิภาพของตัวเร่งปฏิกิริยาในกระบวนการเอทานอลดีไฮเดรชันเพื่อให้ได้ผลผลิตที่ต้องการเช่นกัน

จุฬาลงกรณ์มหาวิทยาลัย
CHULALONGKORN UNIVERSITY

สาขาวิชา วิศวกรรมเคมี
ปีการศึกษา 2562

ลายมือชื่อนิสิต

ลายมือชื่อ อ.ที่ปรึกษาหลัก

5971476021 : MAJOR CHEMICAL ENGINEERING

KEYWORD: catalytic ethanol dehydration, tungsten, titania, palladium

Anchale Tresatayawed : . Advisor: Prof. BUNJERD JONGSOMJIT

In this research, the characteristics and catalytic activity of WO_3/TiO_2 prepared by sol-gel and solvothermal and their metal modified were investigated. The research was divided into two parts. In the first part, the catalyst performance of WO_3/TiO_2 catalysts using titania derived from sol-gel and solvothermal methods over ethanol dehydration reaction was examined. The results showed that the different preparation methods essentially altered the physicochemical properties of TiO_2 supports. It revealed that the titania derived from solvothermal method denoted as $\text{TiO}_2\text{-SV}$ exhibited higher surface area and pore volume, and larger amounts acid sites than the one obtained from sol-gel method ($\text{TiO}_2\text{-SG}$). As a result, the different characteristics of support catalyst seemingly influenced the catalytic properties of WO_3/TiO_2 catalysts. It showed that the highest ethanol conversion (ca. 88%) at 400°C was achieved by the $\text{WO}_3/\text{TiO}_2\text{-SV}$ catalysts due to its high acidity. Furthermore, $\text{WO}_3/\text{TiO}_2\text{-SV}$ catalyst is promising to convert ethanol into ethylene and diethyl ether, having the highest ethylene yield of ca. 77% at 400°C and highest diethyl ether yield of ca. 26% at 250°C. These can be attributed to proper pore structure, acidity and distribution of tungsten. In the second part, the Pd modification and supporting effect of WO_3/TiO_2 catalysts on catalytic ethanol dehydration to ethylene and diethyl ether were investigated. The catalyst characterization and activity examination results indicated that the different sequence during impregnation influenced the physicochemical properties and catalyst activity. The Pd incorporated into catalysts enhanced the ethanol conversion depending on the sequence of impregnation. The diethyl ether is the main product at low temperature, whereas ethylene is the main product at high temperature. At low temperature (ca. 200 to 300°C), the Pd incorporated over W/TiO_2 catalyst resulted in an increasing of diethyl ether yield. It is worth noting that the ethanol conversion increased by palladium modification, while diethyl ether selectivity did not change. This can be attributed to the higher amount of weak acids sites present after Pd modification into catalyst. Among the catalysts, the PdW/TiO_2 catalyst (co-impregnation) accomplished the highest diethyl ether yield of 41.4% at 300°C. At high temperature (ca. 350 to 400°C), the $\text{W}/\text{Pd}/\text{TiO}_2$ catalyst (with sequential impregnation of Pd on TiO_2 followed by W) achieved the highest ethylene yield of 68.1% at 400°C. Thus, the modification of Pd onto W/TiO_2 upon different sequence of Pd and W impregnation improved diethyl ether and ethylene yield in catalytic ethanol dehydration.

จุฬาลงกรณ์มหาวิทยาลัย
CHULALONGKORN UNIVERSITY

Field of Study: Chemical Engineering
Academic Year: 2019

Student's Signature
Advisor's Signature

ACKNOWLEDGEMENTS

In my doctoral dissertation research, I would like to express the deepest gratitude to my research advisor, Prof. Dr. Bunjerd Jongsomjit for his guidance, useful critiques of my research work and constructive suggestions during the planning and development of my research work. This doctoral dissertation cannot be achieved without him.

Furthermore, I would like to thank Asst. Prof. Ekrachan Chaichana, as chairman, Assoc. Prof. Dr. Kasidit Nootong, Assoc. Prof. Dr. Seerong Prichanont and Dr. Rungthiwa Methaapanon as the members of the thesis committee for their suggestion and revision of my thesis.

My grateful thanks are also extended to the funding sources of my research. I would like to thank the Grant for International Research Integration: Chula Research Scholar, Ratchadaphiseksomphot Endowment Fund, Endowment Fund, Grant for Research: Government Budget, Chulalongkorn University (2019), and the National Research Council of Thailand (NRCT) for their financial support of this project.

I would also like to thank the technicians of the CECC laboratory for their help in catalyst characterization. Moreover, I wish to thank my colleagues in laboratory for cooperation and encouragement through my dissertation study.

Finally, I wish to thank my parent for their encouragement and support through my doctoral study.

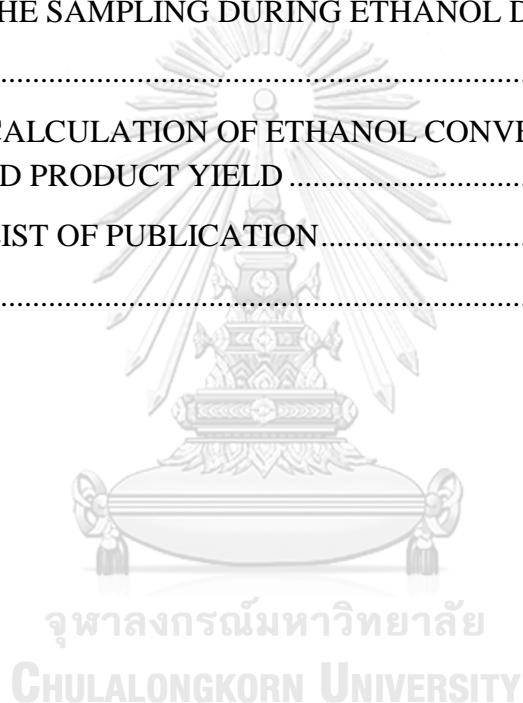
Anchale Tresatayawed

TABLE OF CONTENTS

	Page
ABSTRACT (THAI)	iii
ABSTRACT (ENGLISH).....	iv
ACKNOWLEDGEMENTS.....	v
TABLE OF CONTENTS.....	vi
LIST OF TABLES.....	ix
LIST OF FIGURES	xi
CHAPTER I - INTRODUCTION.....	1
1.1 General introduction.....	1
1.2 Research objectives	3
1.3 Research scopes	4
1.4 Research methodology.....	4
CHAPTER II – THEORY AND LITERATURE REVIEW	7
2.1 Ethanol.....	7
2.2 Catalytic ethanol dehydration reaction to ethylene and diethyl ether.....	7
2.2.1 Catalyst.....	7
2.2.2 Ethylene and diethyl ether.....	8
2.2.3 Catalytic ethanol dehydration.....	9
2.3 Titanium oxide catalyst.....	9
2.3.1 Structure and property of titanium oxide	10
2.3.2 Synthesis of titanium oxide	10
2.3.2.1 The sol-gel method	11
2.3.2.2 The solvothermal method	11
2.4. Tungsten oxide catalyst	12
2.5 Palladium catalyst.....	13
2.6. Literature Reviews.....	13

CHAPTER III – EXPERIMENTAL.....	19
3.1 Catalyst preparation	19
3.1.1 Chemicals	19
3.1.2 Preparation of TiO ₂ supports and WO ₃ /TiO ₂ catalysts	19
3.1.3 Preparation of Pd doped-WO ₃ /TiO ₂ catalysts	20
3.2 Catalyst characterization.....	21
3.2.1 X-ray diffraction (XRD).....	21
3.2.2 Nitrogen Physisorption.....	21
3.2.3 Temperature-programmed desorption of ammonia (NH ₃ -TPD) and carbon dioxide (CO ₂ -TPD).....	21
3.2.4 Scanning electron microscopy (SEM) and energy dispersive X-ray spectroscopy (EDX)	22
3.2.5 X-ray fluorescence spectrometer (XRF)	22
3.2.6 X-ray photoelectron spectroscopy (XPS).....	22
3.3 Reaction study in dehydration of ethanol	22
3.3.1 Chemicals and reagents	22
3.3.2 Instrument and apparatus.....	23
3.3.3 Ethanol dehydration reaction procedure.....	25
CHAPTER IV – RESULTS AND DISCUSSION.....	26
4.1 The catalytic ethanol dehydration to ethylene and diethyl ether over the WO ₃ /TiO ₂ prepared by sol-gel and solvothermal methods	26
4.1.1 Catalyst characterization	26
4.1.2 Ethanol Dehydration Reaction study.....	33
4.2 The catalytic ethanol dehydration to ethylene and diethyl ether carried on the W/TiO ₂ catalyst modified with Pd in different sequence impregnation	38
4.2.1 Catalyst characterization	38
4.2.2 Ethanol dehydration Reaction study.....	46
CHAPTER V – CONCLUSIONS AND RECOMMENDATION	53
5.1 Conclusion	53
5.2 Recommendation	54

REFERENCES	55
APPENDIX.....	62
APPENDIX A – COMPARING PD/TIO ₂ AND WPD/TIO ₂ CATALYST IN ETHANOL DEHYDRATION.....	63
APPENDIX B - CALCULATION CATALYST PREPARATION	68
APPENDIX C - CALCULATION OF ACIDITY AND BASICITY	70
APPENDIX D – GC CALIBRATION CURVES	72
APPENDIX E – CHROMATOGRAM	75
APPENDIX F – THE SAMPLING DURING ETHANOL DEHYDRATION.....	76
.....	76
APPENDIX G – CALCULATION OF ETHANOL CONVERSION, PRODCUT SELCTIVITY AND PRODUCT YIELD	77
APPENDIX H – LIST OF PUBLICATION.....	78
VITA.....	79



LIST OF TABLES

	Page
Table 1: The chemicals used for catalyst preparation.....	19
Table 2: The chemicals for catalytic ethanol dehydration reaction	23
Table 3: Operation conditions for gas chromatograph	24
Table 4: Physical properties of TiO ₂ supports and catalysts	28
Table 5: Elemental compositions (wt%) on external surface of catalysts obtained from EDX	28
Table 6: The amount of surface acidity of supports and catalysts measured by NH ₃ -TPD	32
Table 7: The amount of surface basicity of supports and catalysts measured by CO ₂ -TPD	32
Table 8: The amount of carbon elemental compositions (wt%) on external surface supports and catalysts after reaction obtained from EDX	33
Table 9: Ethanol conversion, product selectivity and product yield as a function of reaction temperature. (the reaction condition: T = 200 – 400°C, WHSV = 22.9 g _{ethanol} /g _{cat} ⁻¹ · h ⁻¹ , and catalyst weight = 0.05 g.).....	37
Table 10: Physical properties of catalysts.....	39
Table 11: Elemental distribution (%wt, %mol) on external surface of catalysts obtained from EDX.....	39
Table 12: The amount surface acidity and acid density of catalysts measured by NH ₃ -TPD	43
Table 13: XPS analysis of catalysts	46
Table 14: Product yield (%) obtained from each catalyst as function of reaction temperature (the reaction condition at T = 200 – 400°C, WHSV = 3.13 g _{ethanol} · g _{cat} ⁻¹ · h ⁻¹ , and catalyst weight = 0.1 g)	51
Table 15: Comparison of various catalysts for ethylene and diethyl ether yield and catalytic performance.....	52
Table 16: Physical properties of PdW/TiO ₂ and Pd/TiO ₂ catalysts.....	64
Table 17: Elemental distribution (%wt, %mol) on external surface of PdW/TiO ₂ and Pd/TiO ₂ catalysts obtained from EDX.....	64

Table 18: The amount surface acidity and acid density of catalysts measured by NH ₃ -TPD	64
Table 19: XPS analysis of PdW/TiO ₂ and Pd/TiO ₂ catalysts	65
Table 20: Catalytic activity and product yield (%) obtained from PdW/TiO ₂ and Pd/TiO ₂ catalyst as function of reaction temperature (the reaction condition at T = 200 – 400°C, WHSV = 3.13 g _{ethanol} ·g _{cat} ⁻¹ ·h ⁻¹ , and catalyst weight = 0.1 g)	66



LIST OF FIGURES

	Page
Figure 1: Flow diagram research methodology in Part I	5
Figure 2: Flow diagram research methodology in Part II	6
Figure 3: Crystal structure of rutile, anatase and brookite	10
Figure 4 : General scheme of preparation by sol-gel method	11
Figure 5: General scheme of preparation by solvothermal method	12
Figure 6: The crystal structure of tungsten observed during in situ heat treatment from temperature to 950°C	13
Figure 7: Process diagram of the ethanol dehydration system	23
Figure 8: X-ray powder diffraction patterns of supports and catalysts	27
Figure 9: Elemental distribution by EDX mapping for (a) WO ₃ /TiO ₂ -SG and (b) WO ₃ /TiO ₂ -SV catalyst	28
Figure 10: Nitrogen adsorption-desorption isotherms for supports and catalysts	30
Figure 11: The pore size distribution for supports and catalysts	30
Figure 12: NH ₃ -TPD profiles of TiO ₂ supports and WO ₃ /TiO ₂ catalysts	31
Figure 13: CO ₂ -TPD profile of TiO ₂ supports and WO ₃ /TiO ₂ catalysts	32
Figure 14: X-ray powder diffraction patterns for Pd/W/TiO ₂ , W/Pd/TiO ₂ , PdW/TiO ₂ and W/TiO ₂ catalysts	39
Figure 15: The energy-dispersive X-ray spectroscopy (EDX) mapping analysis of a) Pd/W/TiO ₂ , b) W/Pd/TiO ₂ and c) PdW/TiO ₂ catalysts	41
Figure 16: Scanning electron microscopy (SEM) micrograph of Pd/W/TiO ₂ , W/Pd/TiO ₂ , PdW/TiO ₂ and W/TiO ₂ catalysts	42
Figure 17: Nitrogen adsorption-desorption isotherms for Pd/W/TiO ₂ , W/Pd/TiO ₂ , PdW/TiO ₂ , and W/TiO ₂ catalysts	43
Figure 18 : The pore size distribution of catalysts using the BJH method	44
Figure 19: NH ₃ -TPD profiles for Pd/W/TiO ₂ , W/Pd/TiO ₂ , PdW/TiO ₂ and W/TiO ₂ catalysts	44
Figure 20: XPS analysis at O 1s for Pd/W/TiO ₂ , W/Pd/TiO ₂ , PdW/TiO ₂ and W/TiO ₂ catalysts	46

Figure 21: Ethanol conversion of Pd/W/TiO ₂ , W/Pd/TiO ₂ , PdW/TiO ₂ , and W/TiO ₂ catalysts.....	50
Figure 22: Product selectivity of Pd/W/TiO ₂ , W/Pd/TiO ₂ , PdW/TiO ₂ and W/TiO ₂ catalysts.....	50
Figure 23: X-ray powder diffraction patterns for PdW/TiO ₂ and Pd/TiO ₂ catalysts....	63
Figure 24: Product selectivity of PdW/TiO ₂ and Pd/TiO ₂ catalysts	67
Figure 25: The calibration curve of NH ₃ -TPD	70
Figure 26: The calibration curve of CO ₂ -TPD.....	71
Figure 27: The calibration curve of ethanol.....	72
Figure 28: The calibration curve of ethylene.....	73
Figure 29: The calibration curve of diethyl ether	73
Figure 30: The calibration curve of acetaldehyde.....	74
Figure 31: The gas chromatography analysis report.....	75
Figure 32: The sampling during the reaction testing	76

CHAPTER I - INTRODUCTION

1.1 General introduction

Nowadays, the ethanol dehydration to produce ethylene and diethyl ether over the solid catalyst has been paid attention for numerous research due to its cleaner technology and efficient utilization of ethanol, which is a renewable raw material obtained from fermentation of biomass. For instance, the production of ethylene from ethanol is considered as an alternative way to produce ethylene, which is currently produced by the catalytic thermal cracking of petroleum feed stocks such as naphtha and dehydrogenation of ethane from natural gas. In fact, dehydration of ethanol to ethylene is cleaner technology due to lower operating temperature, uncomplicated process and less impurity. Generally, ethylene is one of the most important raw materials for petrochemical industry, which is used as a starting material for production of polyethylene, ethylene oxide, vinyl acetate, ethyl benzene, etc. Considering the production of commercialized diethyl ether at present, although it is produced from dehydration of ethanol, the process is not benign since it uses mineral liquid acids such as H_2SO_4 to catalyze the reaction. Consequently, this reaction is further required the separation and purification processes. In this case, the solid acid catalysts are preferred since they are reusable and easy to separate from the product. Although the consumption of diethyl ether is much lesser than ethylene, it is very important chemical. In particular, diethyl ether is mainly employed as a solvent for fragrance and pharmaceutical industries. In transport fuel function, diethyl ether is employed as an ignition improving additive in engines according to its high volatility and cetane and octane number. The blending of diethyl ether in diesel improves the performance-emission characteristics with thermal efficiency and reduced emission of NO_x , CO and HC [1]. Hence, the production of ethylene and diethyl ether from ethanol using suitable solid catalysts is very captivating.

In general, the catalytic ethanol dehydration to ethylene and diethyl ether requires acid sites on the solid catalyst. This reaction essentially undergoes via thermodynamic and kinetic controls. The formation of ethylene is dominated by high reaction temperature since it is endothermic reaction, whereas diethyl ether mainly

occurs at lower reaction temperature due to its exothermic reaction. However, during dehydration of ethanol, a side reaction such as dehydrogenation can occur resulting in the formation of acetaldehyde as a byproduct. From previous researches, many solid acid catalysts have been investigated in ethanol dehydration reaction including the transition metal oxides [2-4], zeolites [5], silica-alumina [6, 7] and heteropolyacids [8]. Many investigators found that the transition metal oxides such as TiO_2 , ZrO_2 , SiO_2 , and Nb_2O_5 play an important role in heterogeneous catalysis acting as an active phase, promoter or support of solid catalysts. Those solid catalysts have been developed on structure characteristics and acid properties to build up the product selectivity, catalytic activity and stability. Among the transition metal oxides, TiO_2 has been widely used as a support in heterogeneous catalysts due to its suitable surface areas, thermal stability and mechanical resistance [9, 10]. Besides, the modification by incorporated the additional active noble and transition metals such as Cs [11], Au/Ag/Cu [12], Al [13], Ru [14], Pt, Pd [15], Mo [16], and W [17, 18] into catalyst supports apparently affected both the catalyst selectivity and activity.

Furthermore, the presence of tungsten (W) metal on catalysts was found to be very interesting since it contributes Bronsted acid site and develops the catalyst stability and activity [19-21]. It has been accepted that WO_3/TiO_2 catalyst is widely used in various reactions and process including glycerol hydrogenation, reforming, oxidation of dibenzothiophene [22], selective catalytic reduction [23], dehydration [24], and photoelectrocatalytic degradation [25]. WO_3/TiO_2 is promising for the catalytic dehydration of ethanol to ethylene and especially diethyl ether at low temperature as described by Phung *et al.* [26]. They discovered that the addition of tungsten on transition metal oxide provided the Brønsted acids sites that are active to the ethanol dehydration reaction to produce ethylene and diethyl ether and also prevent the formation of byproducts such as acetaldehyde and higher hydrocarbons. In addition, with various tungsten loading on TiO_2 , ZrO_2 and SiO_2 catalyst support, the WO_3/TiO_2 catalyst was found to be the most active in this reaction giving the highest yield of diethyl ether. However, besides the active metals, one needs to consider on the properties of a wide variety of supports themselves. The variations of support characteristics mostly arise from different preparation methods including the sol-gel [27, 28] and solvothermal methods [29, 30]. In most cases, they found that different

preparation methods can alter the properties of support and consequently different catalytic properties were observed. As a result, the effect of different preparation methods on the properties of support is crucial for better understanding.

Recently, researchers have developed new designed catalysts with adequate textual properties, controlled acidity and stability to enhance the catalytic properties. The bimetallic catalysts have been proven to be important for many catalyst applications [30-33]. The presence of Pd oxides has been known to be an active for a wide range of reactions such as ethanol reforming [34], hydrogenolysis [35], oxidation [36], dehydration [37, 38]. Armenta et al.[39] reported that the bimetallic (CuO-PdO/ γ - Al_2O_3) performed higher catalyst activity when compared to monometallic catalysts (CuO/ γ - Al_2O_3 and PdO/ γ - Al_2O_3) in methanol dehydration to dimethyl ether. To improve the structure and catalyst performance of catalysts, the metal impregnation technique on support catalyst is promising to be an attractive on catalyst development [40].

Consequently, the objective of this present study is to develop a better understanding on different preparation methods including the sol-gel and solvothermal methods to synthesize the titania oxide supports for tungsten oxide catalysts used in catalytic ethanol dehydration to ethylene and diethyl ether. The change in catalytic properties was also investigated via the catalytic ethanol dehydration in a fixed-bed microreactor at the temperature range of 200 to 400°C. Ethanol conversion and product selectivity of different WO_3/TiO_2 catalysts were reported and discussed further. Besides, the catalyst which showed the highest performance in ethanol dehydration was selected to be further modified by loading with the palladium metal to improve the catalytic activity and performance. The effect of sequence in impregnation method of palladium modification has been explored on their characteristics and catalyst properties.

1.2 Research objectives

1. To investigate the characteristics and activities of WO_3/TiO_2 catalysts synthesized by sol-gel and solvothermal methods for ethanol dehydration to ethylene and diethyl ether.

2. To examine the catalyst performance when the TiO₂-supported W catalyst was modified with palladium (Pd) as well as different sequence incipient wetness impregnation into W/TiO₂ catalysts for ethanol dehydration reaction to ethylene and diethyl ether.

1.3 Research scopes

1. Preparation of TiO₂ supports catalyst by sol-gel and solvothermal methods, followed by the incipient wetness impregnation with tungsten (W) into TiO₂ catalysts. These catalysts were used for studying in part I.

2. Modification the palladium (Pd) into W/TiO₂ catalysts with different sequence of incipient wetness impregnation. These catalysts were used for studying in part II.

3. Evaluation on the catalytic activity for all catalysts in ethanol dehydration to ethylene and diethyl ether under atmospheric pressure and temperature in range of 200°C to 400°C

4. The structural and surface properties on the supports and all catalysts were characterized by several techniques including the catalyst structures and crystallinity by X-ray diffraction (XRD), the morphology and elemental distribution over the catalyst granules by scanning electron microscopy (SEM) and energy dispersive X-ray spectroscopy (EDX), the surface area, pore volume and pore size diameter by N₂ physisorption (BET), the acidity of catalysts by NH₃-temperature programmed desorption (NH₃-TPD), the basicity of catalysts by CO₂-temperature programmed desorption (CO₂-TPD), the coke deposit on surface catalysts after reaction by energy dispersive X-ray spectroscopy (EDX), amount of metal loading by X-ray fluorescence spectrometer (XRF) and binding energy and chemical oxidation states of the catalysts by X-ray photoelectron spectroscopy (XPS).

1.4 Research methodology

The research methodology is divided into 2 parts, which are as following.

Part I: The catalytic ethanol dehydration to ethylene and diethyl ether over the WO_3/TiO_2 prepared by sol-gel and solvothermal methods

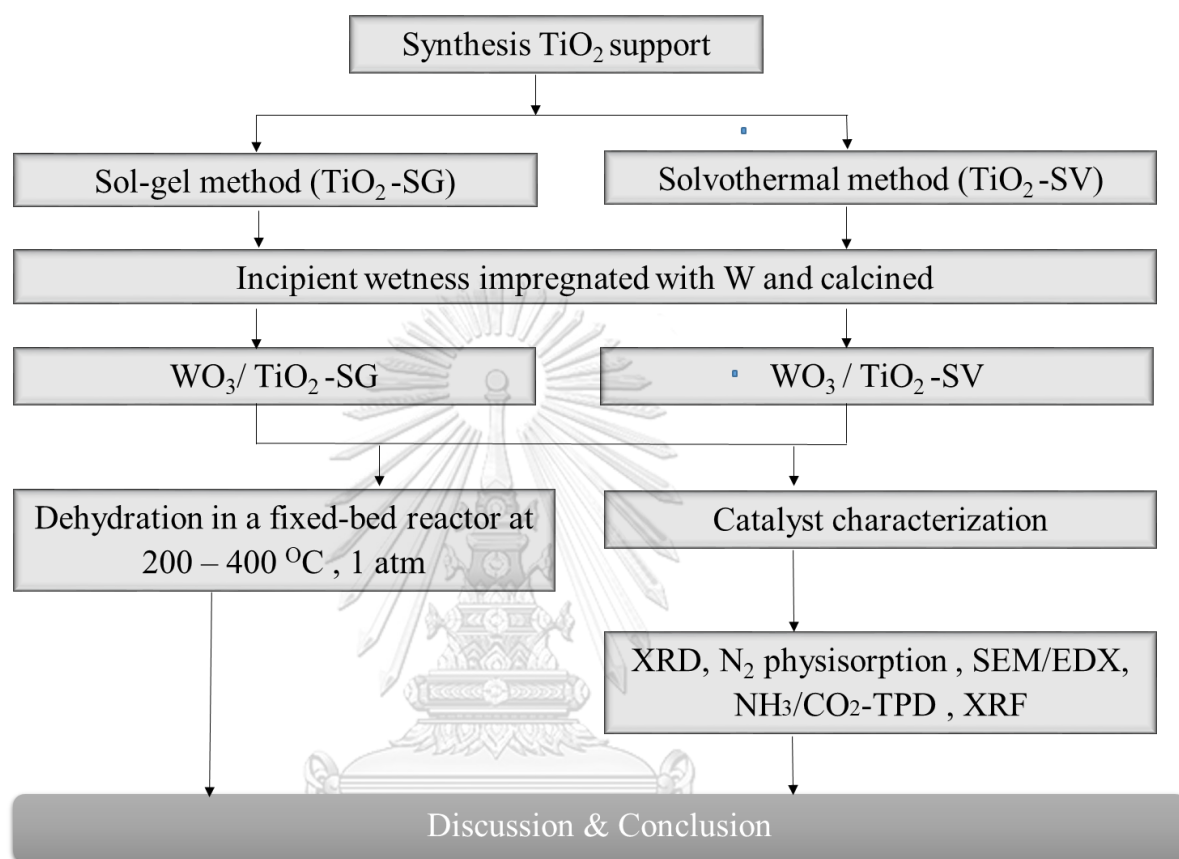


Figure 1: Flow diagram research methodology in Part I

Part II: The catalytic ethanol dehydration to ethylene and diethyl ether over the W/TiO₂ catalyst modified with Pd in different sequence impregnation

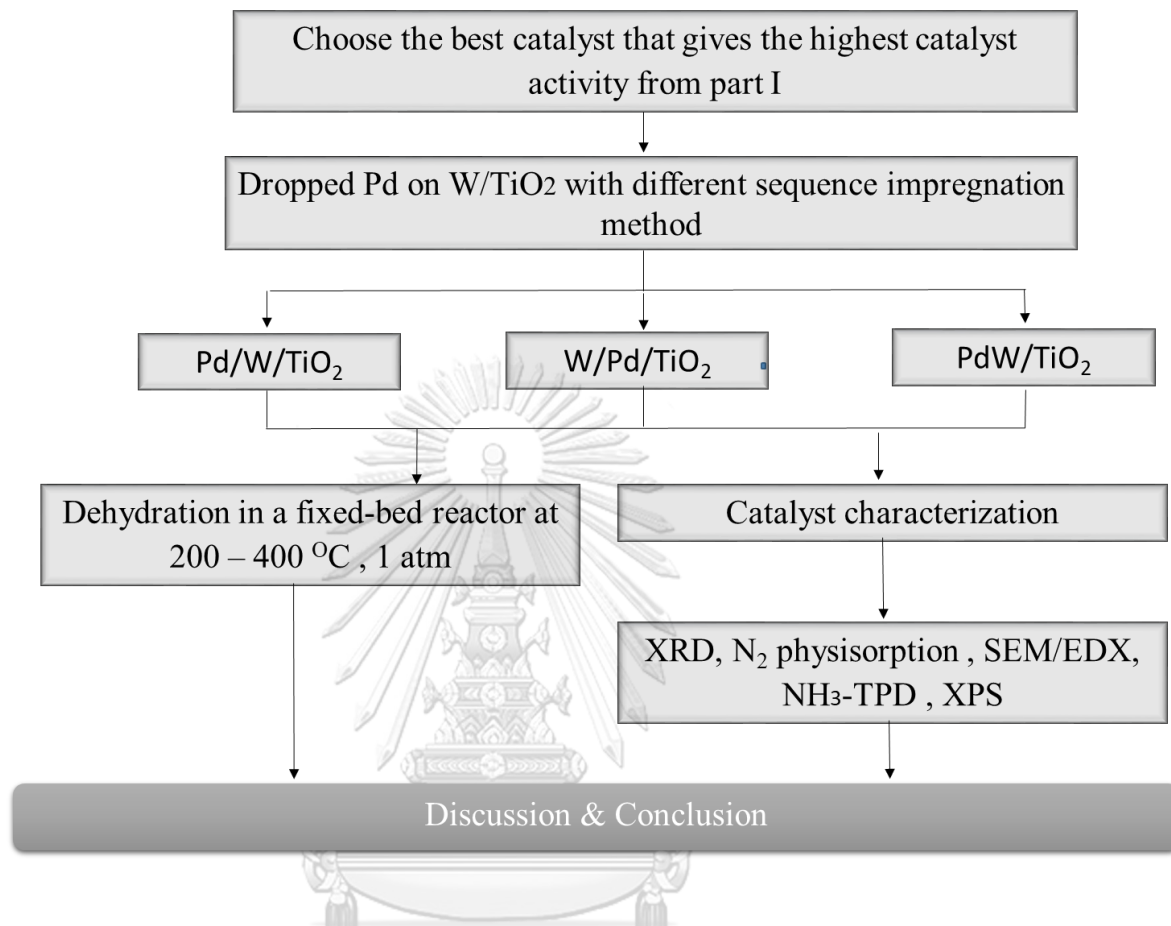


Figure 2: Flow diagram research methodology in Part II

CHAPTER II – THEORY AND LITERATURE REVIEW

This chapter is described the knowledge of catalysts including an ethanol, catalytic ethanol dehydration reaction to ethylene and diethyl ether, titanium oxide catalyst, tungsten oxide catalyst, palladium catalyst and literature reviews.

2.1 Ethanol

Ethanol (bio-ethanol) is derived from fermentation of various types of agricultural products such as corn, sugarcane and cassava [39]. Bio-ethanol has become an attractive renewable source to produce the value-added chemicals such as ethylene, diethyl ether, acetaldehyde, etc., which are widely consumed in many petroleum and petrochemical industries. Recently, bio-ethanol is the main potential source that becomes a sustainable source instead of fossil fuel due to an environmental concern about the emission of greenhouse gas from burning of fossil fuel (coal, oil and gas) and reducing of non-renewable feedstock supply in future. Besides, many researchers have played attention to convert the biomass-derived ethanol to the valued-added chemical compounds with several feasible process and technologies mostly applied with catalytic reactions.

2.2 Catalytic ethanol dehydration reaction to ethylene and diethyl ether

2.2.1 Catalyst

The catalyst is used to change the reaction kinetics of a reaction. It cannot change the equilibrium of a reaction, but it can change the rate of reaction toward the equilibrium by decreasing the activation energy of the reaction. The catalyst is not consumed during the reaction, but it can be deactivated and loose its ability to catalyze the wanted reaction. Many researches develop catalyst in its activity, selectivity and deactivation. The activity is a measurement of how fast the reaction reaches the equilibrium. Selectivity describes the capability to produce a desired product. Deactivation is when a catalyst loses its ability to catalyze a reaction and becomes less active.

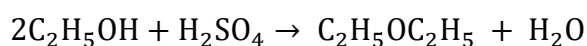
The heterogeneous catalyst can be widely used for many reactions including the catalytic ethanol dehydration. Heterogeneous catalyst is performed in many functions including the carrier, support and active site of catalyst. The carrier provides the structure and the reactor bed, which determine the mass transfer properties and governs the pressure drop over the reactor. The catalyst support provides the surface area in which the reaction can occur and can be the same material as the carrier. The active sites are where the reaction occurs and can be the material of the catalyst support.

2.2.2 Ethylene and diethyl ether

The ethanol dehydration mainly produced ethylene and diethyl ether. The ethylene is normally produced by steam cracking (pyrolysis) of hydrocarbons from fossil feedstock such as naphtha from distillation of crude oil or ethane, propane and butane from natural gas. These gases (ethane, propane or butane) or the liquids (naphtha) are preheated, vaporized and then mixed with steam. It is performed at very high temperatures, 600 - 1000 °C, at approximately normal pressure in a tubular reactor before converted to low relative molecular mass alkenes (plus by-products). Since the fossil feedstock reserves have been continuing depletion and the steam cracking consumes intensive high temperature, high energy and generate large amounts of CO₂ greenhouse gas emissions. The biomass as a nonpetroleum resource has been attractive and go through in many reactions as a raw material, such as bioethanol, to produce ethylene and others petroleum based chemical. Lately, the catalytic ethanol dehydration is an alternative to the steam cracking process.

The diethyl ether is industrially synthesized by the reaction of ethanol with concentrate H₂SO₄ at the temperatures lower than 150°C, which is as shown in **Equation 1**.

Equation 1: Acid ether synthesis reaction



With the reversible reaction, the diethyl ether shall be distilled out of the reaction mixture before it reverts to ethanol to achieve the maximum ether yield. This process has been improved due to its low yield, by product formation and difficult on removal liquid catalyst. During the last few decades, the gas phase ethanol

dehydration to diethyl ether over solid heterogeneous catalyst including alumina, zeolites, transition metal oxide, and heteropolyacids is played in role interested in many researches.

2.2.3 Catalytic ethanol dehydration

The ethanol dehydration reaction is the direct conversion of ethanol to ethylene or diethyl ether by using the acid catalyst. The chemical equation of ethanol dehydration reaction occurs in parallel are shown in **Equation 2** and **3**.

Equation 2: Ethanol dehydration to ethylene



Equation 3: Ethanol dehydration to diethyl ether



The **Equation 2** is endothermic and prefers the moderate to high temperature at 320 °C and 500 °C, while **Equation 3** is exothermic and prefers the low to moderate temperature at ranged 150°C and 300 °C [41]. Besides, acetaldehyde can be formed as a side reaction or hydrogenation reaction in **Equation 4**.

Equation 4: Ethanol dehydrogenation to acetaldehyde reaction



2.3 Titanium oxide catalyst

Titanium dioxide (TiO₂) has been known as titanium oxide or titanium IV oxide or titania which is naturally occurring oxide of titanium. It is in a group of a versatile transition-metal oxide and widely uses in various applications related to catalysis, electronics, photonics, sensing, medicine, and controlled drug release. TiO₂ is recognized as a heterogeneous catalyst and contributed a high catalytic activity due to its strong metal support interaction, chemical stability, and acid-base property. TiO₂ as a catalyst has been revealed that TiO₂ improve the performance of catalysts in many reactions including dehydrogenation, water gas shift, and thermal catalytic decomposition.

2.3.1 Structure and property of titanium oxide

TiO_2 exists in three crystalline bulk structure which are anatase, rutile and brookite. The crystal structures of rutile, anatase and brookite titanium dioxide is showed as **Figure 3**. The rutile and anatase are arranged in the tetragonal structure which are the common types. The rutile crystalline size is always larger than the anatase phase. The Brookite is formed as an orthorhombic structure which is rarely utilized and seldom interest in any applications.

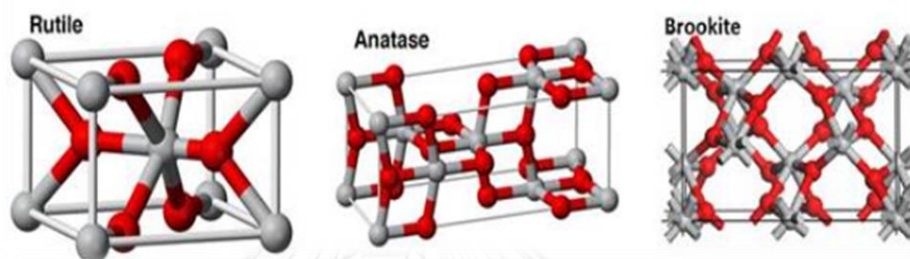


Figure 3: Crystal structure of rutile, anatase and brookite

The phase formation has been achieved by hydrothermal treatment at elevated temperatures with the appropriate reactants. The anatase and brookite crystalline transform phase to rutile crystalline at temperature 550 and 750 °C, respectively. Among of them, TiO_2 in anatase phase is frequently utilized as a catalyst support for metal heterogeneous catalyst since it provided the high specific surface area, strong interaction with metal nanoparticles and showed high actively on ethanol conversion. The interaction influences the catalytic activity and selectivity of the metal heterogeneous catalyst. Nevertheless, the instability of anatase transform to rutile structure is carry out at high temperature reactions.

Regarding to characterization in term of acidity, TiO_2 has highly ionic oxides with medium – strong Lewis acidity and weak Bronsted acidity. The anatase phase is rather stronger Lewis acidity and weaker Bronsted acidity than the rutile structure.

2.3.2 Synthesis of titanium oxide

TiO_2 structures have been prepared through various preparation methods, including the sol–gel method, hydrothermal method and solvothermal method.

2.3.2.1 The sol-gel method

The sol-gel method has been interested in the preparing for inorganic ceramic, glass materials and catalyst. The method is performing in the low temperature and cost effective. Additionally, sol-gel is favored in catalyst preparing due to its potential to fabricate catalysts with high purity, homogeneity, fine-scale and controllable morphology. As showed in Figure 4, the sol-gel method is the process of transforming sols (solid particles suspended in liquid) into gels (particulate networks of sols). The sol-gel procedure includes the process of hydrolysis and condensation.

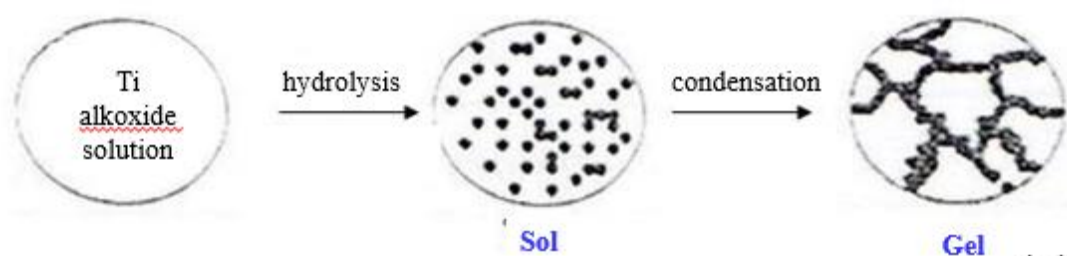
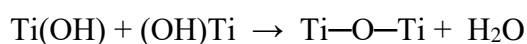
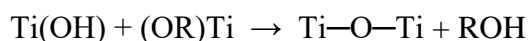
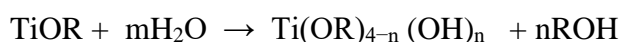


Figure 4 : General scheme of preparation by sol-gel method

In the presence of water, the alkoxy groups (OR) are replaced by the hydroxyl groups from water which is called hydrolysis. The metal hydroxide groups will link and generate a hydrated metal-oxide network which is called condensation. To obtain the crystalline TiO_2 particles, the TiO_2 network (gel) is further dried and calcined. The hydrolysis and condensation reaction is exhibited in **Equation 5**.

Equation 5: the hydrolysis and condensation



2.3.2.2 The solvothermal method

The solvothermal method has been interested in preparing ceramic materials and catalyst such as ZrO_2 , CeO_2 , and Fe_2O_3 . It has a better control on size, crystal phase, narrow size distribution and minimal agglomeration than hydrothermal process. As shown in **Figure 5**, all reagents including metal oxide precursor solution

and solvent the method are mixed together, placed into a Teflon-lined stainless steel autoclave, and heated [42]. The method is process in a closed reaction vessel inducing a decomposition or a chemical reaction between precursors in the presence of a solvent at a temperature higher than the boiling temperature of this solvent. The precipitates obtained should be washed and dried. The calcination process is not necessarily due to the high crystallinity of TiO_2 prepared by the solvothermal method [43]. The crystallization and growth of particles is controlled by parameters such as temperature, pressure, and time.

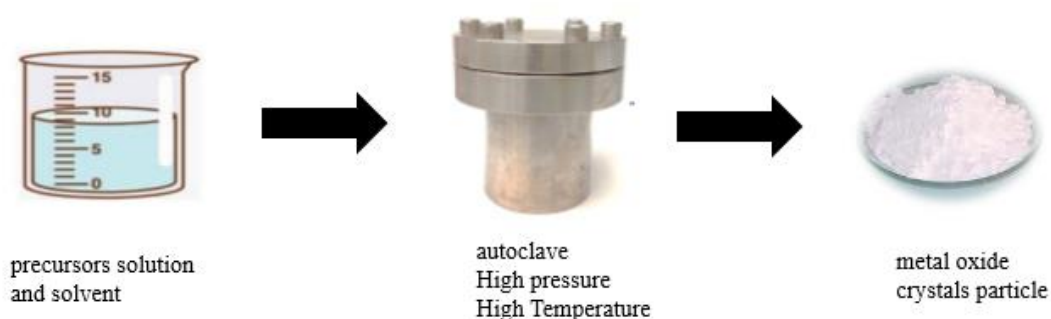


Figure 5: General scheme of preparation by solvothermal method

2.4. Tungsten oxide catalyst

Tungsten oxide plays an important role in a variety of electrochromic devices, catalysts and chemical sensors. The formula of tungsten trioxide is WO_3 . It exhibits several different crystal structures in different temperature ranges which are [tetragonal](#) structures at temperatures above $740\text{ }^\circ\text{C}$, [orthorhombic](#) structures from $330\text{ to }740\text{ }^\circ\text{C}$ and [monoclinic](#) structures from $17\text{ to }330\text{ }^\circ\text{C}$. The WO_3 structure is showed in **Figure 6** [44].

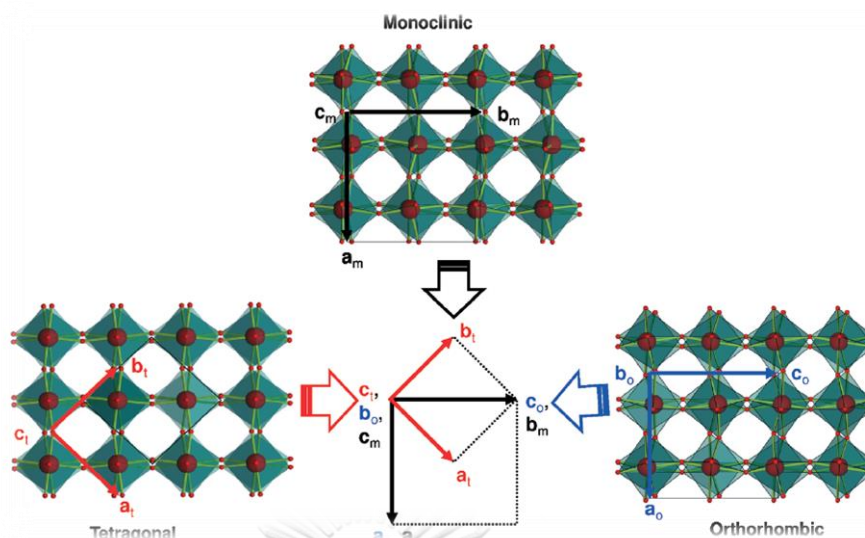


Figure 6: The crystal structure of tungsten observed during in situ heat treatment from temperature to 950°C

2.5 Palladium catalyst

Palladium (Pd) catalyst is one of the precious metal catalysts used to increase catalytic activity in a chemical reaction including dehydration and dehydrogenation. The activity of palladium catalyst depends upon the volume of palladium present in the catalyst, method of depositing palladium, type of support, and distribution of palladium on the support.

2.6. Literature Reviews

Lately, many researchers have been improving and developing the various catalysts in many reactions with various technique such as oxidation, dehydration and dehydrogenation to produce the desired valuable chemicals in many industries. They have been investigated by considering the behavior of catalyst in term of the active phase, metal support interaction, causes of deactivation. This chapter reviewed works on the catalyst spending in catalytic dehydration reaction which are attractive in field of heterogeneous catalyst while it has been used in many applications.

In general, the activity and selectivity of alcohol dehydration are controlled by the physical and chemical catalyst properties. Over the solid catalyst, the acids site and acid strength play an important role in ethanol dehydration. Among the catalyst

studied, the metal oxide as support catalysts such as CeO_2 , ZnO_2 , MgO , Al_2O_3 , Fe_2O_3 , Mn_2O_3 , TiO_2 and SiO_2 are widely investigated and used in many applications. Titania oxide is one of an acidic character and well known as a solid acid catalyst enhancing the performance of ethanol dehydration.

Sohn *et al.* (2002) [45] investigated the characterization of titanium sulfate supported on zirconia and activity for acid catalysis. The catalyst prepared by impregnation of powdered $\text{Zr}(\text{OH})_4$ with titanium sulfate aqueous solution followed by calcining in air at high temperature. The specific surface area and acidity of catalysts increased in proportion to the titanium sulfate content up to 5 wt % of $\text{Ti}(\text{SO}_4)_2$. The $\text{Ti}(\text{SO}_4)_2/\text{ZrO}_2$ which is incorporate of titanium component exhibited the higher catalytic activity for the 2-propanol dehydration reaction than $\text{Zr}(\text{SO}_4)_2/\text{ZrO}_2$ without titanium.

Zhang *et al.* (2008) [46] learned the gamma alumina catalyst to perform in ethanol dehydration. The gamma alumina promoted with TiO_2 catalyst can improve the ethylene selectivity from 90.1% to 99.4% at 500°C.

Wu *et al.* (2009) [47] examined the TiO_2 -supported zeolite carried out the ethanol dehydration to ethylene. The TiO_2 anatase as an acceptor of electrons enhance the moderate acid site on TiO_2 -supported zeolite. The composite catalyst showed the much better catalytic performance than the aluminosilicate zeolite or TiO_2 in the ethanol dehydration to ethylene.

Ladera *et al.* (2015) [48] investigated on two heteropoly acids (HPAs) which are $\text{H}_3\text{PW}_{12}\text{O}_{40}$ (HPW) and $\text{H}_4\text{SiW}_{12}\text{O}_{40}$ (HSiW) deposited on TiO_2 to perform in the methanol dehydration reaction to dimethyl ether. The effect of the HPA loading on TiO_2 to produce dimethyl ether has been correlated with the structure and acid properties of the catalyst. The optimum loading for both TiO_2 -supported HPW and HSiW is 2.3 KU nm^{-2} . All catalysts exhibited very high dimethyl ether productivities and high methanol conversion rates at temperature as low as 413 K. These catalysts are more active than bulk HPA for dehydration of methanol to dimethyl ether.

Héroguel *et al.* (2017) [49] demonstrated the deposition catalysts coated by non-hydrolytic sol gel to improve the catalyst selectivity and stability. The deposition of

TiO₂ on SBA-15 generated the medium strength Lewis acid sites, which catalyzed 1-phenylethanol dehydration at high selectivity and decreased deactivation rates compared to typically used HZSM-5.

Recently, the addition of promoters over solid acid catalyst is one strategy to increase the catalytic activity by facilitated the desired reaction or increased the catalyst selectivity by reducing the unwanted processes. The tungsten oxide metal (WO₃) is well known as promoter metal oxide exhibited the high catalyst activity in various reaction due to the created of active site and increased of the surface areas.

Sohn *et al.* (2000) [50] investigated the characterization of tungsten oxide supported on TiO₂ prepared by drying a mixed solution of ammonium metatungstate with Ti(OH)₄ and calcining in air for 2-propanol dehydration and cumene dealkylation. The interaction between tungsten oxide and titania influences the physicochemical properties of catalysts with calcination temperature. The specific surface area and acidity of catalysts increase in proportion to the tungsten oxide content up to 20 wt%. The addition of only a small amount of tungsten oxide (2 wt%) to titania, both the acidity and acid strength of the catalyst increases remarkably, showing the presence of Bronsted and Lewis acid sites on the surface of WO₃/TiO₂ catalyst.

Pae *et al.* (2004) [51] studied the catalytic activity of 10-NiO-TiO₂/WO₃ in the 2-propanol dehydration reaction. When adding the tungsten oxide on titania up to 25 wt%, the specific surface area and acidity of catalysts increased in proportion to the tungsten oxide content due to the interaction between tungsten oxide and titania.

Lebarbier *et al.* (2006) [52] investigated the relations between structure, acidity, and activity of WO_x modified on titanium oxyhydroxide, and titanium oxide. Both catalysts containing W up to 4.4 atoms of W/nm² were prepared by the impregnation of titanium oxyhydroxide dried at 393 K or titanium oxide calcined at 773 K. Both catalysts exhibited similar surface structure, acidity, and catalytic activity. The Bronsted acidity was detected for W > 1.3 atoms of W/nm² and increased steadily with increasing W surface density and directly related to catalytic activity for 2-propanol dehydration for both catalysts.

Kourieh *et al.* (2011) [53] investigated the various tungsten oxide loadings from 1 to 20 wt.% on ZrO₂ prepared by co-precipitation. The amount Bronsted sites increased with an increasing the loading WO₃. The catalytic reaction of cellobiose disaccharide hydrolysis showed a better catalytic performance on the highest WO₃ loaded catalysts.

Phung *et al.* (2015) [26] examined the effect of tungsta over titania and zirconia oxide under ethanol dehydration with 1.43 h⁻¹ WHSV at 423 - 773 K. The addition of WO₃ to both TiO₂ and ZrO₂ leads the strong Bronsted acid sites that are represent the active sites in the reaction and inhibits the formation of acetaldehyde.

Dalil *et al.* (2015) [10] studied the acrolein selectivity of glycerol dehydration over 13.9 wt% WO₃/TiO₂. They achieved high values of acrolein selectivity by exceeding 73% after 6 h time-on-stream.

Cecilia *et al.* (2016) [19] investigated the tungsten oxide and tungsten oxide phosphorous supported on a zirconium and doped on mesoporous SBA-15 silica The catalyst is prepared by sol-gel followed by incipient wetness impregnation method before testing in the dehydration of glycerol to acrolein. When incorporate WO₃ to SiO₂/ZrO₂ support, it improved the total acidity, Bronsted acid sites and stability catalyst over the glycerol dehydration. The 20W catalyst displayed the highest glycerol conversion and acrolein yield values (97% and 41% after 2 h, and 90% and 38% after 8 h of TOS, respectively, at 325 °C) which may be related to the existence of WO₃ phases on catalyst surface.

Said *et al.* (2016) [54] investigated the catalytic performance of tungsten oxide during the dehydration of isopropyl and methyl alcohols. The WO₃ is more active toward isopropanol dehydration than methanol dehydration. Moreover, it is found that the reaction mechanism and yield of propene and dimethyl ether produced from alcohols are controlled by the strength of acids sites.

Hong *et al.* (2016) [55] suggested on the effect of Bronsted acidity of WO₃/ZrO₂ catalysts in dehydration reactions of C3 and C4 alcohols. WO₃/ZrO₂ catalysts were prepared by impregnation method. The catalytic activity was maximized when loading WO₃ at 20 wt% on ZrO₂ catalysts. The Bronsted acidity is affected to the

catalytic activity over the dehydration reaction. In addition, the propene selectivity increases with an increasing Bronsted acidity while the iso-butene, 1-butene, cis-2-butene and trans-2-butene selectivity were not affected by Bronsted acidity at 200 and 250 °C.

Cunha *et al.* (2017) [56] investigated the effect of texture and acidic properties of bimetallic Cu-(WO₃ or ZrO₂)/Al₂O₃ catalysts carried out in glycerol dehydration to acetol. The metal supported on Al₂O₃ were prepared by wetness impregnation and calcined at 800°C. Cu-Zr/Al catalyst showed a greater acetal selectivity. Cu-W/Al catalyst promoted the hydrogenation reaction by forming 1,2 propanediol. The results showed that an acidic plays a key role in the reaction.

However, besides the active metals, one needs to consider on the properties of a wide variety of supports themselves. The variations of support characteristics mostly arise from different preparation methods. There are many reports focusing on using different methods to prepare various metal oxide supports including the sol-gel and solvothermal methods.

Wannaborworn *et al.* (2015) [28] inspected the ethanol dehydration to ethylene over alumina catalysts prepared by solvothermal and sol-gel methods. The experiments were performed at temperature ranged 200 to 400°C under atmospheric pressure using a feed composition of 99.95% ethanol. The alumina synthesized by solvothermal method exhibited the highest activity due to the higher surface area and larger amount of acid site, especially the ratio of weak/strong acid strength. The results confirmed that the textural and acidic properties is affect to catalytic dehydration.

Go´mez-gutie´rrez *et al.* (2015) [30] examined the solvothermal synthesis of nickel-tungsten sulfides catalyst for 2-propanol dehydration. The solvothermal method influenced the morphology and texture of catalyst and catalytic performance. The catalytic 2-propanol dehydration was selective to propene in 100% at 250 °C for the sample with 0.7 of atomic ratio of Ni/(Ni + W).

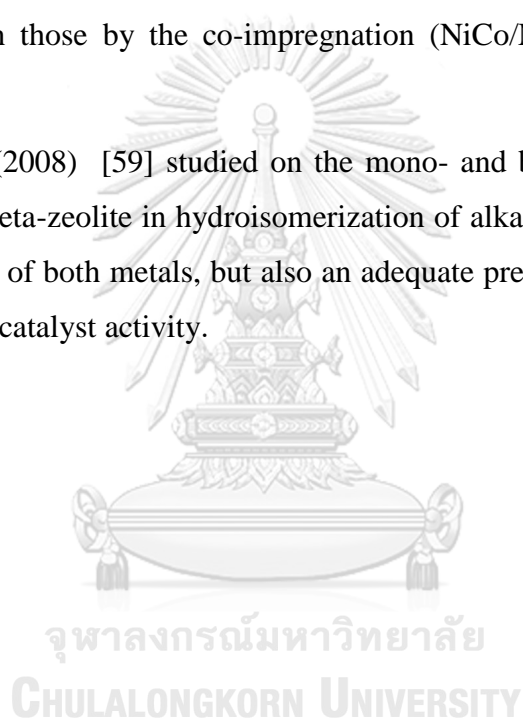
From the literature review, the bimetallic catalysts have been proven to be important for many catalyst applications. The presence of Pd oxides have been

known to be an active site in the dehydration reaction [57]. In addition, the different impregnated preparation technique is affected to the interaction between metal and promoter and/or metals and support catalyst.

Jinshuang *et al.* (2013) [58] examined that Pd/Al₂O₃–TiO₂ catalyst showed higher catalytic activity than Pd/TiO₂ in ethanol oxidation.

Jing *et al.* (2019) [40] discovered that the metal impregnation technique affect the structure and catalyst performance. They revealed that the catalyst prepared by first Co precursor impregnation (Ni/Co/MgO) resulted in the stronger catalytic activity and stability than those by the co-impregnation (NiCo/MgO) in steam reforming reaction.

Roldan *et al.* (2008) [59] studied on the mono- and bi- metallic (Pt and/or Pd) impregnated on beta-zeolite in hydroisomerization of alkanes. They claimed that not only the presence of both metals, but also an adequate preparation method providing an improving the catalyst activity.



CHAPTER III – EXPERIMENTAL

This chapter explains the laboratory procedures, including the support catalyst preparation and modified with metal oxide by impregnation, the characterization of catalyst and the experimental for ethanol dehydration reaction.

3.1 Catalyst preparation

3.1.1 Chemicals

The chemical used to synthesis all catalysts in this research were shown in

Table 1.

Table 1: The chemicals used for catalyst preparation

Chemical	Formula	Supplier
Titanium ethoxide (Ti ~ 20%)	$Ti_4(OCH_2CH_3)_{16}$	Aldrich
Ethanol (99.99%)	C_2H_5OH	Merck
Titanium (IV) n-butoxide (97%)	$C_{16}H_{36}O_4Ti$	Aldrich
1,4 – butanediol	$C_4H_{10}O_2$	Aldrich
Tungsten (VI) chloride	WCl_6	Aldrich
Tetraamminepalladium (II) chloridemonohydrate (99.99%)	$Pd(NH_3)_4Cl_2 \cdot H_2O$	Aldrich

3.1.2 Preparation of TiO_2 supports and WO_3/TiO_2 catalysts

The TiO_2 catalyst supports were synthesized by performing with two different methods which are sol-gel and solvothermal methods [60]. To prepare TiO_2 support catalyst by the sol-gel method, the titanium ethoxide was used as the precursor. Firstly, the precursor with excess ethanol dissolved in deionized water with the molar ratio of 165. The solution was stirred under 20 rpm/min at room temperature for 2 h. The white precipitates of hydrous oxides formed instantly and separated by centrifugation. The sample was then washed with ethanol at least 5 times and then performed centrifugation. The sample was dried and calcined at $450^\circ C$ for 2 h at the

heating rate of 10 °C/min. Finally, the white powder of TiO₂ prepared by the sol–gel method was obtained and denoted as TiO₂-SG.

To synthesis TiO₂ support catalyst by solvothermal method, 25 g of titanium (IV) n-butoxide (TNB) was used as the precursor. Firstly, TNB was suspended in 100 ml of 1,4-butanediol in a test tube and placed in the autoclave. The autoclave was completely purged with nitrogen at pressure of 30 bars before increasing the temperature to 320 °C at a heating rate of 2.5 °C/min and following held at 320 °C for 6 h. Autogenous pressure during the reaction gradually increased as the temperature increased. The autoclave was next cooled down to room temperature. The white powder was collected, and then washed with ethanol followed by centrifugation at least 5 times. The sample was dried over night at 110°C and finally the white powder of TiO₂ prepared by the solvothermal method was obtained and denoted as TiO₂-SV.

The TiO₂-SG and TiO₂-SV catalyst supports obtained as mentioned above were implemented with an incipient wetness impregnation process to provide the tungsten (W) loading of 13.5 wt%. It was accomplished by using the tungsten (VI) chloride as a precursor, followed by drying the catalyst sample overnight at 110 °C and calcined at 400°C with a heating rate of 10 °C/min for 3 h. Consequently, the obtained WO₃/TiO₂ catalysts are denoted as WO₃/TiO₂-SG and WO₃/TiO₂-SV.

3.1.3 Preparation of Pd doped-WO₃/TiO₂ catalysts

The TiO₂ supports catalyst were synthesis by solvothermal methods according to the practice as mentioned in item 3.1.2. After synthesis the TiO₂-SV support catalysts, the support catalysts were further modification with tungsten (W) and palladium (Pd) by incipient wetness impregnation with sequence impregnation and co-impregnation technique as follows.

Preparation of sequence impregnation catalyst (Pd/W/TiO₂): Firstly, The Tungsten (W) precursor and Palladium (Pd) precursor were firstly dissolved in deionized water to obtain W at 13.5 wt% and Pd at 0.5 wt%. Secondly, the tungsten (VI) chloride solution (W 13.5 wt%) was dropped into TiO₂ catalyst. Afterwards, the impregnated sample was dried for overnight at 110 °C and calcined in air at 500°C with a heating rate of 10 oC/min for 3 hrs. The white power of W/TiO₂ catalyst was obtained. Thirdly, tetraamminepalladium (II) chloride monohydrate solution (Pd 0.5

wt%) was dropped into W/TiO₂ catalyst. Afterward, the impregnated sample was dried for overnight at 110 °C and calcined in air at 500°C with a heating rate of 10 °C/min for 3 h. Finally, the white sample of Pd/W/TiO₂ was provided.

Preparation of sequence impregnation catalyst (W/Pd/TiO₂): The synthesis of W/Pd/TiO₂ catalyst was the same as the synthesis of Pd/W/TiO₂ catalyst as mention above except for the sequence of the first step and second step shall be exchanged.

Preparation of co-impregnation catalyst (PdW/TiO₂): Firstly, both tetraamminepalladium (II) chloride monohydrate solution and tungsten (VI) chloride solution was dissolved together in deionized water to obtain W at 13.5 wt% and Pd at 0.5 wt%. Secondly, those precursor solutions were dropped into TiO₂ catalyst. Thirdly, the impregnated sample was dried over night at 110 °C and followed by calcined in air at 500 °C with a heating rate of 10 °C/min for 3 h. Finally, the sample of PdW/TiO₂ catalyst was obtained.

3.2 Catalyst characterization

3.2.1 X-ray diffraction (XRD)

The SIEMENS D-5000 X-ray diffractometer using CuK α radiation ($\lambda = 1.54439 \text{ \AA}$) was used to determine the crystalline phase structure of supports and catalysts. The crystalline domain sizes were calculated from the Scherrer equation. The supports and catalysts were scanned at a rate of $2.4^\circ \text{ min}^{-1}$ in the range 2θ from 20 to 80 degrees with the resolution of 0.02° .

3.2.2 Nitrogen Physisorption

The adsorptiometer Micromeritics ASAP 2010 automated system instrument was used to determine surface area (BET method), pore volume/diameter and pore size distribution (BJH method) by nitrogen gas adsorption-desorption at liquid nitrogen temperature at -196°C .

3.2.3 Temperature-programmed desorption of ammonia (NH₃-TPD) and carbon dioxide (CO₂-TPD)

The Micromeritics Chemisorb 2750 Pulse chemisorption system instrument was employed to identify the acidity and basicity on supports and catalysts. The 0.03 g quartz wool and 0.05 g catalysts were packed in a quartz tube and pretreated at

500°C under He flow for 1 hr. Next, the catalyst surface was saturated with NH₃ or CO₂ in He at 40°C for 30 min. Then, the excess adsorbed gas (the physisorbed NH₃ or CO₂) was purged with He until the baseline was constant. Afterwards, the catalysts were heated from 40°C to 500°C at a heating rate of 10°C/min to desorb NH₃ or CO₂. The amount of NH₃ or CO₂ in effluent was measured via the thermal conductivity detector (TCD) signal as a function of temperature.

3.2.4 Scanning electron microscopy (SEM) and energy dispersive X-ray spectroscopy (EDX)

The SEM model JEOL mode JSM-6400 and EDX with stand Link Isis series 300 program were operated for analysis the morphology, element composition and distributions over supports and catalysts.

3.2.5 X-ray fluorescence spectrometer (XRF)

The Olympus model Vanta M Series was performed to determine the amount of tungsten loading on catalysts. XRF spectrometer has an X-ray tube with Rh anode. The spectra were collected during 120 s, with the tube operating with a current of 100 µA and a voltage of 40 KV.

3.2.6 X-ray photoelectron spectroscopy (XPS)

The AMICUS spectrometer with MgK α X-ray radiation at voltage 15kV and current of 12 mA was used to determine the binding energy and chemical oxidation states of catalysts.

3.3 Reaction study in dehydration of ethanol

The catalytic ethanol dehydration reaction was carried out in gas phase at atmospheric pressure in the fixed bed glass reactor. The reaction was investigated for all catalysts using the apparatus as exhibited in **Figure 7**.

3.3.1 Chemicals and reagents

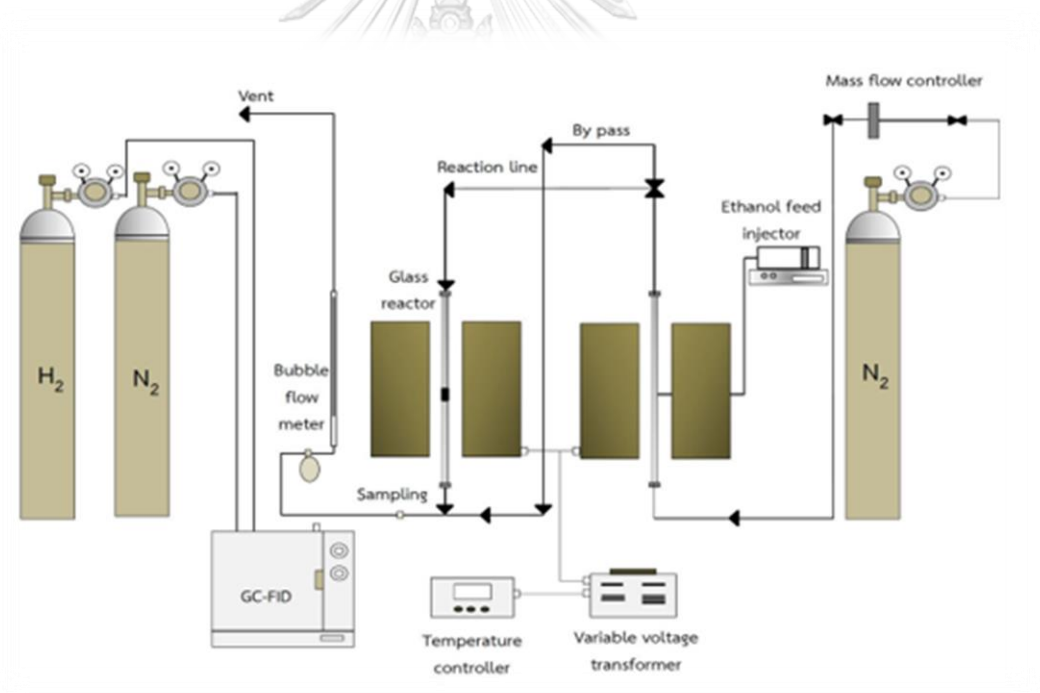
The chemicals and the reagents employed in the ethanol dehydration reaction in present research were displayed in **Table 2**.

Table 2: The chemicals for catalytic ethanol dehydration reaction

Chemical and Reagents	Supplier
Hydrogen gas ultra-high purity of 99.99%	Linde
Nitrogen gas ultra-high purity of 99.99%	Linde
Air zero balance nitrogen	Linde
Absolute ethanol purity of 99.99%	Merck

3.3.2 Instrument and apparatus

The system of the ethanol dehydration including the equipment to carry out the catalytic ethanol dehydration reactions were shown in **Figure 7**. The set up experimental for the reaction are shown as follows:

**Figure 7:** Process diagram of the ethanol dehydration system

- 1) Reactor: In part I, the borosilicate reactor tube was made from glass tube with an inside diameter of 0.7 cm and length of 33 cm. length. In part II, the borosilicate reactor tube has an inside diameter of 1 cm and length of 49.5 cm.
- 2) Syringe pump: Liquid ethanol is injected to the vaporizer by syringe pump.

- 3) Vaporizer: Liquid ethanol was vaporized in vaporizer at temperature of 120°C.
- 4) Furnace and heating cable: The reactor and vaporizers are heated by furnace. The temperature of the furnace was controlled by temperature controller with the maximum voltage of 220 volt. For heating cable, it was warped with the line at outlet of reactor. The heating cable was used to prevent the condensation of water dehydrated from reaction.
- 5) Temperature controller: The temperature of furnace was established a set point at any temperatures in range between 200°C to 400°C. The temperature controller is connected to thermocouple attached to the reactor and a variable voltage transformer.
- 6) Gas controlling system: The flow rate of nitrogen (carrier gas) and air are adjusted by mass flow controller. The system is set up with a pressure regulator and an on-off valve to control the gas flow.
- 7) Gas chromatography (GC): A gas chromatography equipped (Shimadzu GC14B) with flame ionization detector (FID) and DB-5 capillary column. It is used to analyze the feed and product including ethanol, ethylene, diethyl ether, acetaldehyde etc. The operating condition for gas chromatography was described in the **Table 3**.

Table 3: Operation conditions for gas chromatograph

Gas chromatograph	Shimadzu GC14B
Detector	FID
Column	DB5
Maximum temperature	350 °C
Carrier gas	N ₂ (99.999%)
Column temperature	
- Initial (°C)	40
- Final (°C)	40
Injector temperature (°C)	150
Detector temperature (°C)	150
Analyzed gas	ethanol, ethylene, acetaldehyde, diethyl ether

3.3.3 Ethanol dehydration reaction procedure

The ethanol dehydration reaction was performed in a fixed-bed continuous flow micro-reactor at temperature varied from 200 to 400 °C. Firstly, 0.01 g of quartz wool and 0.05 g (part I), 0.1 g (part II) of catalysts were packed in the middle of reactor. The catalyst was preheated by flowing N₂ with a flow rate of 60 ml/min at 200 °C for 1 h under atmospheric pressure to remove the moisture and impurity on surface of catalyst prior to the reaction. Afterwards, the reaction was started by feeding vaporized ethanol and N₂ as a carrier gas. The ethanol flow rate was controlled at 1.45 ml/h (WHSV = 22.9 g_{ethanol}g_{cat}⁻¹. h⁻¹) and 0.397 ml/h (WHSV = 3.13 g_{ethanol} g_{cat}⁻¹. h⁻¹) in the research in part I and II respectively. After reaching steady-state condition, the reaction product compositions at reactor effluent were analyzed by a Shimadzu gas chromatography (GC14B) with flame ionization detector (FID) using DB-5 capillary column.

CHAPTER IV – RESULTS AND DISCUSSION

In this chapter, the results and discussion of WO_3/TiO_2 catalysts using titania derived from sol-gel and solvothermal methods with palladium modification are expressed on the catalyst characterization and activities. All catalysts were prepared as revealed in chapter III and characterized by various techniques including XRD, XRF, SEM, EDX, NH_3 -TPD, CO_2 -TPD, N_2 -physisorption and XPS. All catalysts were studied on the catalytic performance in fixed-bed tubular reactor with the ethanol dehydration reaction under vapor phase of ethanol at temperature between 200 °C and 400 °C. The results and discussion are divided into 2 parts. The first part described on the characteristics and catalytic activity of WO_3/TiO_2 catalysts using titania derived from sol-gel and solvothermal methods. The TiO_2 support catalyst was incipient wetness impregnated with tungsten loading of 13.5 wt%. The second part is to develop the W/TiO_2 catalyst, which gave the best catalyst performance in part one by palladium impregnation of 0.5 wt%. The catalysts were then comparison on their characteristics and catalytic activity.

4.1 The catalytic ethanol dehydration to ethylene and diethyl ether over the WO_3/TiO_2 prepared by sol-gel and solvothermal methods

4.1.1 Catalyst characterization

The XRD patterns of both TiO_2 supports and WO_3/TiO_2 catalysts are demonstrated in **Figure 8**. When compared the intensity of XRD peaks between TiO_2 -SG and TiO_2 -SV, they exhibited the similar XRD patterns having the strong diffraction peaks located at 2θ degree of 25° (major), 38 ° and 48 °, which are assigned to the tetragonal anatase phase of crystalline TiO_2 [61, 62]. When the support was impregnated with 13.5 wt % of tungsten, the XRD patterns were also similar with those of titania supports. The intensities were lower indicating the smaller crystallite size of WO_3/TiO_2 catalysts than the TiO_2 supports. Furthermore, the low intensity peaks were noticed at 24° and 34° for WO_3/TiO_2 -SG and WO_3/TiO_2 -SV catalysts, which were designated to the formation of the WO_3 crystals with tetragonal phase [63, 64]. Based on the Scherrer equation, the average crystalline size

of $\text{WO}_3/\text{TiO}_2\text{-SG}$ was smaller than $\text{WO}_3/\text{TiO}_2\text{-SV}$ as established in **Table 4**, where the TiO_2 crystalline size were in the range of 10.7 to 14.3 nm indicating the mesoporous structure.

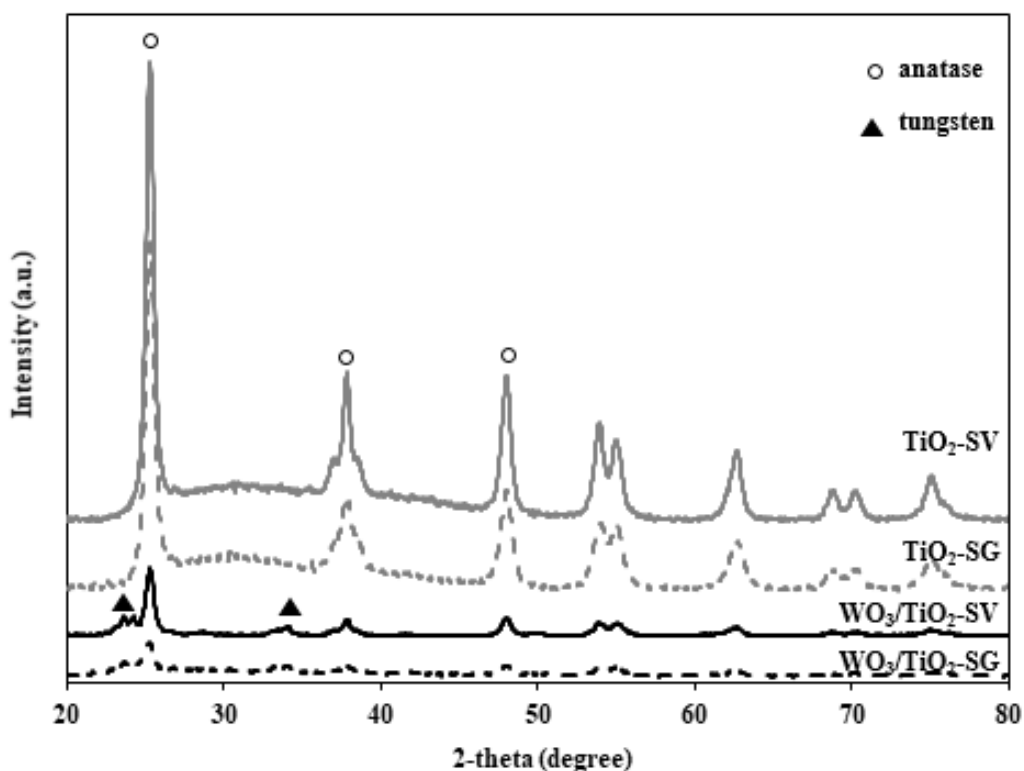


Figure 8: X-ray powder diffraction patterns of supports and catalysts

The morphology of TiO_2 supports and WO_3/TiO_2 catalysts prepared by different methods showed the different morphologies. The $\text{TiO}_2\text{-SG}$ formed irregular shape particles, while $\text{TiO}_2\text{-SV}$ formed small agglomerated spherical and porous particles. When loading of tungsten into $\text{TiO}_2\text{-SG}$ and $\text{TiO}_2\text{-SV}$ supports, both samples exhibited more porous particles. This suggested that the presence of tungsten into TiO_2 resulted in an increase of porosity. The EDX mapping of $\text{WO}_3/\text{TiO}_2\text{-SG}$ and $\text{WO}_3/\text{TiO}_2\text{-SV}$ catalysts are illustrated in **Figure 9**. It shows the elemental distribution of Ti, O, and W dispersing on the external surface of catalysts. The tungsten was well dispersed at the outer surface of both $\text{TiO}_2\text{-SG}$ and $\text{TiO}_2\text{-SV}$. The weight ratios of W/Ti are also listed in **Table 5**. The amount of tungsten present at outer surface of $\text{TiO}_2\text{-SG}$ were larger than $\text{TiO}_2\text{-SV}$. Nevertheless, according to the XRF analysis the

amount of tungsten in the bulk of TiO₂-SV catalyst was larger than TiO₂-SG showing that the distribution of tungsten for TiO₂-SV catalyst were mostly located inside the pore of catalyst.

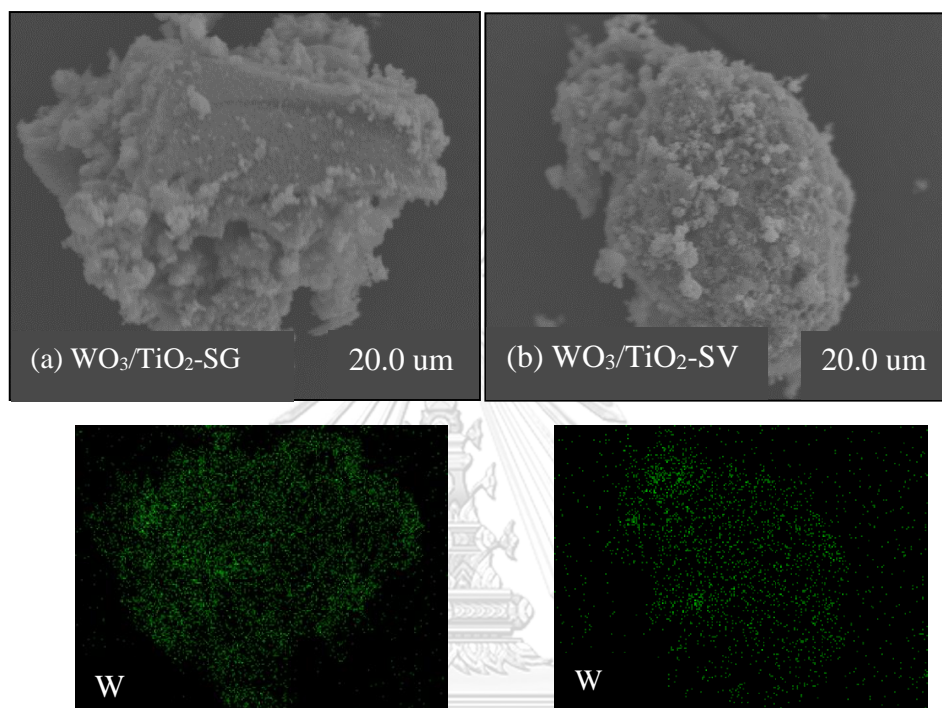


Figure 9: Elemental distribution by EDX mapping for (a) WO₃/TiO₂-SG and (b) WO₃/TiO₂-SV catalyst

Table 4: Physical properties of TiO₂ supports and catalysts

Sample	S _{BET} ^a (m ² /g)	Pore Volume ^b (cm ³ /g)	Pore Diameter ^c (nm)	Crystallite TiO ₂ size ^d (nm)	Crystallite WO ₃ size ^d (nm)	W content ^e (wt %)
TiO ₂ -SG	73	0.13	4.8	12.4	-	-
TiO ₂ -SV	85	0.42	16.5	15.3	-	-
WO ₃ /TiO ₂ -SG	61	0.11	5.1	10.7	6.1	16.3
WO ₃ /TiO ₂ -SV	78	0.30	13.0	14.3	9.0	18.9

^a Measured by BET method, ^{b,c} Measured by BJH desorption method, ^d measured by XRD using the Scherrer equation, ^e measured by XRF

Table 5: Elemental compositions (wt%) on external surface of catalysts obtained from EDX

Sample	O	Ti	W	Cl	W/Ti
TiO ₂ -SG	44.67	55.33	n.a.	n.a.	n.a
TiO ₂ -SV	44.37	55.63	n.a.	n.a.	n.a
WO ₃ /TiO ₂ -SG	30.71	35.17	33.84	0.28	0.96
WO ₃ /TiO ₂ -SV	39.00	48.25	12.36	0.39	0.26

The BET surface area (S_{BET}), pore volume and pore size diameter of TiO₂ supports and WO₃/TiO₂ catalysts analyzed by N₂ physisorption are shown in **Table 4**. The results exposed that the TiO₂-SG exhibited smaller surface area (73 m²/g) and pore volume (0.13 cm³/g) than those of TiO₂-SV BET surface area (85 m²/g) and pore volume (0.42 cm³/g). The large surface area essentially enhances catalytic activity in ethanol dehydration by increasing possibility of ethanol to attach on the acid site [28]. Besides, the BET surface area, pore volume and pore size diameter decreased with the presence of tungsten due to some pore blockage [65].

The N₂ adsorption-desorption isotherms at -196°C for the TiO₂ supports and WO₃/TiO₂ catalysts is presented in **Figure 10**. The results revealed the Type IV adsorption isotherms with the H1 hysteresis loop indicating the mesoporous structure according to the IUPACS. After incorporated the tungsten to obtain WO₃/TiO₂-SG and WO₃/TiO₂-SV, it was realized that the Type IV isotherm was still observed. The hysteresis loop moved toward lower pressure for WO₃/TiO₂-SG and WO₃/TiO₂-SV suggesting that the tungsten addition onto TiO₂ support catalyst resulted in decreased pore volume. The pore size distribution (PSD) for the TiO₂ support catalysts and WO₃/TiO₂ catalysts are shown in **Figure 11**. All catalysts were in the average pore diameter range of 2-50 nm classified as mesoporous particles. The WO₃/TiO₂ showed the narrower pore size distribution than that of TiO₂-SV. The average pore sizes for all samples calculated by Barrett-Joyner-Halenda (BJH) are shown in **Table 4**, which were corresponding to the results from N₂ adsorption – desorption isotherm as seen from **Figure 10**.

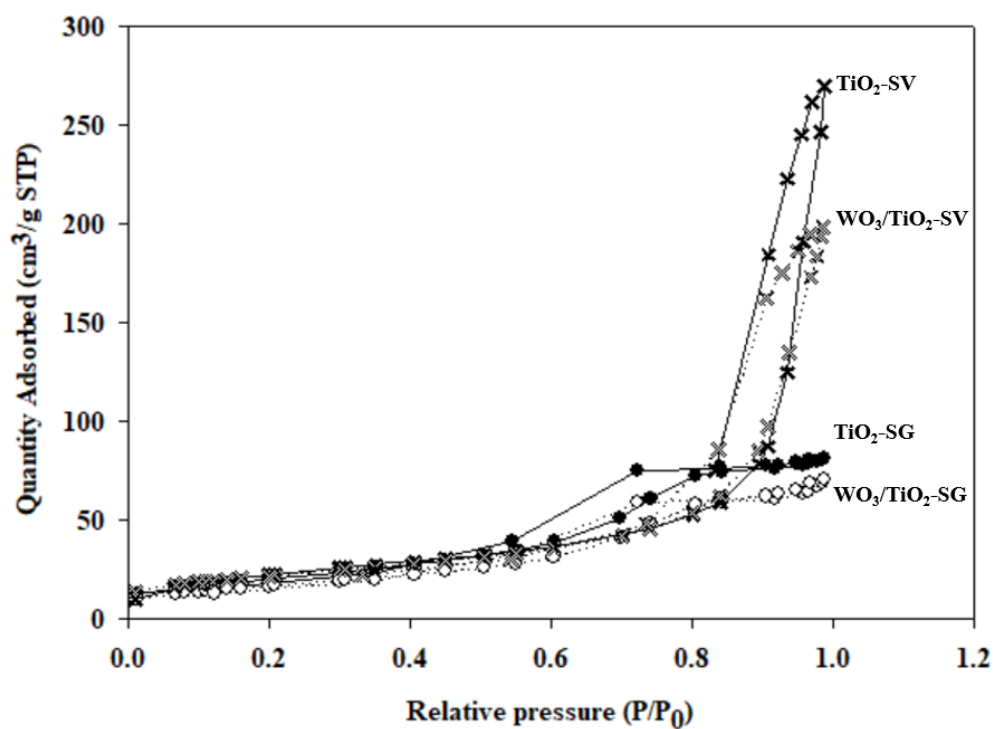


Figure 10: Nitrogen adsorption-desorption isotherms for supports and catalysts

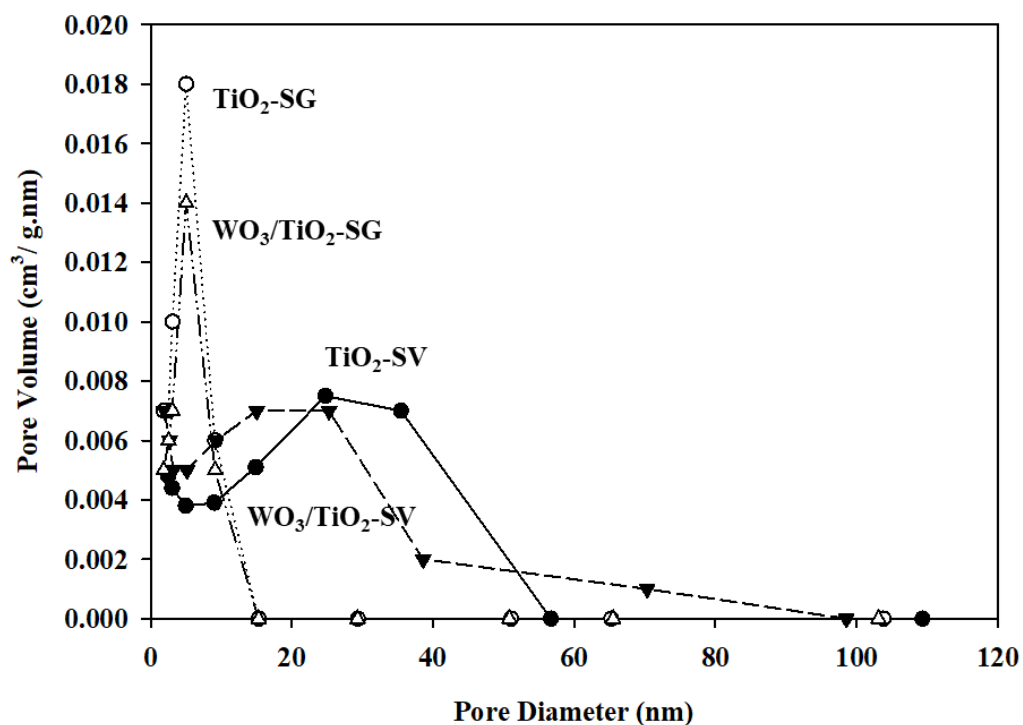


Figure 11: The pore size distribution for supports and catalysts

It is well known that acidity of catalyst is the key factor relating to the catalytic activity for ethanol dehydration process. The acidity of supports and catalysts was evaluated by NH_3 -temperature-programmed desorption as displayed in **Figure 12**. As observed, the NH_3 -TPD profiles for all samples displayed the broad desorption peaks in range of 150-500 °C. The NH_3 -TPD desorption temperature of acidic sites are classified into 3 classifications. The desorption of NH_3 between 150 and 300 °C is designated to weak acidic sites, whereas the desorption between 300 and 450 °C is moderate acid sites and the desorption above 450 °C is strong acid sites [66].

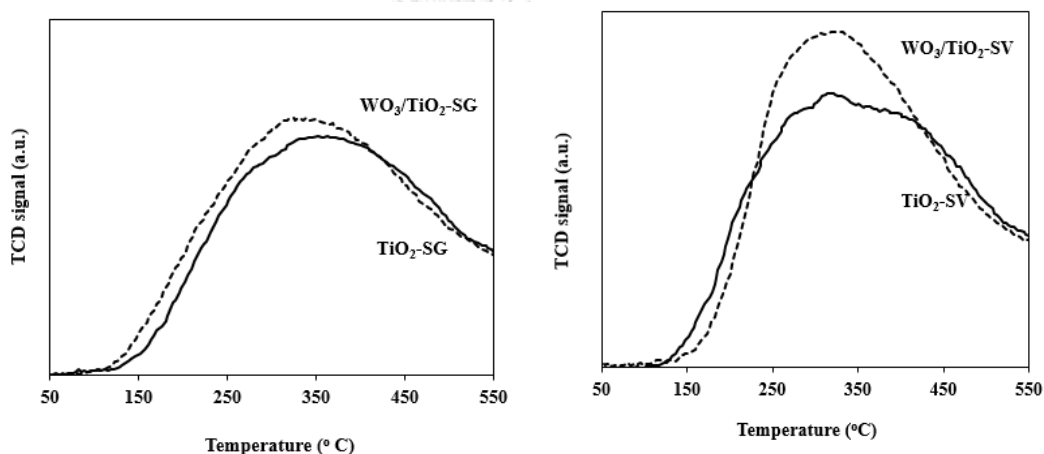


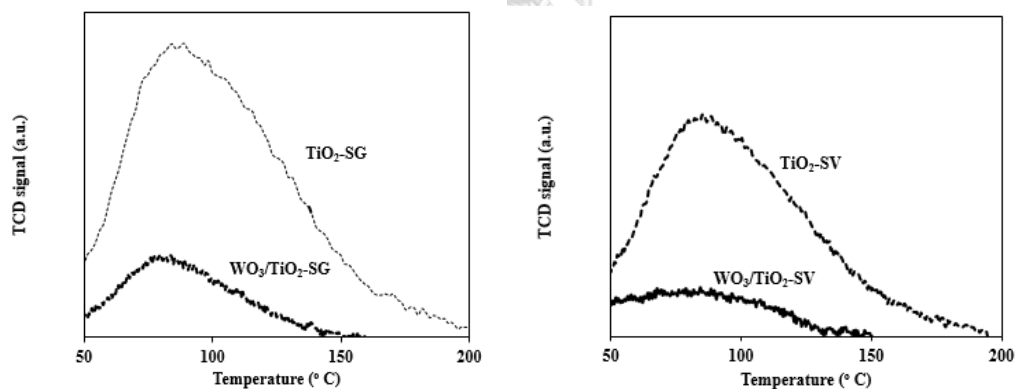
Figure 12: NH_3 -TPD profiles of TiO_2 supports and WO_3/TiO_2 catalysts

The TiO_2 -SG presented the lower amount of acid site than the TiO_2 -SV as presented in **Table 6**. As observed with tungsten loading on both supports, it showed significant increase in weak and total acid sites for both WO_3/TiO_2 -SG and WO_3/TiO_2 -SV catalysts, which is essential for enhancing the ethylene and diethyl ether [67, 68]. Furthermore, it can be detected that the WO_3/TiO_2 -SV catalyst exposed the highest amount of total acid sites at 3645 $\mu\text{mol/g}$ cat.

Table 6: The amount of surface acidity of supports and catalysts measured by NH₃-TPD

Sample	NH ₃ Desorption (μmol/g cat)			Total Acidity (μmol/g cat)
	Weak	Medium	Strong	
TiO ₂ -SG	895	662	717	2274
TiO ₂ -SV	1152	1232	841	3224
WO ₃ /TiO ₂ -SG	1030	1054	681	2765
WO ₃ /TiO ₂ -SV	1558	1263	823	3645

When considering the CO₂-TPD profiles as revealed in **Figure 13**, the desorption peak exposed the narrow desorption in the temperature range of 50-200 °C. Both TiO₂ supports showed the low temperature CO₂ desorption around 87°C delegated to weak basic sites [69, 70]. The impregnated of tungsten into the support catalysts resulted in a decrease of peak intensity around 80°C. Besides, it discovered that WO₃/TiO₂-SG had the higher amount of basicity site than WO₃/TiO₂-SV as presented in **Table 7**.

**Figure 13:** CO₂-TPD profile of TiO₂ supports and WO₃/TiO₂ catalysts**Table 7:** The amount of surface basicity of supports and catalysts measured by CO₂-TPD

Sample	CO ₂ Desorption (μmol/g cat)		Total Basicity (μmol/g cat)
	Weak	Medium/Strong	
TiO ₂ - SG	27	4	31
TiO ₂ -SV	18	2	20
WO ₃ /TiO ₂ - SG	6	1	7
WO ₃ /TiO ₂ - SV	4	0	4

In **Table 8**, it showed the amounts of carbon deposition after reaction obtained by EDX measurement. The $\text{WO}_3/\text{TiO}_2\text{-SG}$ and $\text{WO}_3/\text{TiO}_2\text{-SV}$ exhibited higher amounts of carbon deposition than those of the TiO_2 supports due to their higher acidity. It is recognized that high acidity yields high amount of carbon deposition on catalysts.

Table 8: The amount of carbon elemental compositions (wt%) on external surface supports and catalysts after reaction obtained from EDX

Sample	$\text{TiO}_2\text{-SG}$	$\text{TiO}_2\text{-SV}$	$\text{W}/\text{TiO}_2\text{-SG}$	$\text{W}/\text{TiO}_2\text{-SV}$
C (%)	1.0	1.2	1.8	4.5

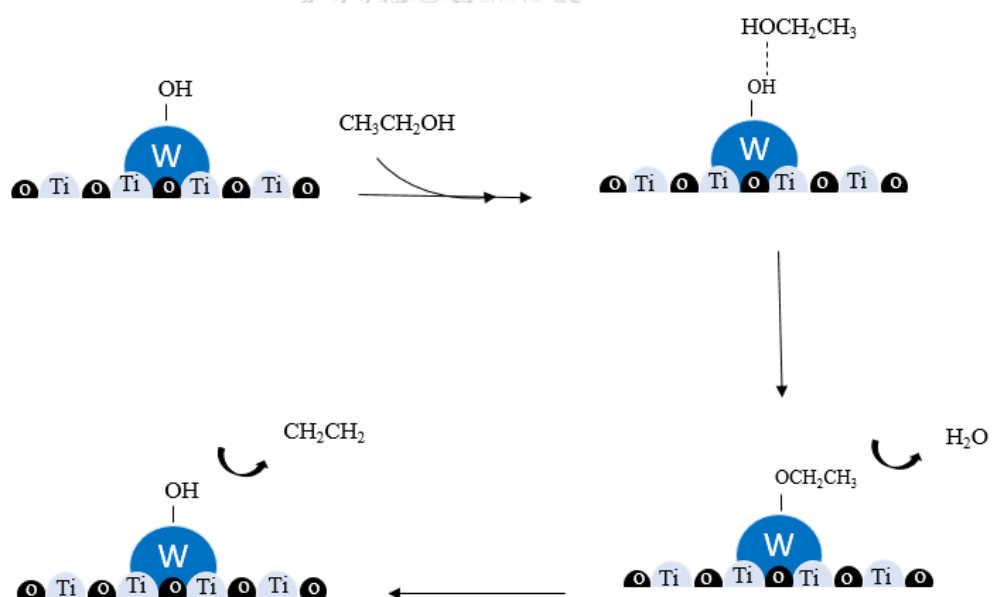
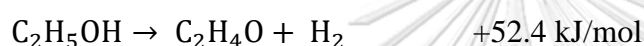
4.1.2 Ethanol Dehydration Reaction study

The supports and catalysts were investigated on the catalytic performance via the ethanol dehydration reaction in gas-phase at atmospheric pressure and temperature ranging from 200 °C to 400 °C. As shown in **Table 9**, the ethanol conversion for all samples increased with an increased reaction temperature which is signified that no deactivation of supports and catalysts occurred. The highest ethanol conversion was achieved at 400°C for all samples. The ethanol conversion was found in order of $\text{WO}_3/\text{TiO}_2\text{-SV}$ (87.6%) > $\text{TiO}_2\text{-SV}$ (56.3%) > $\text{WO}_3/\text{TiO}_2\text{-SG}$ (45.4%) > $\text{TiO}_2\text{-SG}$ (33.9%), which are corresponding to total amount acid sites of catalysts. Besides, it is detected that the conversion of $\text{TiO}_2\text{-SV}$ was still higher than that of $\text{WO}_3/\text{TiO}_2\text{-SG}$, which is quite interesting.

The selectivity to ethylene, diethyl ether and acetaldehyde are obtained in **Table 9**. It is realized that the TiO_2 rendered acetaldehyde as a main product. However, it is interesting that when incorporated the tungsten on TiO_2 supports, ethylene and diethyl ether are turned out to be the main products at different temperature. The formation of the ethylene occurs by acid catalyst protonating to hydroxyl group of ethanol molecule (proton transfers from acid to O atom to form alkyloxonium ion), and then the water molecules is created. Afterward, an ethoxide surface group forms and deprotonates its methyl group to produce the ethylene. The diethyl ether formation performs by either dissociative pathway or associative pathway [57]. The dissociative pathway is happened by one ethanol adsorption on

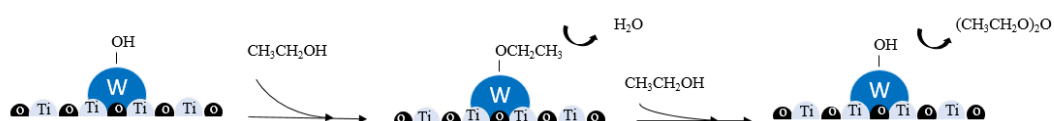
catalyst and water elimination providing an adsorbed ethyl group. Subsequently, the ethyl group reacts with the second ethanol molecule and finally the diethyl ether is produced. The associative pathway takes place from co-adsorption of two ethanol reacted and formed into diethyl ether. It is well known that the dehydration from the alcohol essentially happened on Bronsted acid sites [68, 71], while Lewis acid sites rarely contribute for this reaction [72, 73]. The mechanism of ethanol dehydration to ethylene and diethyl ether over the W/TiO₂ catalysts are demonstrate in **Schemes 1** and **2**, respectively. Furthermore, acetaldehyde is formed under the side reaction (dehydrogenation reaction) in **Equation 6** which is preferred on the basic sites of catalysts.

Equation 6: The dehydrogenation reaction

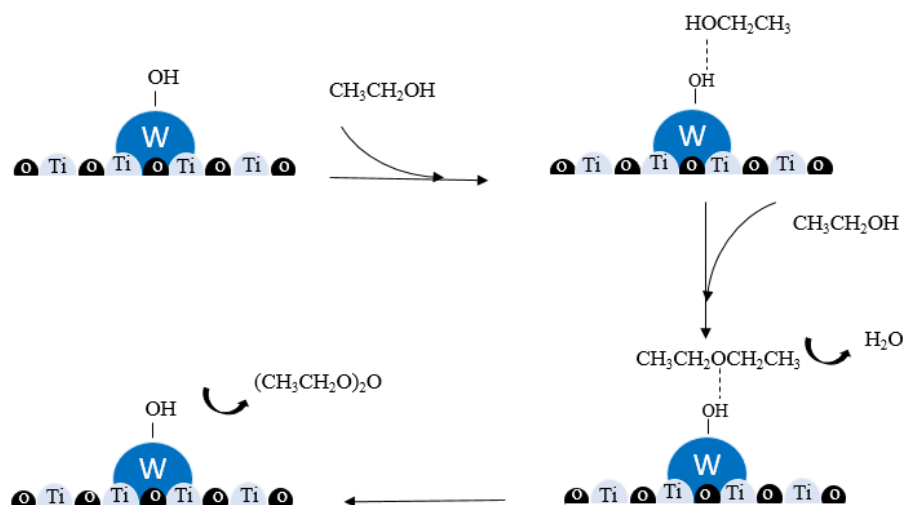


Scheme 1: The mechanism of ethanol dehydration ethylene over WO₃/TiO₂ catalyst

(a) dissociative pathway



(b) associative pathway

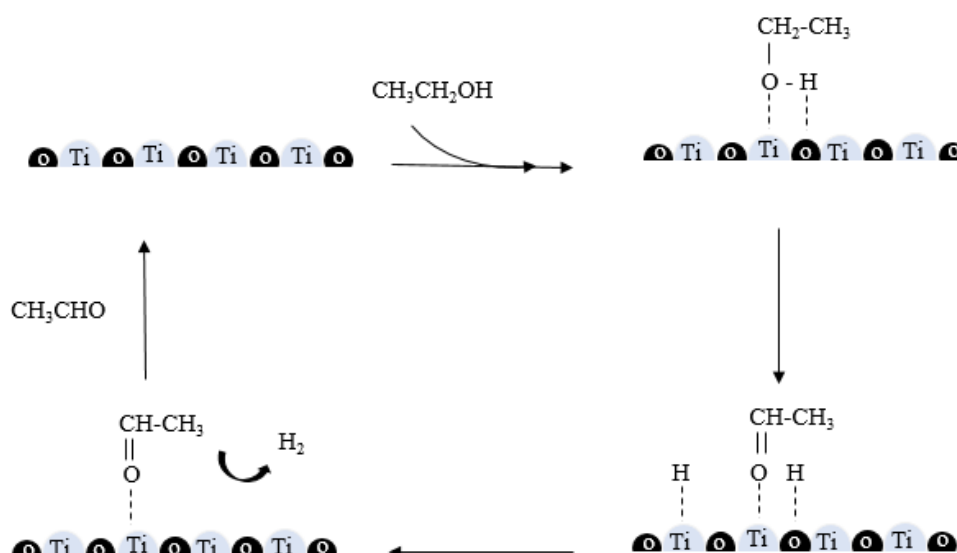


Scheme 2: The mechanism of ethanol dehydration to diethyl ether with (a) dissociative and (b) associative pathways over WO₃/TiO₂ catalyst

With the experimental studying, the TiO₂-SG and TiO₂-SV support catalysts still showed high acetaldehyde selectivity at ca. 81 °C and ca. 71 °C, respectively. This is because the high reaction temperature or the heat treatment effect to an oxidation of Lewis oxygen in pure TiO₂ structure with the basic site is more dominant than acid as seen from the pure SBA-15 catalyst used in ethanol dehydration reported by Autthanit and Jongsomjit in 2018 [60]. The mechanism of ethanol dehydrogenation to acetaldehyde over TiO₂ support is explained in **Scheme 3**. Acetaldehyde forms by ethanol molecule firstly adsorbed on the catalyst surface. An ethoxy group is further produced and transform into acetaldehyde. When introduced the tungsten on the TiO₂ supports, it exposed an increased ethylene selectivity at high temperature and increased diethyl ether selectivity at low temperature. The ethylene and diethyl ether selectivity over WO₃/TiO₂-SV catalyst was higher than those of WO₃/TiO₂-SG catalyst. It was learned on the highest ethylene selectivity of ca. 88 % under the reaction temperature at 400 °C and the highest diethyl ether selectivity of ca. 68 % under the reaction temperature at 250 °C for WO₃/TiO₂-SV. The influence to increase the ethylene and diethyl ether selectivity is the high amount of weak acid or Brønsted acid, which is the active site for ethanol dehydration after impregnated the tungsten on TiO₂ supports. As shown in **Table 6**, the weak acid sites for WO₃/TiO₂ catalyst were extensively higher than TiO₂ support catalyst, whereas the

strong acid sites for TiO_2 were higher than the WO_3/TiO_2 catalyst. It is familiar that amount of weak acid site is probably associated to Bronsted acid site of the catalyst, while the Lewis acid site relate to the strong acid site [60].

In the meantime, the acetaldehyde was formed as byproduct over WO_3/TiO_2 -SG and WO_3/TiO_2 -SV catalysts under dehydrogenation reaction. The acetaldehyde selectivity over WO_3/TiO_2 -SG was higher than that of WO_3/TiO_2 -SV correlating to higher amounts of basic site display in WO_3/TiO_2 -SG catalyst. The mass balance (carbon balance) in the experimental typically closed to 90 %. Such a deviation which were not detected by GC analysis were the heavy components and coke.



Scheme 3 : The mechanism of ethanol dehydrogenation to acetaldehyde over TiO_2 support catalyst

Table 9: Ethanol conversion, product selectivity and product yield as a function of reaction temperature. (the reaction condition: $T = 200 - 400^{\circ}\text{C}$, $\text{WHSV} = 22.9 \text{ g}_{\text{ethanol}}/\text{g}_{\text{cat}}^{-1} \cdot \text{h}^{-1}$, and catalyst weight = 0.05 g.)

Catalyst	Temp ($^{\circ}\text{C}$)	Ethanol Conversion (%)	Product Selectivity (%)			Product Yield (%)		
			Ethylene	Diethyl ether	Acetal dehyde	Ethylene	Diethyl ether	Acetal dehyde
TiO ₂ -SG	200	4.5	0.0	0.0	100.0	0.0	0.0	4.5
	250	8.6	1.8	0.0	98.2	0.2	0.0	8.5
	300	13.2	4.0	2.6	93.4	0.5	0.3	12.3
	350	32.3	11.4	1.6	87.0	3.7	0.5	28.1
	400	33.9	17.7	0.9	81.4	6.0	0.3	27.6
TiO ₂ -SV	200	21.1	0.0	0.0	100.0	0.0	0.0	21.1
	250	23.2	0.0	0.0	100.0	0.0	0.0	23.2
	300	35.7	2.5	2.1	95.3	0.9	0.8	34.1
	350	54.3	9.7	2.4	87.8	5.3	1.3	47.7
	400	56.3	25.5	3.4	71.1	14.4	1.9	40.0
WO ₃ /TiO ₂ - SG	200	12.4	4.7	37.4	57.9	0.6	4.6	7.2
	250	16.4	17.1	40.9	42.0	2.8	6.7	6.9
	300	25.0	39.5	10.4	50.1	9.9	2.6	12.5
	350	33.4	54.5	3.3	42.3	18.2	1.1	14.1
	400	45.4	64.6	1.3	34.1	29.3	0.6	15.5
WO ₃ /TiO ₂ - SV	200	33.2	5.2	42.6	52.2	1.7	14.2	17.3
	250	37.7	22.4	67.7	10.0	8.4	25.5	3.8
	300	51.8	52.6	42.4	5.0	27.3	22.0	2.6
	350	71.7	76.4	17.8	5.8	54.8	12.8	4.1
	400	87.6	88.2	3.5	8.3	77.2	3.1	7.3

The comparison of product yield for each temperature over supports and catalysts is reported in **Table 9**. It is revealed that the incorporated of tungsten effectively developed the ethylene and diethyl ether yields. The highest ethylene yield was found to be ca. 77 % at 400 $^{\circ}\text{C}$ over WO₃/TiO₂-SV. Furthermore, it was realized that the highest diethyl ether yield of ca. 26 % at 250 $^{\circ}\text{C}$ was achieved with WO₃/TiO₂-SV. However, diethyl ether yield was fairly small due to the low conversion at low temperature. It should be mentioned that the highest acetaldehyde yield of ca. 48% at 350 $^{\circ}\text{C}$ provided from TiO₂-SV was noticeable, which is quite interesting.

4.2 The catalytic ethanol dehydration to ethylene and diethyl ether carried on the W/TiO₂ catalyst modified with Pd in different sequence impregnation

4.2.1 Catalyst characterization

The XRD patterns of catalysts are presented in **Figure 14**. All catalysts exposed the high intensity peak located at 2θ degree of 25° (major), 38° and 48° corresponding to the crystal structure of (101), (004) and (200), respectively. The diffraction peak is noticed as the formation tetragonal anatase phase of TiO₂ crystalline [74]. Besides, the low intensity peaks was occurred at 24° and 34° on Pd/W/TiO₂, W/Pd//TiO₂, WPd/TiO₂ and W/TiO₂ catalysts correlated to the tetragonal phase of WO₃ formation [54]. It is declared that the diffraction patterns of all catalysts were similar. It is noticed that peak of palladium did not appeared due to the small loading of Pd metal and/or the very small size of crystallites being in the highly dispersed form on the TiO₂ support[75]. Referring to the Scherrer equation, $D = K \lambda / \beta \cos \theta$, the crystalline sizes of bimetallic Pd/W/TiO₂, W/Pd//TiO₂ and WPd/TiO₂ are provided and exposed in **Table 10**. When the palladium presented into W/TiO₂ catalysts, the Pd/W/TiO₂ presented the largest crystalline size of ca. 15.9 nm, whereas WPd/ TiO₂ disclosed the smallest crystalline size of ca. 11.8 nm. It is realized that the different sequence of metal impregnation slightly affected the crystalline size of catalysts.

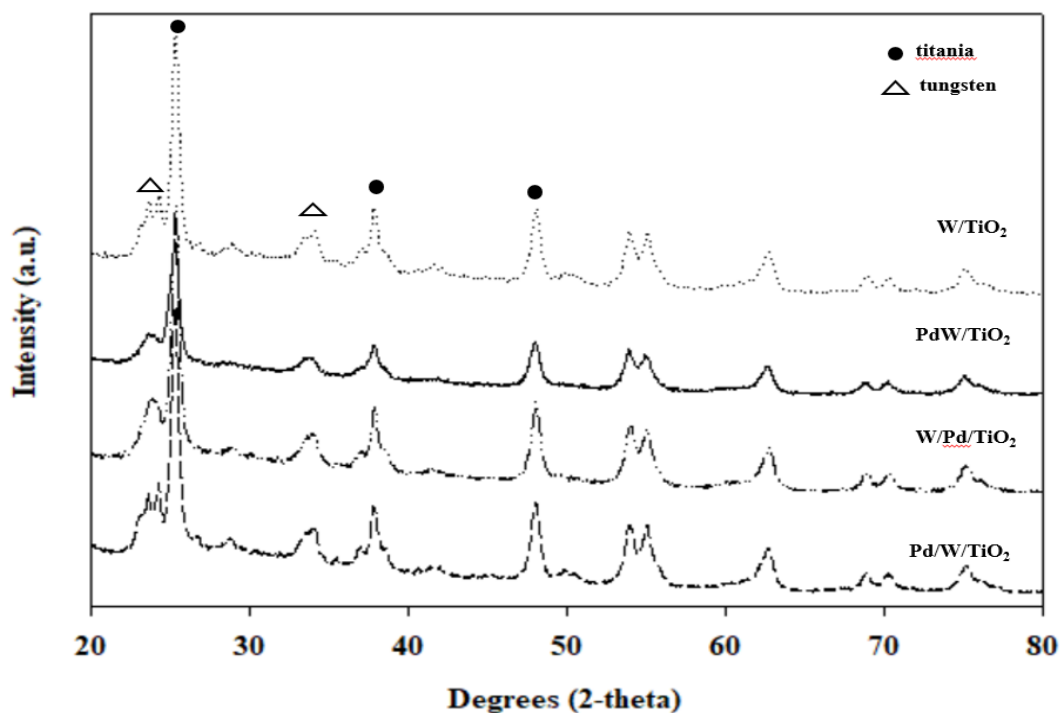


Figure 14: X-ray powder diffraction patterns for Pd/W/TiO₂, W/Pd/TiO₂, PdW/TiO₂ and W/TiO₂ catalysts

Table 10: Physical properties of catalysts

Sample	S _{BET} ^a (m ² /g)	Pore Volume ^b (cm ³ /g)	Pore Size ^c (nm)	Crystalline size ^d (nm)
Pd/W/TiO ₂	54.5	0.23	14.6	15.9
W/Pd/TiO ₂	44.3	0.26	15.7	15.4
PdW/TiO ₂	30.4	0.13	13.9	11.8
W/TiO ₂	58.9	0.25	13.4	15.4

^a Measured by BET method, ^{b,c} Measured by BJH desorption method, ^d Measured by XRD using the Scherrer equation

Table 11: Elemental distribution (% wt, % mol) on external surface of catalysts obtained from EDX

Catalyst	Element							
	% weight				% mol			
	O	W	Pd	Ti	O	W	Pd	Ti
Pd/W/TiO ₂	35.48	11.69	1.97	50.86	65.90	1.90	0.60	31.60
W/Pd/TiO ₂	39.55	12.32	1.81	46.32	70.10	1.90	0.50	27.50
PdW/TiO ₂	38.87	10.51	1.7	48.92	68.90	1.60	0.50	29.00
W/TiO ₂	35.1	8.29	-	56.61	64.10	1.30	-	34.60

In order to investigate the dispersion of elements, the energy-dispersive X-ray spectroscopy (EDX) analysis was performed. The typical EDX mapping of catalysts is illustrated in **Figure 15**. The results revealed good distribution of metals, which are elements of Ti, O, W and Pd on external surface of catalysts. The amounts of elements near the surface of catalysts are displayed in **Table 11**. It was found that the Pd particles were mostly located at outer surface of Pd/W/TiO₂, W/Pd/TiO₂ and WPd/TiO₂ catalysts in the order of 1.97, 1.81, and 1.7 wt%, which are higher than the amounts of Pd loading (0.5 wt%) in bulk catalyst.

The morphology of the catalysts obtained by scanning electron microscopy (SEM) is shown in **Figure 16**. It can be noticed that the shape of the Pd incorporated into W/TiO₂ exhibited the small agglomerated spherical and porous particles, which is similar to the morphology of the unmodified one. It suggested that the Pd impregnation process and thermal treatment of catalysts results in a slightly change on the morphology of the catalyst.

In **Table 10** is the Brunauer-Emmett-Teller surface area (S_{BET}), pore volume, and pore size diameter of catalysts explored by N₂ physisorption method. It demonstrated that the Pd modification onto W/TiO₂ slightly decreased the surface area (S_{BET}). The surface area of W/TiO₂ evidently diminished from 58.9 m²/g to 54.5 m²/g, 44.3 m²/g and 30.4 m²/g for Pd/W/TiO₂, W/Pd/TiO₂ and WPd/TiO₂, respectively due to some pore blockage from Pd particles in W/TiO₂, especially for WPd/TiO₂ [67]. The catalysts pore sizes calculated by Barrett–Joyner–Halenda (BJH) method are shown in **Table 10**. The pore sizes of all catalysts were in ranged between 13-16 nm identifying their mesoporous structure. When consider the different sequence impregnation of Pd on W/TiO₂, it discovered that the highest S_{BET} was showed in Pd/W/TiO₂ (54.5 m²/g), while the lowest S_{BET} was showed in PdW/TiO₂ (30.4 m²/g). It is concluded that the different sequence impregnation influences the textual property of the catalysts.

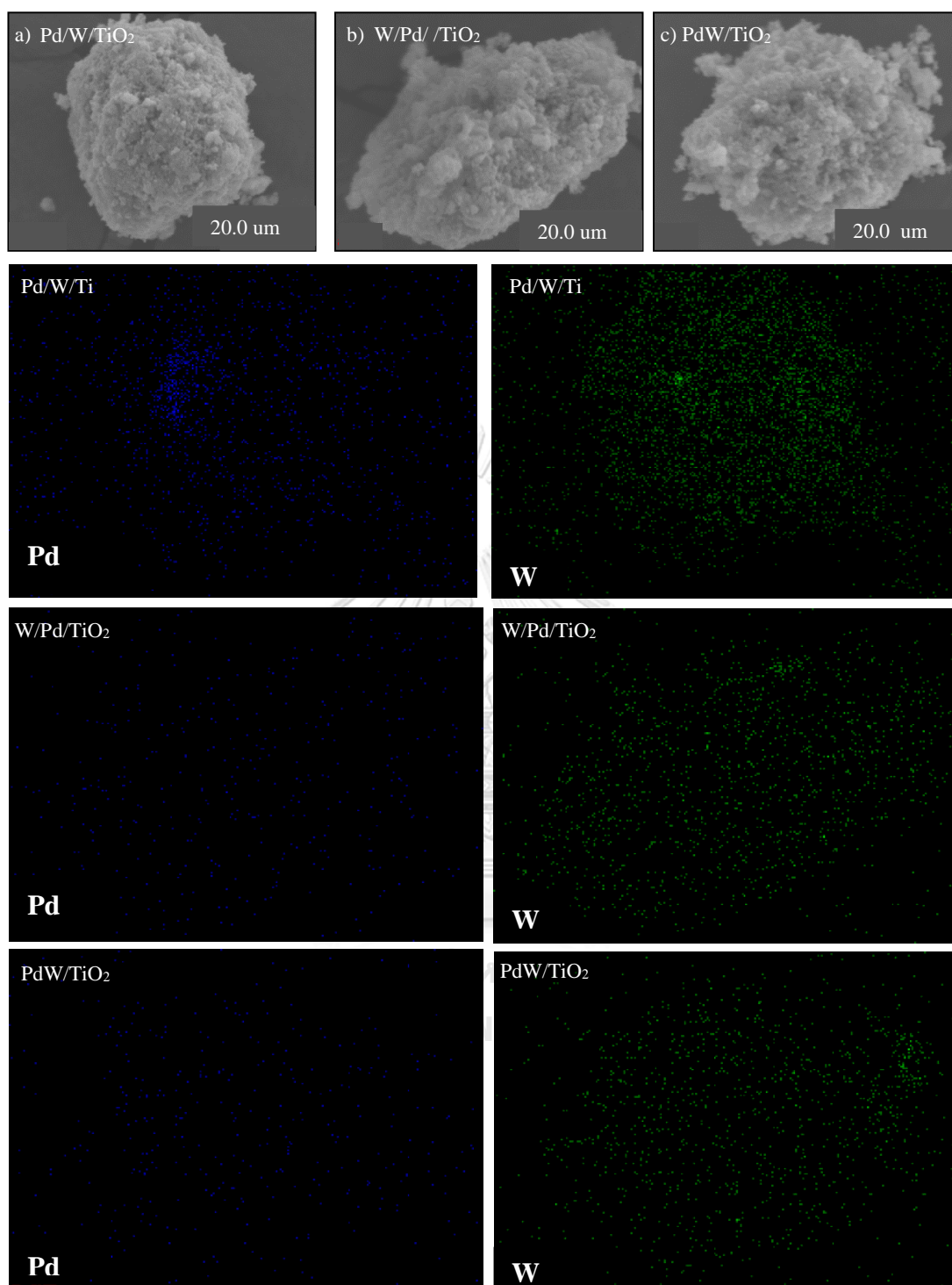


Figure 15: The energy-dispersive X-ray spectroscopy (EDX) mapping analysis of a) Pd/W/TiO₂, b) W/Pd/TiO₂ and c) PdW/TiO₂ catalysts

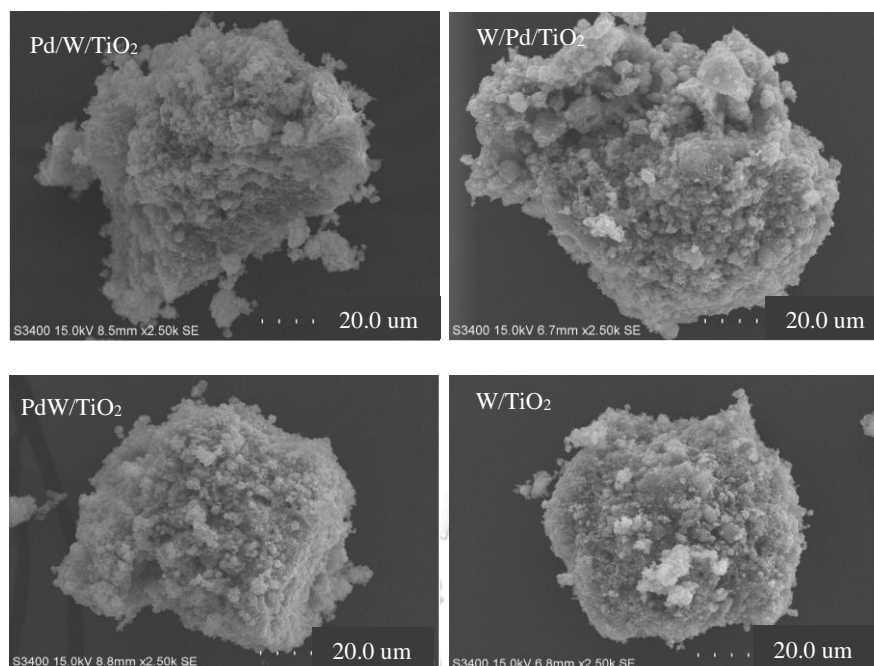


Figure 16: Scanning electron microscopy (SEM) micrograph of Pd/W/TiO₂, W/Pd/TiO₂, PdW/TiO₂ and W/TiO₂ catalysts

The N₂ adsorption-desorption isotherms of the catalysts were revealed in **Figure 17**. All catalysts played the isotherm type IV with a hysteresis loop type H1 at high relative pressures ($P/P_0 = 0.7-0.9$), which were signified to mesoporous structure according to the IUPAC (International Union of Pure and Applied Chemistry) classification. In **Figure 18**, it exposed the pore size distribution (PSD) for the catalysts which were in the average pore diameter range of 13-16 nm and broad distribution. These results were resembling to the ones obtained from Barrett–Joyner–Halenda (BJH) method as seen in **Table 10**.

The NH₃ temperature - programmed desorption (NH₃-TPD) profiles of the catalysts were presented in **Figure 19**. It displayed the NH₃ desorption between 150° and 300° C, which is attributed to weak acid sites. The desorption peaks between 300° and 450° C are the moderate and strong acid sites, respectively [76]. **Table 12** is exhibited the acid properties such as acid strength, acid site and acid density of catalysts. It is noticed that the presented of Pd in to catalysts provided an increase of acidity on W/TiO₂, especially for weak acid sites. The acidity tended to increase in the order of W/TiO₂ < Pd/W/TiO₂ < W/Pd/TiO₂ < PdW/TiO₂. Considering the effect of different sequence impregnation of Pd into catalysts, the PdW/TiO₂ catalyst

established the highest acidity of 2,884 $\mu\text{mol NH}_3/\text{g}$, while Pd/W/TiO₂ exposed the lowest acidity of 1,926 $\mu\text{mol NH}_3/\text{g}$. It was suggested that different sequence impregnation of Pd improved the acidity of W/TiO₂ catalysts. It is generally accepted that weak and/or medium acid sites is the key factor for ethanol dehydration to diethyl ether and ethylene, whereas the formation of the higher hydrocarbon takes place in the strong acid sites [68, 77].

Table 12: The amount surface acidity and acid density of catalysts measured by NH₃-TPD

Sample	Acidity ($\mu\text{mol/g cat}$)				
	Weak	Moderate	Strong	Weak to Moderate/Strong	Total
Pd/W/TiO ₂	837	848	240	7.02	1926
W/Pd/TiO ₂	1263	1154	251	9.62	2668
PdW/TiO ₂	1311	1215	357	7.07	2884
W/TiO ₂	804	823	241	6.76	1867

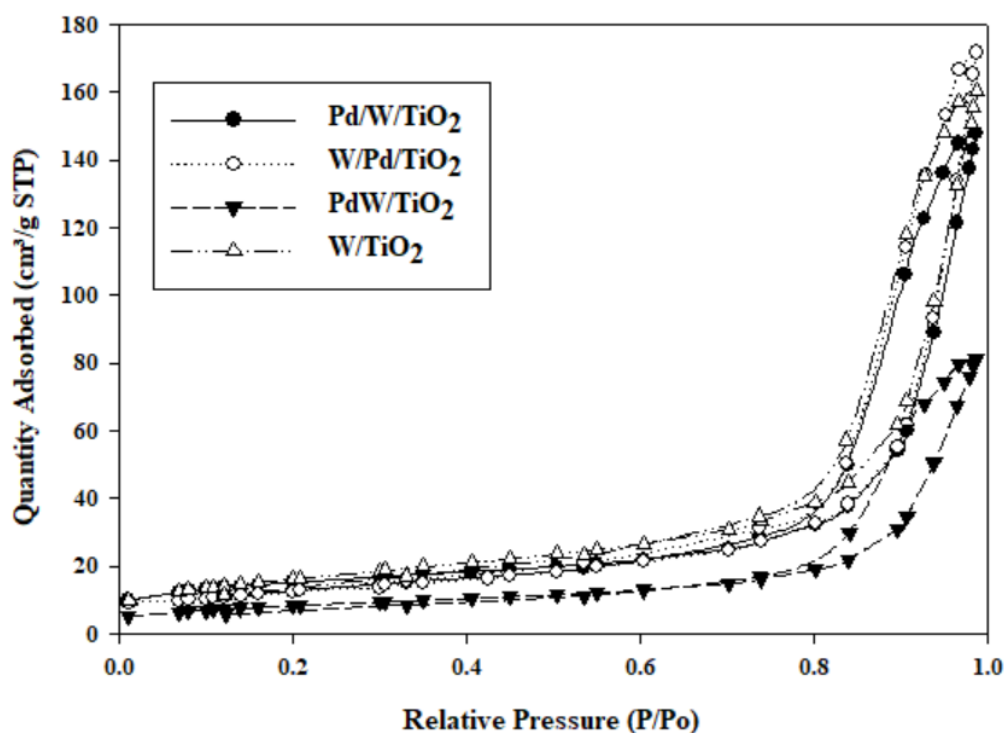


Figure 17: Nitrogen adsorption-desorption isotherms for Pd/W/TiO₂, W/Pd/TiO₂, PdW/TiO₂, and W/TiO₂ catalysts

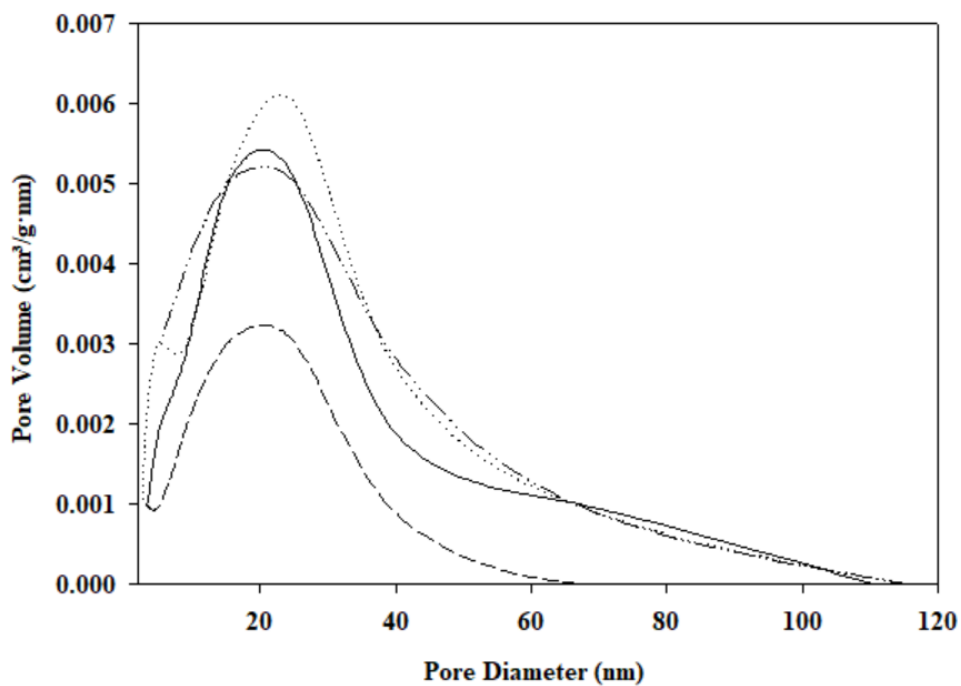


Figure 18 : The pore size distribution of catalysts using the BJH method

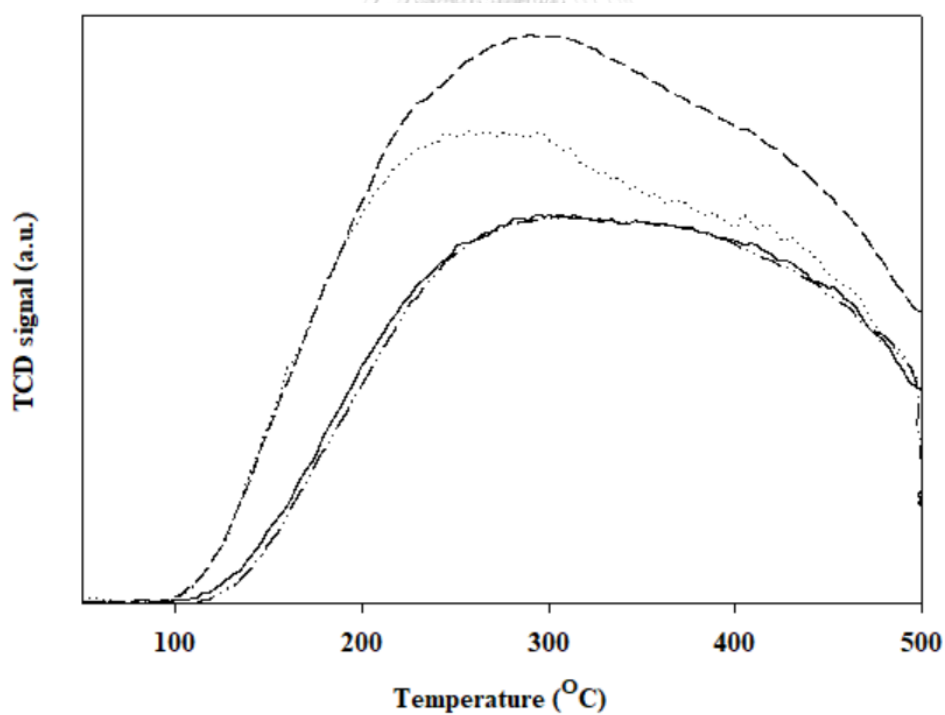


Figure 19: NH₃-TPD profiles for Pd/W/TiO₂, W/Pd/TiO₂, PdW/TiO₂ and W/TiO₂ catalysts

The surface characterization of catalysts such as elemental composition on the catalysts was analyzed by using XPS method. In **Table 13**, it summarizes the binding energy for all elements in catalysts. As expected, the binding energies for Ti, W, Pd and O were detected, which are in well agreement to those of EDX analysis. Considering the binding energy of Pd, it can be observed at 341.5, 334.8 and 336.1 eV for Pd/W/TiO₂, W/Pd/TiO₂ and PdW/TiO₂, respectively indicating the PdO₂ formation for Pd/W/TiO₂, metallic Pd for W/Pd/TiO₂ and PdO for PdW/TiO₂ [38, 78]. However, the binding energy of metal can be shifted to the lower or higher by electron donate from or to neighboring atom. Moreover, the spectral analysis of the XPS focused on O 1s core-level spectra providing the additional information for oxygen species on catalyst surface. The deconvolution of the O 1s spectra was fitted and separated into three kinds of oxygen species as demonstrate in **Figure 20**. The binding energies were noticed at 529.9, 531.6 and 533.2 eV which is corresponding to lattice oxygen (O), surface hydroxyl group (OH) and adsorbed water (H₂O), respectively [79, 80]. Table 13 defined the atomic concentrations of each O 1s on surface catalysts. The results showed that the hydroxyl group area fraction decreased in the following order PdW/TiO₂ (41%) > W/Pd/TiO₂ (37%) > Pd/W/TiO₂ (29%) > W/TiO₂ (9%) consistent to the acidity of catalysts. The results suggested that the presented of Pd into catalysts essentially alters the acidity of catalysts due to the formation of Pd on support catalyst indicating that PdW/TiO₂ has the highest hydroxyl group (Brønsted acid) on the surface catalyst. It is reported that the Brønsted acid site is perhaps related to the weak acidity, while the Lewis acid site is related to the strong acidity [81].

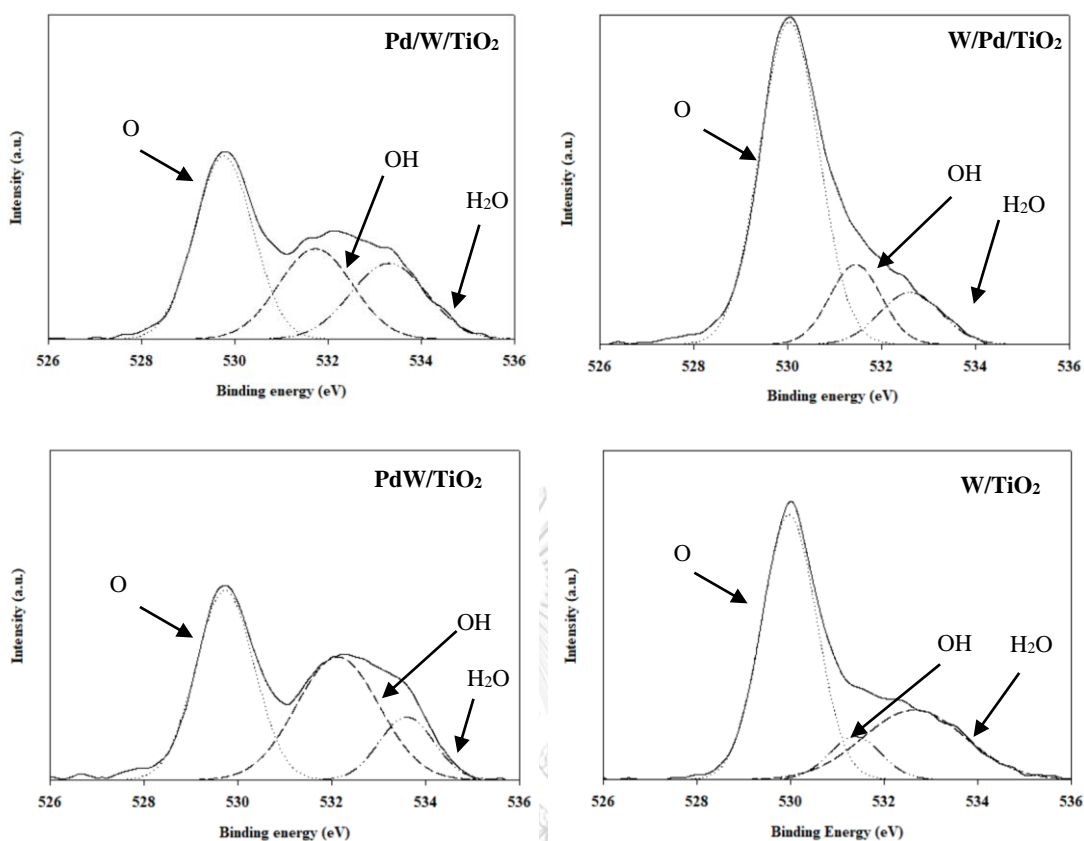


Figure 20: XPS analysis at O 1s for Pd/W/TiO₂, W/Pd/TiO₂, PdW/TiO₂ and W/TiO₂ catalysts

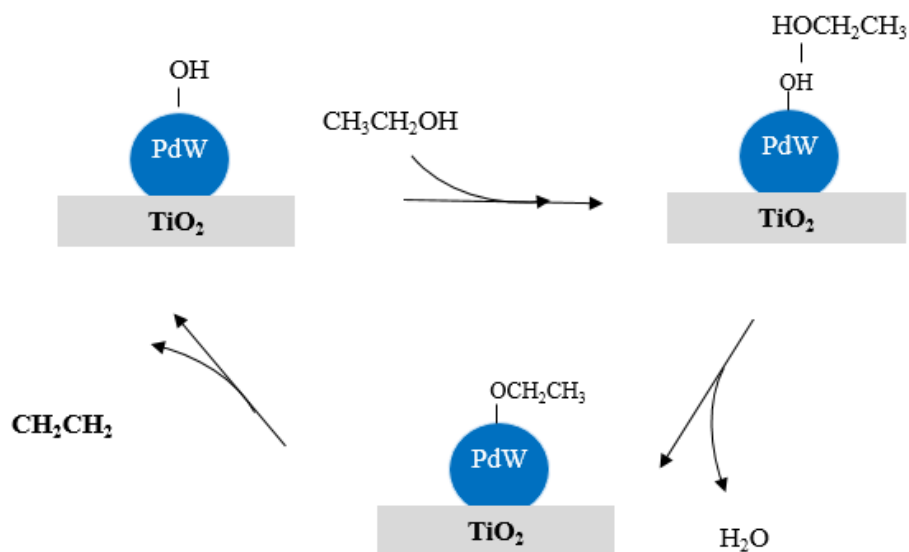
Table 13: XPS analysis of catalysts

Catalysts	Binding Energy (eV)					O 1s	O 1s area portion (%)		
	Ti 2p1	Ti 2p2	Pd 3d	W 4f1	W 4f2		O	OH	H ₂ O
Pd/W/TiO ₂	458.5	464.3	341.5	37.3	35.2	529.8	46	29	25
W/Pd/TiO ₂	458.8	464.5	334.8	37.6	35.4	530.0	44	37	19
PdW/TiO ₂	458.7	464.5	336.1	37.6	35.5	530.0	45	41	14
W/TiO ₂	458.7	464.4	-	37.6	35.4	530.0	61	09	30

4.2.2 Ethanol dehydration Reaction study

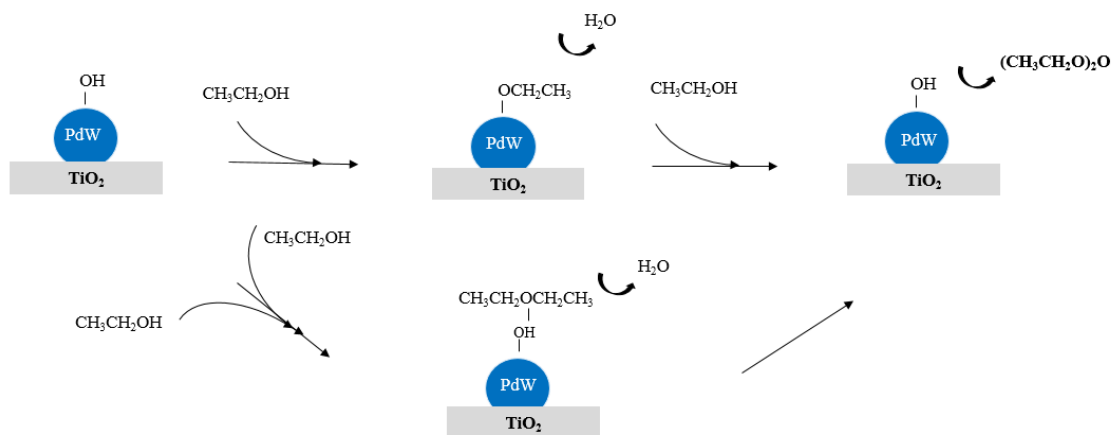
The mechanism of catalytic ethanol dehydration to ethylene over catalyst is displayed in **Scheme 4**. The formation of the ethylene occurs by one ethanol molecule adsorption on PdW/TiO₂ catalyst, followed by water elimination to form an adsorbed ethoxide. Finally, the ethylene is occurred. As exhibited in **Scheme 5**, the diethyl ether formation creates by either dissociative pathway or associative pathway. The

dissociative pathway occurs by one ethanol adsorbed on PdW/TiO₂ catalyst and followed by water elimination to obtain the adsorbed ethoxide. Afterward, the ethoxide on surface PdW/TiO₂ catalyst reacts with the second ethanol molecule to produce diethyl ether. The associative pathway arises from co-adsorption of two ethanol molecule reacted on catalyst, and then formed into diethyl ether [57]. The ethylene formation is mainly favored at high temperature between 320°C and 500°C, while diethyl ether mainly prefers at the low to moderate temperature between 150°C and 300°C [82]. However, diethyl ether can decompose to ethylene at high temperature [80, 83] as displayed in **Scheme 6** resulting in the increased ethylene selectivity and decreased diethyl ether selectivity at high temperature. In addition, acetaldehyde can be formed as a byproduct as a dehydrogenation reaction (side reaction). The formation of acetaldehyde is occurred by one ethanol adsorbed on the catalyst surface, followed by released H₂ to provide the adsorbed ethoxide group.



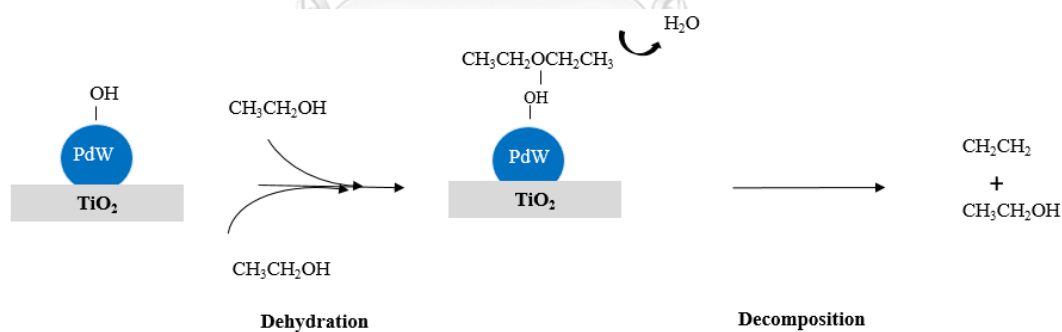
Scheme 4 : The mechanism of catalytic ethanol dehydration to ethylene over PdW/TiO₂ catalysts

a) Dissociative pathway



b) Associative pathway

Scheme 5: The mechanism of catalytic ethanol dehydration to diethyl ether over PdW/TiO₂ catalysts with a) dissociative pathway and b) associative pathway



Scheme 6: Catalytic ethanol dehydration pathway at high temperature

The behavior of the presented Pd into W/TiO₂ catalyst was examined in the ethanol dehydration at temperature range of 200-400°C. The study focused on the catalytic activity, selectivity and yield of ethylene and diethyl ether. The ethanol conversion for all catalysts is revealed in **Figure 21**. All catalysts showed the similar behavior in which the ethanol conversion increased with increasing the reaction temperature. The obtained catalytic activity of all catalysts was the highest at 400°C

without deactivation. The Pd modification on W/TiO₂ catalyst affected on the catalytic activity for W/Pd/TiO₂ and PdW/TiO₂ by a significant increase in ethanol conversion at low temperature (250-300°C). Likewise, the sequence of palladium impregnation into catalysts increased the catalytic activity when Pd was impregnated on the support before W (W/Pd/TiO₂) and Pd and W were co-impregnated on the support (PdW/TiO₂). The catalytic activity was found to increase in the order of PdW/TiO₂ (90.2%) > W/Pd/TiO₂ (89.6%) > Pd/W/TiO₂ (81.5%) > W/TiO₂ (80.2%) at 400°C. It should be realized that this result was correlated to acidity of catalysts as displayed in **Table 12**. The acidity of the catalysts played an importance role to introduce the catalytic activity [11, 26, 50, 54, 84, 85]. In addition, with higher acid density and shorter distance between two acid sites, it is benefit to increase the possibility of the reactant to be adsorbed and rapidly catalyzed to produce the chemical product, especially diethyl ether at low temperature [80]. In summary, the different sequence of impregnated Pd and W into TiO₂ catalyst effect on the interaction between Pd and W and promote the formation of an active site. Besides, it is noticed that the catalytic activity and NH₃ -TPD profile of Pd/W/TiO₂ catalyst is quite similar to those results for W/TiO₂ catalysts. This is probed that incorporated W into TiO₂ catalyst before Pd did not contribute the active site on the catalyst.

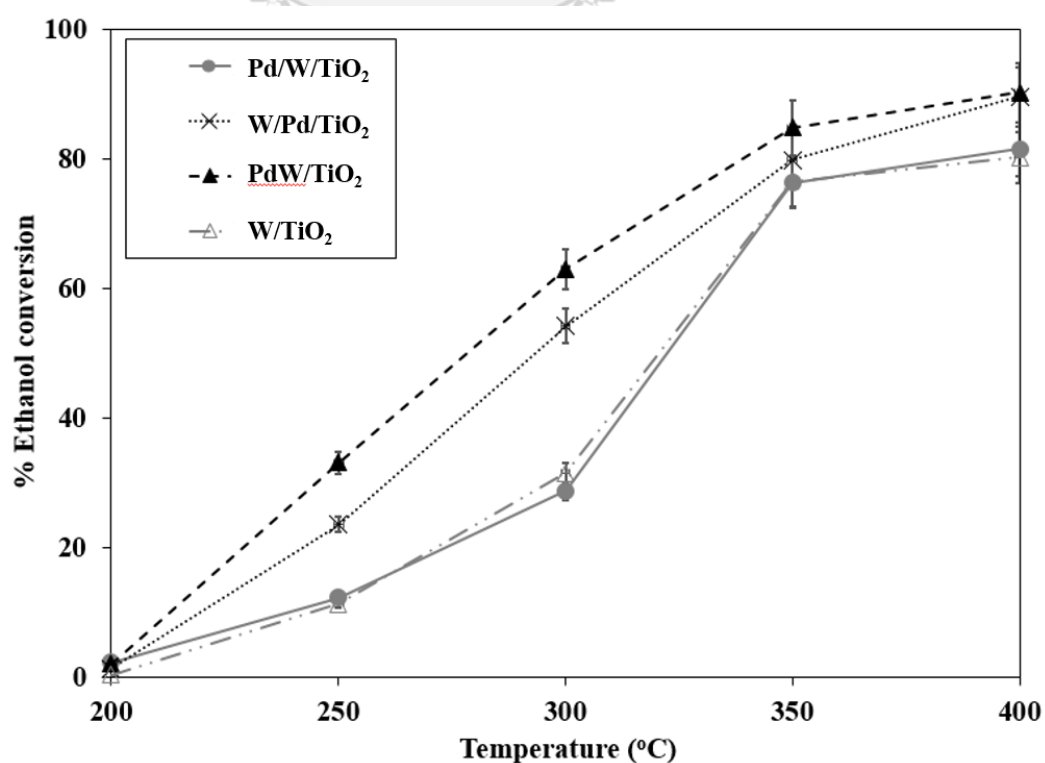


Figure 21: Ethanol conversion of Pd/W/TiO₂, W/Pd/TiO₂, PdW/TiO₂, and W/TiO₂ catalysts

The product selectivity for all catalysts is revealed in the **Figure 22**. It shows that the ethylene selectivity increased with increasing temperature, while the diethyl ether selectivity decreased with increasing temperature. In addition, the acetaldehyde selectivity was increased gradually at reaction temperature 250 - 400°C. All catalysts showed the highest ethylene selectivity at 400°C and diethyl ether selectivity at 300°C. It is remarked that the Pd modification on the catalysts affected the product selectivity by merely increasing the acetaldehyde selectivity. On the other hand, the Pd modification resulted in an increase the ethanol conversion without significant change the main product selectivity. However, it should be noted that only PdW/TiO₂ catalysts exhibited high diethyl ether selectivity at high reaction temperature perhaps due to its weak acidity.

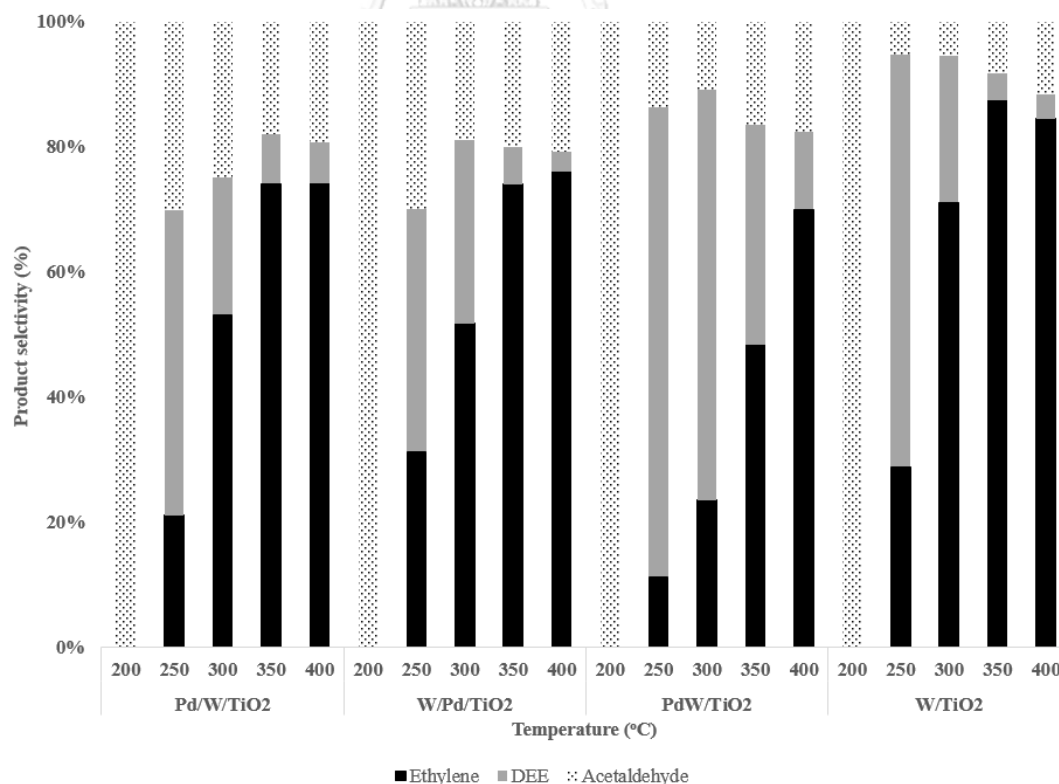


Figure 22: Product selectivity of Pd/W/TiO₂, W/Pd/TiO₂, PdW/TiO₂ and W/TiO₂ catalysts

Table 14 shows the ethylene and diethyl ether yields. It is revealed that the Pd modification on W/TiO₂ catalysts resulted an increasing of ethylene yield of 68.1% for W/Pd/TiO₂ at 400°C corresponding to the highest portion of weak to moderate/strong acid site. Wannaborworn et al.[28]described that the ethanol conversion to ethylene is mainly associated to weak and moderate acid site. Moreover, the incorporated of Pd on W/TiO₂ catalyst improved the diethyl ether yield for both W/Pd/TiO₂ and PdW/TiO₂ catalysts at 15.9% and 41.4% respectively at 300°C. As a result, the Pd modification as a chemical promoter along with the metal sequence impregnation method enriched their catalyst activity and product yield in ethanol dehydration reaction. It is familiar that the dehydration of alcohol really takes place on Brønsted acid sites [86]. The XPS results confirmed that the Pd modification increased amount of hydroxyl groups which is correlated to the Brønsted acid sites on catalyst resulting in an increasing catalyst activity.

Table 14: Product yield (%) obtained from each catalyst as function of reaction temperature (the reaction condition at T = 200 – 400°C, WHSV = 3.13 g_{ethanol}·g_{cat}⁻¹·h⁻¹, and catalyst weight = 0.1 g)

Catalysts	Temp(°C)	Conversion (%)	Product Yield (%) ^a		
			Ethylene	Diethyl ether	Acetaldehyde
Pd/W/TiO ₂	200	2.3	0.0	0.0	2.3
	250	12.3	2.6	6.0	3.7
	300	28.7	15.3	6.3	7.1
	350	76.3	56.6	6.0	13.7
	400	81.5	60.5	5.3	15.7
W/Pd/TiO ₂	200	1.2	0.0	0.0	1.2
	250	23.5	7.3	9.1	7.0
	300	54.2	28.1	15.9	10.3
	350	79.8	59.1	4.8	16.0
	400	89.6	68.1	2.7	18.7
PdW/TiO ₂	200	2.0	0.0	0.0	2.0
	250	33.1	3.7	24.9	4.5
	300	63.0	14.8	41.4	6.8
	350	84.8	41.0	29.9	13.9
	400	90.2	63.2	11.1	15.9
W/TiO ₂	200	0.3	0.0	0.0	0.3
	250	11.3	3.3	7.4	0.6
	300	31.5	22.4	7.4	1.7
	350	76.5	67.0	3.2	6.4

400 80.2 67.8 3.1 9.3

^a product yield is ethanol conversion (%) × product selectivity (%)

The catalytic performance for ethanol dehydration to ethylene and diethyl ether over various catalysts as reported so far are presented in **Table 15**. It was suggested that W/Pd//TiO₂ and PdW/TiO₂ are comparable to those of typical and modified catalysts. Accordingly, the W/Pd//TiO₂ and PdW/TiO₂ is an alternative route to obtain ethylene and diethyl ether in respectively via ethanol dehydration.

Table 15: Comparison of various catalysts for ethylene and diethyl ether yield and catalytic performance

Catalyst	S _{BET} (m ² /g)	Reaction temperature (°C)	Ethanol conversion (%)	Ethylene yield (%)	Diethyl ether yield (%)	Ref.
Pd/W/TiO ₂	55	200 – 400	2 – 90	61	6	This study
W/Pd//TiO ₂	44	200 – 400	1 – 90	68	16	This study
PdW/TiO ₂	30	200 – 400	2 – 82	63	41	This study
WO ₃ /ZrO ₂	81	150 – 500	0 – 100	99	42	[26]
WO ₃ /TiO ₂ (c)	60	150 – 500	12 – 100	98	68	[26]
WO ₃ /MgO– Al ₂ O ₃	168	150 – 500	0 - 100	93	17	[26]
WO ₃ /SiO ₂	110	150 – 500	1-100	42	5	[26]
TiO ₂	70	150 – 500	0 - 100	65	48	[26]
ZrO ₂	94	150 – 500	0 - 100	87	1	[26]
Al ₂ O ₃	199	200 – 400	14 - 89	82	27	[87]
5P/Al ₂ O ₃	151	200 – 400	9 - 86	80	34	[87]
Cr-Co/γ- Al ₂ O ₃	134	200	93	-	0.3	[88]
Fe ₂ O ₃	40	500	97	63	-	[4]

CHAPTER V – CONCLUSIONS AND RECOMMENDATION

5.1 Conclusion

In first part, the TiO_2 supports were prepared by sol-gel and solvothermal methods. TiO_2 supports were then incipient wetness impregnated with tungsten (W) and calcined at temperature of 450°C . The supports and catalysts including WO_3/TiO_2 –SG, WO_3/TiO_2 –SV, TiO_2 –SG and TiO_2 –SV were investigated on their characteristics and catalyst performance in the ethanol dehydration to ethylene and diethyl ether at temperature range of 200°C – 400°C . The result showed that the WO_3/TiO_2 -SV catalyst is promising for dehydration of ethanol to ethylene and diethyl ether having the highest ethylene of 77 % at 400°C and the highest yield of 26 % at 250°C . It showed that the more efficient method to synthesize TiO_2 support was solvothermal method due to its high acidity and surface area. It is worth noting that the TiO_2 -SV itself also rendered the highest yield of acetaldehyde at 48 % at 350°C . This support can be potentially used as support for a catalyst in dehydrogenation of ethanol to acetaldehyde.

In the second part, the W/TiO_2 catalyst was modified with palladium by different sequence of incipient wetness impregnation. The Pd-modified W/TiO_2 catalysts were calcined at temperature of 500°C . The catalyst including $\text{Pd}/\text{W}/\text{TiO}_2$, $\text{W}/\text{Pd}/\text{TiO}_2$, PdW/TiO_2 and WO_3/TiO_2 were investigated on their characteristics and catalyst performance in the ethanol dehydration to ethylene and diethyl ether at temperature range of 200°C – 400°C . The results showed that the effect of Pd modification and the different sequence impregnation of Pd and W on W/TiO_2 catalysts were investigated and their catalytic properties for ethanol dehydration were evaluated. The introduction of 0.5 wt% of Pd into W/TiO_2 apparently affected the structure and surface acidity of the catalysts providing an increasing of catalytic activity for catalysts. The co-impregnated catalyst (PdW/TiO_2) exhibited higher ethanol conversion than those prepared by sequential impregnation method ($\text{W}/\text{Pd}/\text{TiO}_2$ and $\text{Pd}/\text{W}/\text{TiO}_2$). It is summarized that the Pd modification resulted in an increase of diethyl ether yield for PdW/TiO_2 and $\text{W}/\text{Pd}/\text{TiO}_2$, whereas that of $\text{Pd}/\text{W}/\text{TiO}_2$ catalyst was hardly affected. Besides, the Pd modification yielded a slight increase of ethylene

yield for W/Pd/TiO₂ catalyst. From the experiment, PdW/TiO₂ was considered as the most effective catalyst for ethanol conversion to diethyl ether with diethyl ether yield of ca. 41% at 300°C and W/Pd/TiO₂ was the most promising catalyst to convert ethanol into ethylene with ethylene yield of ca. 68% at 400°C. This is attributed to the increased amount of weak acid sites and total acidity with Pd modification onto W/TiO₂ catalyst.

5.2 Recommendation

- 1) The stability of all study catalysts should be investigated in future work.
- 2) The other parameter on reaction condition should be studied such as WHSV and co feeding with oxygen in ethanol dehydration. Adjusting some parameters shall be improved the product selectivity at lower temperature.
- 3) The other method to synthesis the TiO₂ support catalyst such as hydrothermal method shall be investigated. It may affect to the characters and catalyst activity.
- 4) The effect of various amounts of tungsten (W) and/or palladium (Pd) wt% loading on catalysts shall be further investigated on the catalyst performance in ethanol dehydration reaction.
- 5) The TiO₂ support catalyst shall be further developed by loading suitable noble metal in other reaction such as ethanol dehydrogenation to acetaldehyde.

REFERENCES



จุฬาลงกรณ์มหาวิทยาลัย
CHULALONGKORN UNIVERSITY

1. Paul, A., et al., *Effect of diethyl ether and ethanol on performance, combustion, and emission of single-cylinder compression ignition engine*. International Journal of Ambient Energy, 2014. **38**(1): p. 2-13.
2. Mostafa, M.R., Youssef, A.M. and Hassan, S.M., *Conversion of ethanol and isopropanol on alumina, titania and alumina-titania catalysts*. Materials Letters, 1999. **12**: p. 207-213.
3. Nair, H., et al., *Mechanistic insights into the formation of acetaldehyde and diethyl ether from ethanol over supported VO_x, MoO_x, and WO_x catalysts*. Journal of Catalysis, 2011. **279**(1): p. 144-154.
4. Zaki, T., *Catalytic dehydration of ethanol using transition metal oxide catalysts*. J Colloid Interface Sci, 2005. **284**(2): p. 606-13.
5. Xiao, Y., et al., *Catalytic Dehydration of Ethanol to Ethylene on TiO₂/4A Zeolite Composite Catalysts*. Catalysis Letters, 2009. **130**(3-4): p. 308-311.
6. Rossetti, I., et al., *Ethylene production via catalytic dehydration of diluted bioethanol: A step towards an integrated biorefinery*. Applied Catalysis B: Environmental, 2017. **210**: p. 407-420.
7. Phung, T.K. and G. Busca, *Ethanol dehydration on silica-aluminas: Active sites and ethylene/diethyl ether selectivities*. Catalysis Communications, 2015. **68**: p. 110-115.
8. Popa, A. and V. Sasca, *The influence of surface coverage on the catalytic activity of silica-supported heteropolyacids*. Reaction Kinetics, Mechanisms and Catalysis, 2015. **117**(1): p. 205-221.
9. Bagheri, S., N. Muhd Julkapli, and S. Bee Abd Hamid, *Titanium dioxide as a catalyst support in heterogeneous catalysis*. ScientificWorldJournal, 2014. **2014**: p. 727496.
10. Dalil, M., et al., *Transient acrolein selectivity and carbon deposition study of glycerol dehydration over WO₃/TiO₂ catalyst*. Chemical Engineering Journal, 2015. **270**: p. 557-563.
11. Filek, U., et al., *Ethanol conversion over cesium-doped mono- and bi-cationic aluminum and gallium H₃PW₁₂O₄₀ salts*. Journal of Molecular Catalysis A: Chemical, 2015. **407**: p. 152-162.
12. Mai, D.T., I.I. Mikhalenko, and A.I. Pylina, *Hydrothermal ethanol conversion on Ag, Cu, Au/TiO₂*. Russian Journal of Physical Chemistry A, 2014. **88**(10): p. 1637-1642.
13. Pérez-López, G., R. Ramírez-López, and T. Viveros, *Acidic properties of Si- and Al- promoted TiO₂ catalysts: Effect on 2-propanol dehydration activity*. Catalysis Today, 2018. **305**: p. 182-191.
14. Kamsuwan, T., P. Prasertdam, and B. Jongsomjit, *Diethyl Ether Production during Catalytic Dehydration of Ethanol over Ru- and Pt- modified H-beta Zeolite Catalysts*. J Oleo Sci, 2017. **66**(2): p. 199-207.
15. Sudhakar, M., et al., *Vapor phase hydrogenation of aqueous levulinic acid over hydroxyapatite supported metal (M = Pd, Pt, Ru, Cu, Ni) catalysts*. Applied Catalysis B: Environmental, 2016. **180**: p. 113-120.
16. Inmanee, T., P. Pinthong, and B. Jongsomjit, *Effect of Calcination Temperatures and Mo Modification on Nanocrystalline (γ-χ)-Al₂O₃ Catalysts for Catalytic Ethanol Dehydration*. Journal of Nanomaterials, 2017: p. 1-9.

17. Chauvin, J., et al., *Comparative Influence of Surface Tungstate Species and Bulk Amorphous WO₃ Particles on the Acidity and Catalytic Activity of Tungsten Oxide Supported on Silica*. The Journal of Physical Chemistry C, 2015. **119**(22): p. 12345-12355.
18. Lauriol-Garbey, P., et al., *Gas phase dehydration of glycerol to acrolein over WO₃/ZrO₂ catalysts: Improvement of selectivity and stability by doping with SiO₂*. Catalysis Communications, 2011. **16**(1): p. 170-174.
19. Cecilia, J.A., et al., *WO₃ supported on Zr doped mesoporous SBA-15 silica for glycerol dehydration to acrolein*. Applied Catalysis A: General, 2016. **516**: p. 30-40.
20. Ai, M., *The activity of WO₃-based mixed-oxide catalysts _ I. Acidic properties of WO₃-based catalysts and correlation with catalytic activity*. Journal of Catalysis, 1977. **49**(30): p. 305-312.
21. Lebarbier, V., Clet, G. and Houalla, M., *Relations between Structure, Acidity, and Activity of WO_x on TiO₂ _ Influence of the Initial State of the Support, Titanium Oxyhydroxide, or Titanium Oxide*. Journal of Physical Chemistry B, 2006. **110**(45): p. 22608-17.
22. Qin, Y., et al., *Synthesis of mesoporous WO₃/TiO₂ catalyst and its excellent catalytic performance for the oxidation of dibenzothiophene*. New Journal of Chemistry, 2017. **41**(2): p. 569-578.
23. Zhao, X., L. Mao, and G. Dong, *Mn-Ce-V-WO_x/TiO₂ SCR Catalysts: Catalytic Activity, Stability and Interaction among Catalytic Oxides*. Catalysts, 2018. **8**(2): p. 76.
24. Liebig, C., et al., *Glycerol conversion to acrylonitrile by consecutive dehydration over WO₃/TiO₂ and ammoxidation over Sb-(Fe,V)-O*. Applied Catalysis B: Environmental, 2013. **132-133**: p. 170-182.
25. Hunge, Y.M., et al., *Photoelectrocatalytic degradation of oxalic acid using WO₃ and stratified WO₃/TiO₂ photocatalysts under sunlight illumination*. Ultrason Sonochem, 2017. **35**: p. 233-242.
26. Phung, T.K., L. Proietti Hernández, and G. Busca, *Conversion of ethanol over transition metal oxide catalysts: Effect of tungsta addition on catalytic behaviour of titania and zirconia*. Applied Catalysis A: General, 2015. **489**: p. 180-187.
27. Fajardo, H.V., et al., *Synthesis, characterization and catalytic properties of nanocrystalline Y₂O₃-coated TiO₂ in the ethanol dehydration reaction*. Materials Research, 2012. **15**(2): p. 285-290.
28. Wannaborworn, M., P. Prasertthdam, and B. Jongsomjit, *A Comparative Study of Solvothermal and Sol-Gel-Derived Nanocrystalline Alumina Catalysts for Ethanol Dehydration*. Journal of Nanomaterials, 2015. **2015**: p. 1-11.
29. Panpranot, J., K. Kontapakdee, and P. Prasertthdam, *Selective hydrogenation of acetylene in excess ethylene on micron-sized and nanocrystalline TiO₂ supported Pd catalysts*. Applied Catalysis A: General, 2006. **314**(1): p. 128-133.
30. Gomez-Gutierrez, C.M., et al., *Solvothermal synthesis of nickel-tungsten sulfides for 2-propanol dehydration*. Scanning, 2015. **37**(3): p. 165-71.
31. Jiang, T., et al., *Catalytic performance of Pd-Ni bimetallic catalyst for glycerol hydrogenolysis*. Biomass and Bioenergy, 2015. **78**: p. 71-79.

32. Cunha, A., et al., *Bimetallic Cu-(WO₃ or ZrO₂) on Al₂O₃ catalysts for glycerol dehydration to acetol : effect of texture and acidic properties* International Symposium on Acid - Basic Catalysis, 2017.
33. Murcia-López, S., et al., *On the role of Cu, Ag and Pt in active titania for gas-phase ethanol photo-reforming*. Materials Science in Semiconductor Processing, 2018. **73**: p. 30-34.
34. Casanovas, A., et al., *Ethanol reforming processes over ZnO-supported palladium catalysts: Effect of alloy formation*. Journal of Molecular Catalysis A: Chemical, 2006. **250**(1-2): p. 44-49.
35. Kim, N.D., et al., *Promoter effect of Pd in CuCr₂O₄ catalysts on the hydrogenolysis of glycerol to 1,2-propanediol*. Green Chemistry, 2012. **14**(9).
36. Ipadeola, A.K., et al., *Bimetallic Pd/SnO₂ Nanoparticles on Metal Organic Framework (MOF)-Derived Carbon as Electrocatalysts for Ethanol Oxidation*. Electrocatalysis, 2019. **10**(4): p. 366-380.
37. Ma, T., et al., *Pd-H₃PW₁₂O₄₀ /Zr-MCM-41: An efficient catalyst for the sustainable dehydration of glycerol to acrolein*. Chemical Engineering Journal, 2016. **294**: p. 343-352.
38. Díaz de Leon, J.N., et al., *Catalytic dehydration of 2 propanol over Al₂O₃-Ga₂O₃ and Pd/Al₂O₃-Ga₂O₃ catalysts*. Catalysis Today, 2019: p. in press.
39. Armenta, M.A., et al., *Thermodynamic and catalytic properties of Cu- and Pd-oxides over mixed γ - χ -Al₂O₃ for methanol dehydration toward dimethyl ether*. International Journal of Hydrogen Energy, 2019. **44**(14): p. 7276-7287.
40. Jing, J.-y., et al., *Metal precursor impregnation sequence effect on the structure and performance of Ni-Co/MgO catalyst*. International Journal of Hydrogen Energy, 2019. **44**(16): p. 8089-8098.
41. Chong, S.L., Soh, J. C. and Cheng, C. K., *Production of Ethylene from ethanol dehydration over H₃PO₄- Modified cerium oxide catalyst* Malaysian Journal of Analytical Sciences, 2017. **21**(4): p. 839 - 848.
42. Inoue, M., *Handbook of Advanced Ceramics: Chapter 11.1.4. Solvothermal Synthesis of Metal Oxides*. 2013: Elsevier Science.
43. Wang, Y., et al., *Review of the progress in preparing nano TiO₂: an important environmental engineering material*. J Environ Sci (China), 2014. **26**(11): p. 2139-77.
44. Pokhrel, S., et al., *In situ high temperature X-ray diffraction, transmission electron microscopy and theoretical modeling for the formation of WO₃ crystallites*. CrystEngComm, 2015. **17**(36): p. 6985-6998.
45. Sohn, J.R., et al., *Characterization of Titanium Sulfate Supported on Zirconia and Activity for Acid Catalysis*. Langmuir, 2002. **18**: p. 1666-1673.
46. Chen, G., et al., *Catalytic dehydration of bioethanol to ethylene over TiO₂/ γ -Al₂O₃ catalysts in microchannel reactors*. Catalysis Today, 2007. **125**(1-2): p. 111-119.
47. Wu, L.-P., et al., *The fabrication of TiO₂-supported zeolite with core/shell heterostructure for ethanol dehydration to ethylene*. Catalysis Communications, 2009. **11**(1): p. 67-70.
48. Ladera, R.M., et al., *TiO₂-supported heteropoly acid catalysts for dehydration of methanol to dimethyl ether: relevance of dispersion and support interaction*. Catalysis Science & Technology, 2015. **5**(1): p. 484-491.

49. Héroguel, F., et al., *Controlled deposition of titanium oxide overcoats by non-hydrolytic sol gel for improved catalyst selectivity and stability*. Journal of Catalysis, 2018. **358**: p. 50-61.
50. Sohn, J.R. and J.H. Bae, *Characterization of Tungsten Oxide Supported on TiO₂ and Activity for Acid Catalysis*. 2000. **17**: p. 86-92
51. Pae, Y.I., et al., *Characterization of NiO-TiO₂ Modified with WO₃ and Catalytic Activity for Acid Catalysis* Bulletin of the Korean Chemical Society, 2004. **25**: p. 1881-1888.
52. Lebarbier, V., G. Clet, and M. Houalla, *Relations between Structure, Acidity, and Activity of WO_x on TiO₂ – Influence of the Initial State of the Support, Titanium Oxyhydroxide, or Titanium Oxide*. The Journal of Physical Chemistry B, 2006. **110**: p. 22608-22617.
53. Kourieh, R., et al., *Investigation of the WO₃/ZrO₂ surface acidic properties for the aqueous hydrolysis of cellobiose*. Catalysis Communications, 2012. **19**: p. 119-126.
54. Said, A.E.-A.A., M.M.M. Abd El-Wahab, and M. Abd El-Aal, *The Role of Acid Sites in the Catalytic Performance of Tungsten Oxide during the Dehydration of Isopropyl and Methyl Alcohols*. Chemical and Materials Engineering, 2016. **213**: p. 17–25.
55. Hong, E., H.-I. Sim, and C.-H. Shin, *The effect of Brønsted acidity of WO₃/ZrO₂ catalysts in dehydration reactions of C₃ and C₄ alcohols*. Chemical Engineering Journal, 2016. **292**: p. 156-162.
56. Cunha, A.M.d., et al., *Bimetallic Cu-(WO₃ or ZrO₂) on Al₂O₃ catalysts for glycerol dehydration to acetol : effect of texture and acidic properties*. International Symposium on Acid - Basic Catalysis, 2017.
57. Alharbi, W., et al., *Dehydration of ethanol over heteropoly acid catalysts in the gas phase*. Journal of Catalysis, 2014. **319**: p. 174-181.
58. Zhao, J., et al., *Effects of adding Al₂O₃ on the crystal structure of TiO₂ and the performance of Pd-based catalysts supported on the composite for the total oxidation of ethanol*. Inorganica Chimica Acta, 2013. **405**: p. 395-399.
59. Roldan, R., et al., *Effect of the impregnation order on the nature of metal particles of bi-functional Pt/Pd-supported zeolite Beta materials and on their catalytic activity for the hydroisomerization of alkanes*. Journal of Catalysis, 2008. **254**(1): p. 12-26.
60. Autthanit, C. and B. Jongsomjit, *Production of Ethylene through Ethanol Dehydration on SBA-15 Catalysts Synthesized by Sol-gel and One-step Hydrothermal Methods*. J Oleo Sci, 2018. **67**(2): p. 235-243.
61. Thamaphat, K., P. Limsuwan, and B. Ngotawornchai, *Phase Characterization of TiO₂ Powder by XRD and TEM*. Natural Science, 2008. **42**: p. 357 - 361
62. Shirke, B.S., et al., *Synthesis and characterization of pure anatase TiO₂ nanoparticles*. Journal of Materials Science: Materials in Electronics, 2010. **22**(7): p. 821-824.
63. A. A. Said, M.A.E.-W., M. A. El-Aal *The Role of Acid Sites in the Catalytic Performance of Tungsten Oxide during the Dehydration of Isopropyl and Methyl Alcohols*. Chemical and Materials Engineering, 2016 **4**(2): p. 17-25.

64. Maksasithorn, S., et al., *Preparation of super-microporous WO₃-SiO₂ olefin metathesis catalysts by the aerosol-assisted sol-gel process*. Microporous and Mesoporous Materials, 2015. **213**: p. 125-133.
65. M. Abdennouri, R.E., A. Elmhammedi, A. Galadi, M. Baâlala, M. Bensitel, A. Boussaoud, Y. El hafiane, A. Smith, N. Barka, *Influence of tungsten on the anatase-rutile phase transition of sol-gel synthesized TiO₂ and on its activity in the photocatalytic degradation of pesticides* Journal of Materials and Environmental Science, 2013. **4 (6)** p. 953-960
66. Almohalla, M., I. Rodríguez-Ramos, and A. Guerrero-Ruiz, *Comparative study of three heteropolyacids supported on carbon materials as catalysts for ethylene production from bioethanol*. Catalysis Science & Technology, 2017. **7(9)**: p. 1892-1901.
67. Kamsuwan, T. and B. Jongsomjit, *A Comparative Study of Different Al-based Solid Acid Catalysts for Catalytic Dehydration of Ethanol*. Engineering Journal, 2016. **20(3)**: p. 63-75.
68. Xin, H., et al., *Catalytic dehydration of ethanol over post-treated ZSM-5 zeolites*. Journal of Catalysis, 2014. **312**: p. 204-215.
69. David Raju Burri, K.-M.C., Sang-Cheol Han, Abhishek Burri, and Sang-Eon Park, *Dehydrogenation of Ethylbenzene to Styrene with CO₂ over TiO₂-ZrO₂ Bifunctional Catalyst*. Bulletin of the Korean Chemical Society, 2007. **28(1)**: p. 53-58.
70. Chen, D., et al., *CO₂ hydrogenation to methanol over CuO-ZnO-TiO₂-ZrO₂: a comparison of catalysts prepared by sol-gel, solid-state reaction and solution-combustion*. Journal of Sol-Gel Science and Technology, 2018. **86(3)**: p. 719-730.
71. Hong, E., H.-I. Sim, and C.-H. Shin, *The effect of Brønsted acidity of WO₃/ZrO₂ catalysts in dehydration reactions of C₃ and C₄ alcohols*. Chemical Engineering Journal, 2016. **292**: p. 156-162.
72. Moser, W.R., et al., *Silicon-Rich H-ZSM-5 Catalyzed Conversion of Aqueous Ethanol to Ethylene* Journal of Catalysis, 1989. **117** p. 19-32
73. Nash, C.P., et al., *Mixed alcohol dehydration over Brønsted and Lewis acidic catalysts*. Applied Catalysis A: General, 2016. **510**: p. 110-124.
74. Shirke, B.S., et al., *Synthesis and characterization of pure anatase TiO₂ nanoparticles*. Journal of Material Science, 2011. **22**: p. 821-824
75. Min S., W.H., Shandong Y., Hailang Z., Tianqiong C., Jainli W., *Effect of the loading sequence of CeO₂ and Pd*. Molecular catalysis 2018: p. in press.
76. Sun, J. and Y. Wang, *Recent Advances in Catalytic Conversion of Ethanol to Chemicals*. ACS Catalysis, 2014. **4(4)**: p. 1078-1090.
77. Zhang, M. and Y. Yu, *Dehydration of Ethanol to Ethylene*. Industrial & Engineering Chemistry Research, 2013. **52(28)**: p. 9505-9514.
78. Yang, C., et al., *Catalytic activity and crystal structure modification of Pd/ γ -Al₂O₃-TiO₂ catalysts with different Al₂O₃ contents*. Journal of Energy Chemistry, 2016. **25(3)**: p. 375-380.
79. Krutpijit, C. and B. Jongsomjit, *Catalytic Ethanol Dehydration over different acid activated montmorillonite clays*. Journal of Oleo science, 2016. **65** p. 347-355.

80. Janlamool, J. and B. Jongsomjit, *Catalytic Ethanol Dehydration to Ethylene over Nanocrystalline χ - and γ - Al_2O_3 Catalysts*. *J Oleo Sci*, 2017. **66**(9): p. 1029-1039.
81. Buniazet, Z., et al., *Supported oxides catalysts for the dehydration of isobutanol into butenes: Relationships between acidic and catalytic properties*. *Molecular Catalysis*, 2018. **451**: p. 143-152.
82. Chong, S.L., J.C. Soh, and C.K. Cheng, *Production of Ethylene from Ethanol Dehydration over H_3PO_4 -Modified Cerium Oxide Catalysts*. *Malaysian Journal of Analytical Science*, 2017. **21**(4): p. 839–848.
83. Kamsuwan, T. and B. Jongsomjit, *Characterization of Different Si- and Al-based Catalysts with Pd Modification and Their Use for Catalytic Dehydration of Ethanol*. *J Oleo Sci*, 2018. **67**(8): p. 1005-1014.
84. Said, A.E.-A.A., M.M.M. Abd El-Wahab, and M.M. Abdelhak, *The role of Brønsted acid site strength on the catalytic performance of phosphotungstic acid supported on nano γ -alumina catalysts for the dehydration of ethanol to diethyl ether*. *Reaction Kinetics, Mechanisms and Catalysis*, 2017. **122**(1): p. 433-449.
85. Makoto, A. and O. Yoshito, *Kinetics of Glycerol Dehydration with WO_3/TiO_2 in Supercritical Water*. *Industrial & Engineering Chemistry Research*, 2012. **51**: p. 12253–12257.
86. Conner, N., et al., *Mixed alcohol dehydration over Brønsted and Lewis acidic catalysts*. *Applied Catalysis A: General*, 2016: p. 110-124.
87. Limlamthong, M., N. Chitpong, and B. Jongsomjit, *Influence of Phosphoric Acid Modification on Catalytic Properties of γ - χ Al_2O_3 Catalysts for Dehydration of Ethanol to Diethyl Ether*. *Bulletin of Chemical Reaction Engineering & Catalysis*, 2019. **14**(1).
88. Marbun, M.J., et al., *Production of Diethyl Ether Over Cr-Co / γ - Al_2O_3 Catalyst* International Symposium of Indonesian Chemical Engineering, 2019.

APPENDIX

จุฬาลงกรณ์มหาวิทยาลัย
CHULALONGKORN UNIVERSITY

APPENDIX A – COMPARING Pd/TiO₂ AND WPD/TiO₂ CATALYST IN ETHANOL DEHYDRATION

The PdW/TiO₂ which provided the highest catalytic activity in part II and Pd/TiO₂ were investigated and compared on catalyst characterization and performance.

1. Catalyst characterization

The XRD patterns of PdW/TiO₂ and Pd/TiO₂ are demonstrated in **Figure 23**. The intensity of XRD peaks of both catalyst exhibited the similar XRD patterns having the strong diffraction peaks located at 2 θ degree of 25° (major), 38° and 48°, which are assigned to the tetragonal anatase phase of crystalline TiO₂ [61, 62]. The low intensity peaks were noticed at 24° and 34° for PdW/TiO₂ which were designated to the formation of the WO₃ crystals with tetragonal phase [63, 64]. In addition to both catalyst, it is noticed that peak of palladium did not appear due to the small loading of Pd metal and/or the very small size of crystallites being in the highly dispersed form on the TiO₂ support [75]. According to the Scherrer equation, the average crystalline size of PdW/TiO₂ was smaller than Pd/TiO₂ as established in **Table 16**. The pore sizes of catalysts were in ranged of mesoporous structure referring to IUPAC.

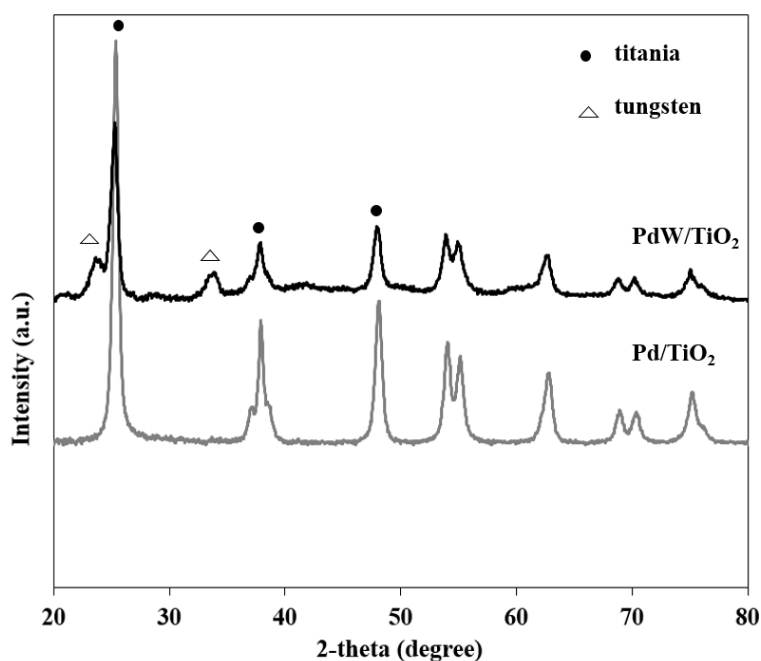


Figure 23: X-ray powder diffraction patterns for PdW/TiO₂ and Pd/TiO₂ catalysts

Table 16: Physical properties of PdW/TiO₂ and Pd/TiO₂ catalysts

	$S_{\text{BET}}^{\text{a}}$	Pore Volume ^b	Pore Size ^c	Crystalline size ^d
Sample	(m ² /g)	(cm ³ /g)	(nm)	(nm)
PdW/TiO ₂	30.4	0.13	13.9	11.8
Pd/TiO ₂	63.6	0.34	16.6	15.7

^a Measured by BET method , ^{b,c} Measured by BJH desorption method , ^d Measured by XRD using the Scherrer equation

The S_{BET} , pore volume, and pore size diameter of catalysts explored by N₂ physisorption method were shown in **Table 16**. It demonstrated that the W modification onto Pd/TiO₂ significantly decreased the surface area (S_{BET}), pore properties due to some pore blockage from W particles in Pd/TiO₂.

The dispersion of elements of PdW/TiO₂ and Pd/TiO₂ catalysts analyzed by the energy-dispersive X-ray spectroscopy (EDX) are displayed in **Table 17**. It was found that the Pd particles were mostly located at outer surface of PdW/TiO₂ and Pd/TiO₂ catalysts in the order of 1.7 and 1.6 wt%, which are higher than the amounts of Pd loading (0.5 wt%) in bulk catalyst.

Table 17: Elemental distribution (% wt, % mol) on external surface of PdW/TiO₂ and Pd/TiO₂ catalysts obtained from EDX

Catalyst	Element							
	% weight				% mol			
	O	W	Pd	Ti	O	W	Pd	Ti
PdW/TiO ₂	38.87	10.51	1.7	48.92	68.90	1.60	0.50	29.00
Pd/TiO ₂	43.9	-	1.6	51.77	72.60	-	0.40	27.00

The acid properties of PdW/TiO₂ and Pd/TiO₂ catalysts measured by NH₃ temperature - programmed desorption (NH₃-TPD) is exhibited **Table 18**. It is noticed that the presented of Pd in to catalysts provided an increase of acidity on W/TiO₂.

Table 18: The amount surface acidity and acid density of catalysts measured by NH₃-TPD

Sample	Acidity ($\mu\text{mol/g cat}$)				Acid density ($\mu\text{mol/m}^2$)			
	Weak	Moderate	Strong	Total	Weak	Moderate	Strong	Total
PdW/TiO ₂	1311	1215	357	2884	43.10	39.93	11.74	94.78
Pd/TiO ₂	1876	2144	400	4420	29.50	33.71	6.28	69.49

The binding energy of surface elemental composition on the catalysts analyzed by XPS technique is shown in **Table 19**. The binding energies for Ti, W, Pd and O were detected which are corresponding to those of EDX analysis. Furthermore, the spectral analysis of the XPS focused on O 1s core-level spectra providing the additional information for oxygen species on catalyst surface is exhibited in **Table 19**. It is observed that PdW/TiO₂ has the higher hydroxyl group (Brønsted acid) than Pd/TiO₂ catalyst.

Table 19: XPS analysis of PdW/TiO₂ and Pd/TiO₂ catalysts

Catalysts	Binding Energy (eV)						O 1s area portion		
	Ti 2p1	Ti 2p2	Pd 3d	W 4f1	W 4f2	O 1s	O	OH	H ₂ O
PdW/TiO ₂	458.7	464.5	336.1	37.6	35.5	530.0	0.45	0.41	0.14
Pd/TiO ₂	458.5	464.2	336.5	-	-	529.7	0.74	0.19	0.08

2. Ethanol dehydration Reaction study

As shown in **Table 20**, the ethanol conversion for catalysts increased with an increased the reaction temperature which is signified that no deactivation of supports and catalysts. The highest ethanol conversion was achieved at 400°C for all samples. At 400°C, it is displayed that the ethanol conversion of PdW/ TiO₂ (ca. 90%) was higher than Pd/TiO₂ (ca 60%), which is correspondence to the total acid density as shown in **Table 18**. It is general accept that the higher acid density and shorter distance between two acid sites, it is benefit to increase the possibility of the reactant to be adsorbed and rapidly catalyzed to produce the chemical product [80]. In **Figure 24**, it showed the product selectivity of PdW/TiO₂ and Pd/TiO₂ catalysts. The resulted

revealed that the Pd/TiO₂ catalysts were mostly selective to acetaldehyde at 200 – 300 °C and selective to diethyl ether at 350 – 400 °C. The modification of Tungsten into Pd/TiO₂ provided the ethylene selectivity at 200 – 400 °C and diethyl ether selectivity at 200 - 300 °C. The ethylene and diethyl ether yields are exposed in **Table 20**. It was discovered that the Pd/TiO₂ catalysts provide the highest acetaldehyde of ca. 21 % at 350°C whereas PdW/TiO₂ provided the highest ethylene and diethyl ether of ca. 63% at 400°C and 41% at 300°C in respectively. The XPS results confirmed that the PdW/TiO₂ contained the higher Brønsted acid sites on catalyst rather than Pd/TiO₂ one which is influenced to the ethanol dehydration to produce ethylene and diethyl ether.

Table 20: Catalytic activity and product yield (%) obtained from PdW/TiO₂ and Pd/TiO₂ catalyst as a function of reaction temperature (the reaction condition at T = 200 – 400°C, WHSV = 3.13 g_{ethanol}·g_{cat}⁻¹·h⁻¹, and catalyst weight = 0.1 g)

Catalysts	Temp(oC)	Conversion (%)	Product Yield (%)		
			Ethylene	DEE	Acetaldehyde
PdW/TiO ₂	200	2.0	0.0	0.0	2.0
	250	33.1	3.7	24.9	4.5
	300	63.0	14.8	41.4	6.8
	350	84.8	41.0	29.9	13.9
	400	90.2	63.2	11.1	15.9
Pd/TiO ₂	200	1.4	0.0	0.0	1.4
	250	3.5	0.4	0.0	3.1
	300	19.5	2.5	6.7	10.2
	350	54.5	10.7	23.0	20.8
	400	60.2	19.8	25.7	14.7

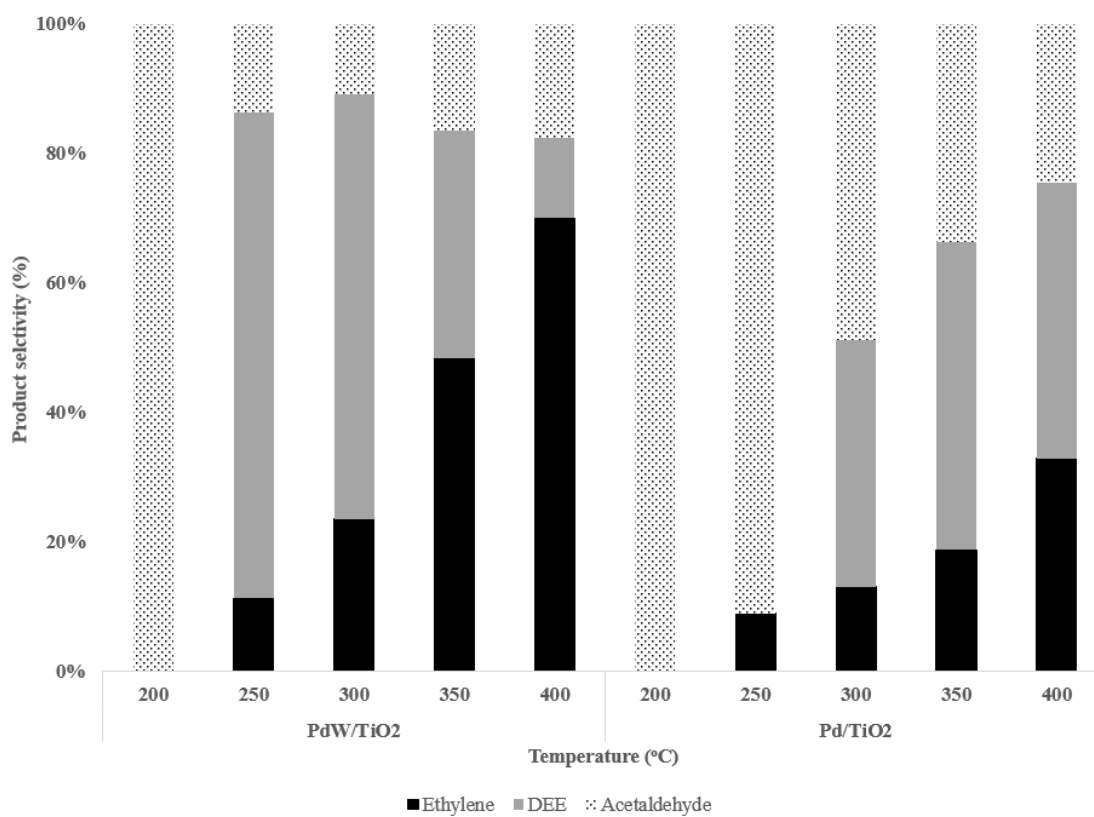


Figure 24: Product selectivity of PdW/TiO₂ and Pd/TiO₂ catalysts

APPENDIX B - CALCULATION CATALYST PREPARATION

The Calculation of metal loading by incipient wetness impregnation is described as follows:

1. Procedure solution

Tungsten (VI) chloride (WCl_6)

Molecular weight = 396.56 g/mol

W atomic weight = 183.84 g/mol

Tetraamminepalladium (II) chloridemonohydrate (99.99%) ($Pd(NH_3)_4Cl_2 \cdot H_2O$)

Molecular weight = 263.44 g/mol

Pd atomic weight = 106.42 g/mol

2. Preparation W/TiO₂ catalyst at W 13.5 wt%

Based on 1 g of catalyst

Tungsten (W) = 0.135 g

TiO₂ support catalyst = $1.00 - 0.135 = 0.865$ g

WCl_6 (precursor) 1 mole contained 1 atom of W, then

Tungsten (W) 183.84 g WCl_6 = 0.396.56 g

Tungsten (W) 0.135 g WCl_6 = 396.56×0.135

183.84

= 0.0626 g

3. Preparation Pd/TiO₂ catalyst at Pd 0.5 wt%

Based on 1 g of catalyst

Palladium (Pd) = 0.005g

TiO₂ support catalyst = $1.00 - 0.005 = 0.995$ g

$Pd(NH_3)_4Cl_2 \cdot H_2O$ (precursor) 1 mole contained 1 atom of Pd, then

$$\begin{array}{rclcl}
 \text{Palladium (Pd)} & 106.42 \text{ g} & \text{Pd(NH}_3)_4\text{Cl}_2 \cdot \text{H}_2\text{O} & = & 263.44 \text{ g} \\
 \text{Palladium (Pd)} & 0.005 \text{ g} & \text{Pd(NH}_3)_4\text{Cl}_2 \cdot \text{H}_2\text{O} & = & \underline{263.44 \times 0.005} \\
 & & & & 106.42 \\
 & & & = & 0.0124 \text{ g}
 \end{array}$$

4. The preparation of Pd/W /TiO₂ , W/Pd/TiO₂ and PdW/TiO₂ were using the same calculation method as mention above.



APPENDIX C - CALCULATION OF ACIDITY AND BASICITY

The acidity of all supports and catalysts is determined from NH₃-TPD by calculating the area under TCD signal versus temperature.

$$\text{Acidity of catalysts} = \frac{\text{mol of desorbed NH}_3}{\text{weight of dry catalyst}} \quad [\mu\text{mol/g cat}]$$

Where:

$$\text{mol of desorbed NH}_3 = (\text{area under TCD signal curve}) \times (30.927 \mu\text{mol})$$

$$\text{weight of dry catalyst} = 0.05 \text{ g}$$

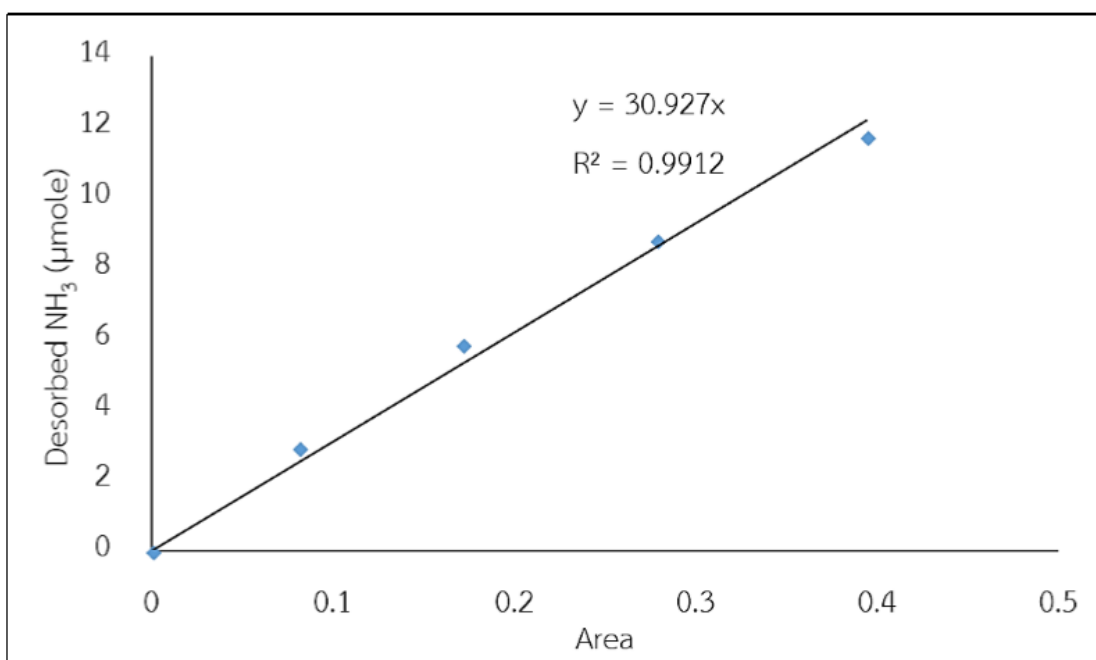


Figure 25: The calibration curve of NH₃-TPD

The basicity of all supports and catalysts is determined from CO₂-TPD by calculating the area under TCD signal versus temperature.

$$\text{Basicity of catalysts} = \frac{\text{mol of desorbed CO}_2}{\text{weight of dry catalyst}} \quad [\mu\text{mol/g cat}]$$

Where:

$$\text{mol of desorbed CO}_2 = (\text{area under TCD signal curve}) \times (0.0176 \mu\text{mol})$$

weight of dry catalyst = 0.05 g

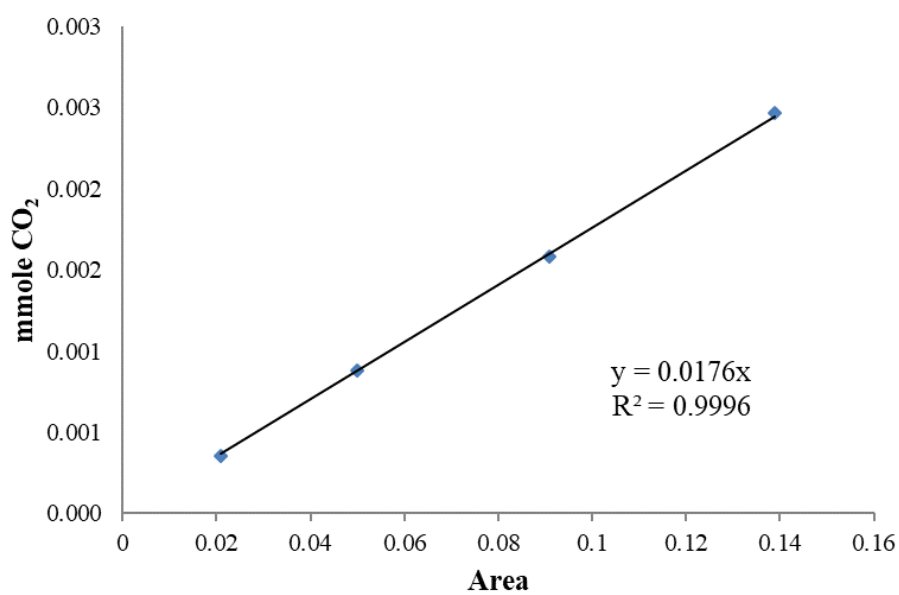


Figure 26: The calibration curve of CO₂-TPD



APPENDIX D – GC CALIBRATION CURVES

The calibration curves were calculated by injection substance into GC with flame ionization detector (GC-FID) and detected by chromatogram in area of substance versus amount of injection substance. The calibration curves of the reactant and products were used to quantitative the reactant and products including ethanol, ethylene, diethyl ether and acetaldehyde as showed in **Figure 27-30**.

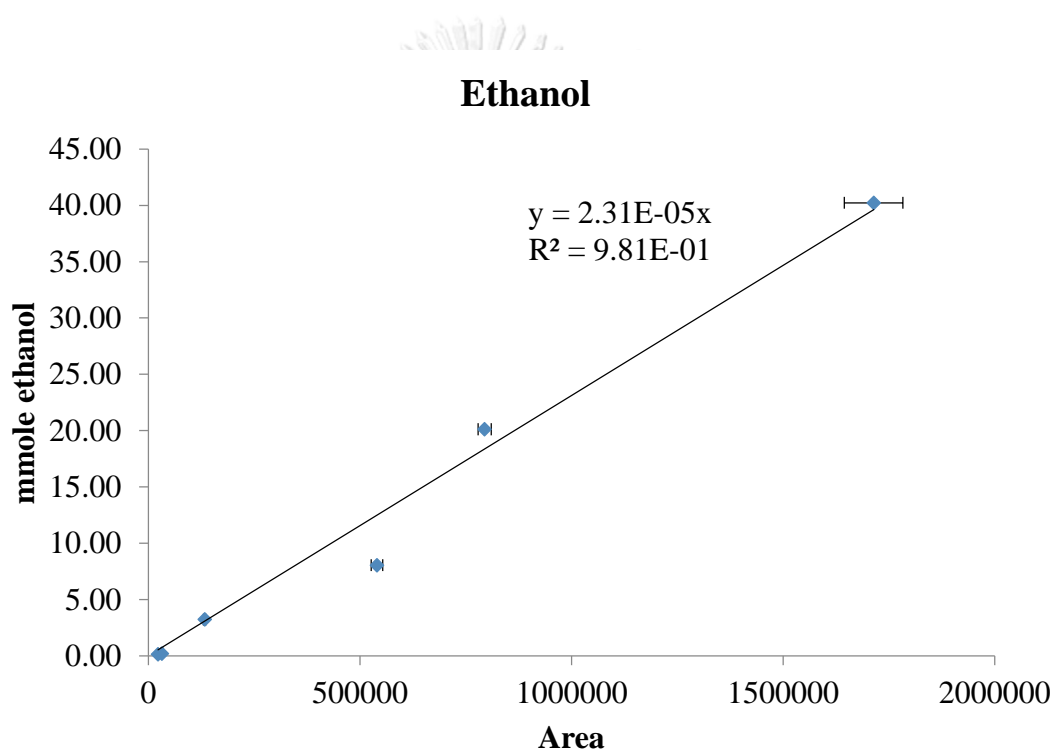


Figure 27: The calibration curve of ethanol

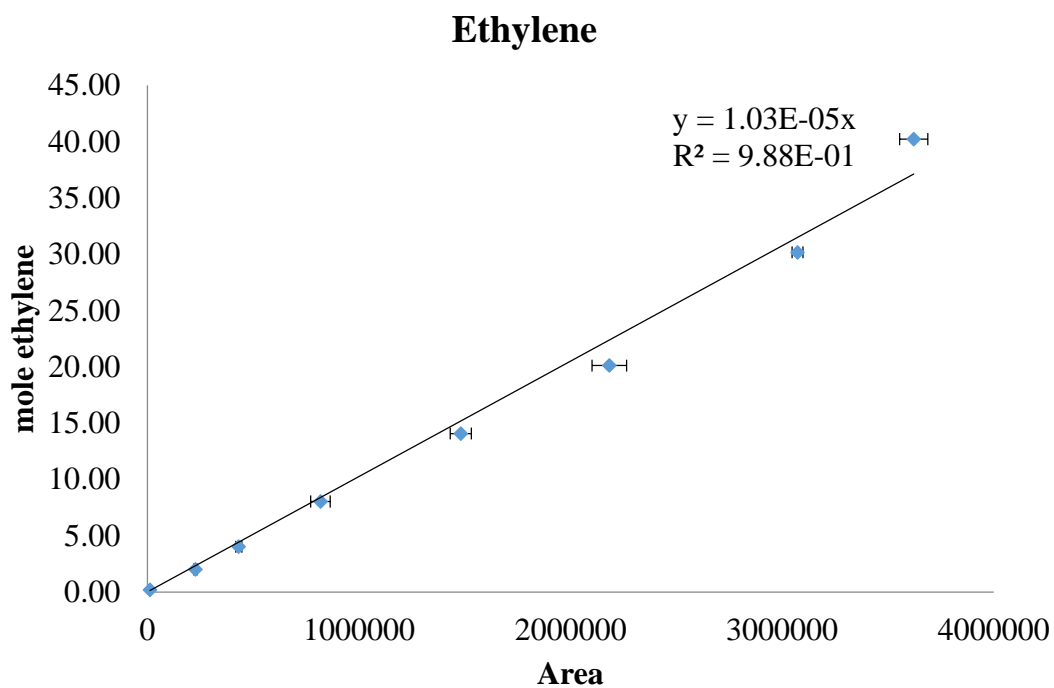


Figure 28: The calibration curve of ethylene

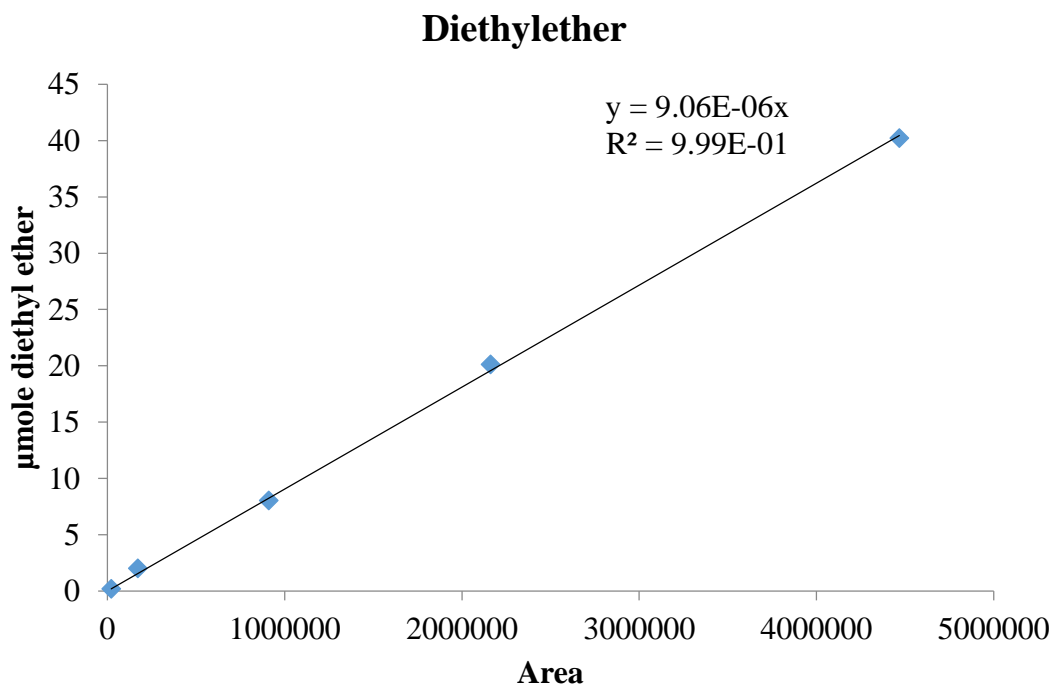


Figure 29: The calibration curve of diethyl ether

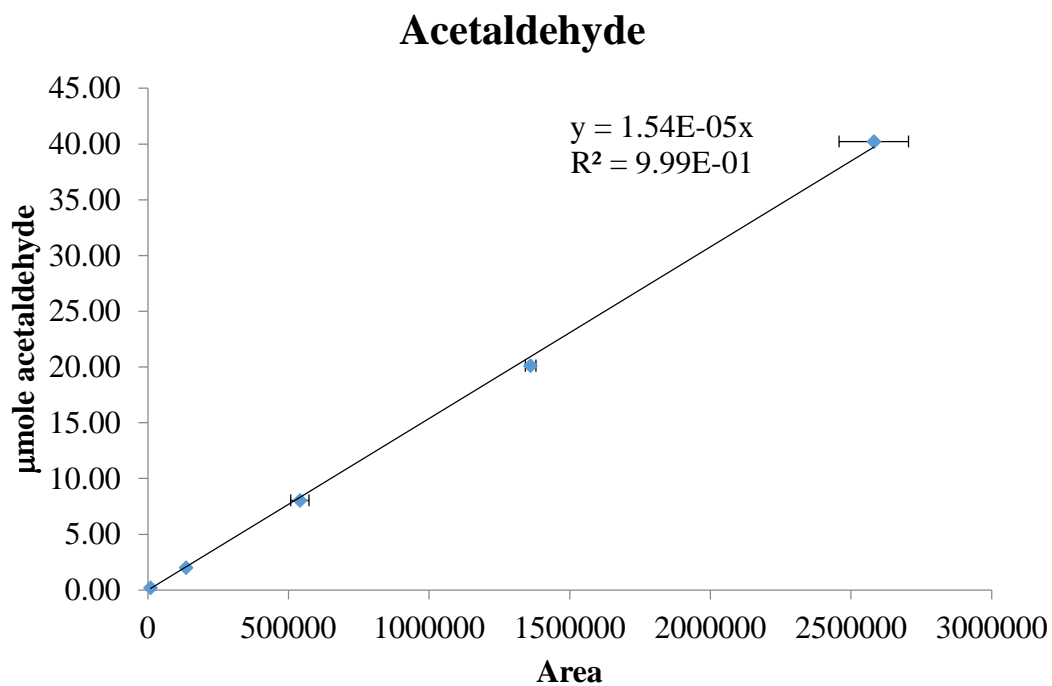


Figure 30: The calibration curve of acetaldehyde



APPENDIX E – CHROMATOGRAM

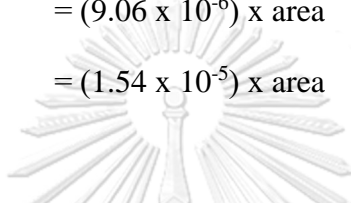
The amount of reactant and products including ethanol, ethylene, diethyl ether and acetaldehyde were quantitatively analyzed by Gas Chromatography (GC). The calculation report analysis by GC are shown as follows:

$$\text{Mole of ethanol} = (2.31 \times 10^{-5}) \times \text{area}$$

$$\text{Mole of ethylene} = (1.03 \times 10^{-5}) \times \text{area}$$

$$\text{Mole of diethyl ether} = (9.06 \times 10^{-6}) \times \text{area}$$

$$\text{Mole of acetaldehyde} = (1.54 \times 10^{-5}) \times \text{area}$$



C-RSA CHROMATOPAC CH=1 Report No.=19 DATA=1:@CHRM1.C00 17/07

** CALCULATION REPORT **

CH	PKNO	TIME	AREA	HEIGHT	MK	IDNO	CONC
1	1	4.127	1912	852			0.4809
	2	4.356	171	34			0.0429
	3	4.581	388870	143427	SV		97.8045
	4	4.878	6647	3210	T		1.6717
TOTAL			397600	147522			100

Figure 31: The gas chromatography analysis report

In **Figure 31**, the gas chromatography report showed the area of the reactant and products by peak positions at 4.127 min, 4.356 min, 4.581 min and 4.878 min for ethylene, acetaldehyde, ethanol and diethyl ether in respectively.

As a result,

$$\begin{aligned} \text{The mole of ethylene} &= (1.03 \times 10^{-5}) \times \text{areas} \\ &= (1.03 \times 10^{-5}) \times 1912 \\ &= 0.02 \text{ mol} \end{aligned}$$

$$\begin{aligned} \text{The mole of diethyl ether} &= (9.06 \times 10^{-6}) \times \text{areas} \\ &= (9.06 \times 10^{-6}) \times 6647 \\ &= 0.06 \text{ mol} \end{aligned}$$

APPENDIX F – THE SAMPLING DURING ETHANOL DEHYDRATION

The ethanol dehydration reaction is carried out at reaction temperature ranged 200 – 400 °C. The sample were taken for analyzed the reactance and products. The sampled shall be taken at effluence after the feed and the reaction is in steady state. The sampling during the reaction is exhibited in **Figure 32**.

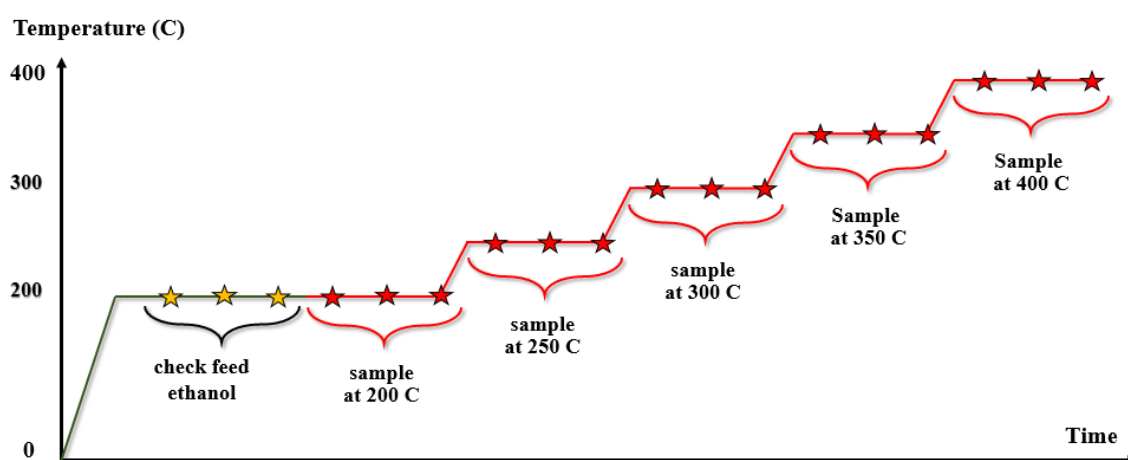


Figure 32: The sampling during the reaction testing

Remark:

The steady state is the parameter condition and system such as concentrations are unchanging in time.

APPENDIX G – CALCULATION OF ETHANOL CONVERSION, PRODUCT SELECTIVITY AND PRODUCT YIELD

The catalytic activities (conversion, selectivity and yield) were calculated as follows:

Ethanol conversion

The ethanol conversion is the amount of the converted ethanol (mole) with respect to ethanol in feed as following equation.

$$\text{Ethanol conversion (\%)} = \frac{(\text{mol of ethanol in feed} - \text{mol of ethanol in product}) \times 100}{\text{mol of ethanol in feed}}$$

Product selectivity

The products selectivity is the amount of each product formed (mole) with respect to total products (mole) as following equation

$$\text{Product selectivity (\%)} = \frac{\text{mol of each product} \times 100}{\text{mol of total products}}$$

Product yield

The product yield is defined by following equation

$$\text{Product yield (\%)} = \frac{\text{ethanol conversion} \times \text{selectivity of each product}}{100}$$

APPENDIX H – LIST OF PUBLICATION

1. Anchale Tresatayawed, Peangpit Glinrun, and Bunjerd Jongsomjit Ethanol. Dehydration over WO_3/TiO_2 Catalysts Using Titania Derived from Sol-Gel and Solvothermal Methods, International Journal of Chemical Engineering, 2019 (3), 1-11. (ISI & Scopus, Q2 by SJR)
2. Anchale Tresatayawed, Peangpit Glinrun, Chaowat Autthanit and Bunjerd Jongsomjit. Pd modification and supporting effects on catalytic dehydration of ethanol to ethylene and diethyl ether over W/TiO_2 catalysts, Journal of Oleo Science, in press. (ISI & Scopus, Impact factor (ISI) = 1.182, Q2 by SJR)

VITA

NAME Anchale Tresatayawed

DATE OF BIRTH 22 May 1974

PLACE OF BIRTH Manila, Philippines

INSTITUTIONS ATTENDED B. Eng (Chemical Engineering), Kasetsart University
M.S. (Petrochemical Technology), Petroleum and Petrochemical College Chulalongkorn University

HOME ADDRESS 416/34 Lardprao 87, Wangtonglang, Bangkok, Thailand

PUBLICATION

1. Anchale Tresatayawed, Peangpit Glinrun, and Bunjerd Jongsomjit Ethanol. Dehydration over WO₃/TiO₂ Catalysts Using Titania Derived from Sol-Gel and Solvothermal Methods, International Journal of Chemical Engineering, 2019 (3), 1-11.
2. Anchale Tresatayawed, Peangpit Glinrun, Chaowat Autthanit and Bunjerd Jongsomjit. Pd modification and supporting effects on catalytic dehydration of ethanol to ethylene and diethyl ether over W/TiO₂ catalysts, Journal of Oleo Science, In press.